



Norwegian University of
Science and Technology

Investigation of a twisted-tube type shell-and-tube heat exchanger

Sven Olaf Danielsen

Master of Science in Energy and Environment

Submission date: June 2009

Supervisor: Erling Næss, EPT

Norwegian University of Science and Technology
Department of Energy and Process Engineering

Problem Description

The following should be considered in the project work:

1. Perform a literature study on the twisted tube heat exchanger concept, which should include:

The heat exchanger design, industrial experience and thermal-hydraulic characteristics. Depending on available information, operational and maintenance experiences shall be presented.

A comparison of the twisted tube heat exchanger concept to other competing heat exchanger concepts.

The information shall be presented and discussed.

2. Collect data of thermal-hydraulic performance on the twisted-tube heat exchanger installed at Melkøya (25-HA-113). Analyze and present the data, and perform an uncertainty analysis.
3. Perform thermal-hydraulic simulations on the heat exchanger by using the HTRI program Xist. Simulate various operation modes. Thereafter, compare and discuss the simulations with the data gathered in point 2. Evaluate and comment deviations between the measured data and the simulations.
4. Comparative thermal-hydraulic designs of the twisted-tube heat exchanger 25-HA-113 with other types of shell-and-tube heat exchanger configurations. The HTRI program Xist shall be used in the design calculations. The results shall be presented and discussed. With basis in the performed designs, a heat exchanger concept/geometry shall be recommended for the present application.
5. Suggest further work on this topic.

Assignment given: 20. January 2009
Supervisor: Erling Næss, EPT

EPT-H-2009-18



MASTER THESIS

for

Stud.techn. Sven Olaf Danielsen

Spring 2009

Investigation of a twisted-tube type shell-and-tube heat exchanger *Undersøkelse av en 'twisted-tube'-type rørsatsvarmeveksler*

Background

StatoilHydro has recently installed a “twisted-tube” heat exchanger on the Hammerfest LNG plant at Melkøya. The heat exchanger is in service as a gas compressor intercooler for a multicomponent refrigerant. As of today, StatoilHydro has limited experience with this type of heat exchangers. Therefore it is desirable to verify the thermal-hydraulic performance of the installed unit. In addition, it is of interest to point out the strengths and weaknesses of the twisted tube heat exchanger concept in comparison to other types of heat exchangers.

Objectives

The aim of the thesis is to verify the thermal-hydraulic performance of the twisted tube heat exchanger installed on StatoilHydro's LNG plant at Melkøya and to perform an evaluation of the strengths and weaknesses of the twisted tube concept with other heat exchanger concepts.

The following questions should be considered in the project work:

1. Perform a literature study on the twisted tube heat exchanger concept, which should include:
 - a. The heat exchanger design, industrial experience and thermal-hydraulic characteristics. Depending on available information, operational and maintenance experiences shall be presented.
 - b. A comparison of the twisted tube heat exchanger concept to other competing heat exchanger concepts.
The information shall be presented and discussed.
2. Collect data of thermal-hydraulic performance on the twisted-tube heat exchanger installed at Melkøya (25-HA-113). Analyze and present the data, and perform an uncertainty analysis.
3. Perform thermal-hydraulic simulations on the heat exchanger by using the HTRI program Xist. Simulate various operation modes. Thereafter, compare and discuss the simulations with the data gathered in point 2. Evaluate and comment deviations between the measured data and the simulations.

4. Comparative thermal-hydraulic designs of the twisted-tube heat exchanger 25-HA-113 with other types of shell-and-tube heat exchanger configurations. The HTRI program Xist shall be used in the design calculations. The results shall be presented and discussed. With basis in the performed designs, a heat exchanger concept/geometry shall be recommended for the present application.
5. Suggest further work on this topic.

Within 14 days of receiving the written text on the diploma thesis, the candidate shall submit a research plan for his project to the department.

When the thesis is evaluated, emphasis is put on processing of the results, and that they are presented in tabular and/or graphic form in a clear manner, and that they are analyzed carefully.

The thesis should be formulated as a research report with summary both in English and Norwegian, conclusion, literature references, table of contents etc. During the preparation of the text, the candidate should make an effort to complete a well presented report. In order to ease the evaluation of the thesis, it is important that the cross references are correct. In the making of the report, strong emphasis should be placed on both a thorough discussion of the results and an orderly presentation.

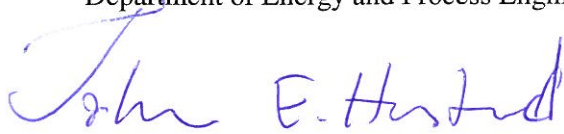
The candidate is requested to initiate and keep close contact with his/her specialist teacher and academic supervisor(s) throughout the working period. The candidate must follow the rules and regulations of NTNU as well as passive directions given by the Department of Energy and Process Engineering.

Pursuant to "Regulations concerning the supplementary provisions to the technology study program/Master of Science" at NTNU §20, the Department reserves the permission to utilize all the results for teaching and research purposes as well as in future publications.

One – 1 complete original of the thesis shall be submitted to the authority that handed out the set subject. (A short summary including the author's name and the title of the thesis should also be submitted, for use as reference in journals (max. 1 page with double spacing)).

Two – 2 – copies of the thesis shall be submitted to the Department. Upon request, additional copies shall be submitted directly to research advisors/companies. A CD-ROM (Word format or corresponding) containing the thesis, and including the short summary, must also be submitted to the Department of Energy and Process Engineering

Department of Energy and Process Engineering, 12. January 2009



Johan E. Hustad
Department manager



Erling Næss
Academic supervisor

Research advisors:

Øystein Larsen, StatoilHydro
Jan Kristiansen, StatoilHydro

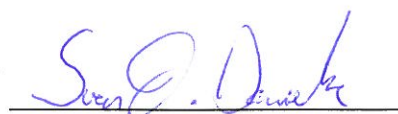
Acknowledgments

This master thesis is a result of collaboration between StatoilHydro ASA and Department of Energy and Process Engineering, Norwegian University of Science and Technology (NTNU). The work presented has been mainly performed at NTNU in Trondheim, but computer simulations have been carried out at the StatoilHydro office in Stavanger.

It has been very interesting for me to work on this thesis. This is due to a fascinating topic and inspiring supervisors. I especially wish to thank professor Erling Næss for excellent supervision and for giving me the opportunity to choose this topic. He has been very helpful when I have faced theoretical problems during the work. I also want to thank PhD student Pål-Tore Storli who assisted me on the uncertainty analysis.

Øystein Larsen and Jan Kristiansen at StatoilHydro have assisted with specification of the tasks in the thesis. They have also, with their experience with heat exchanger computer software, helped me to perform the computer simulations. In addition they have taken initiative and supported me during the whole development of the thesis. Arne Olav Fredheim at StatoilHydro has provided me all needed measurement data and given me valuable information on how the measurements were performed.

Thank you all for your help.



Trondheim 14.06.2009

Abstract

This master thesis investigates twisted tube type shell-and-tube heat exchangers with emphasis on thermal-hydraulic characteristics, fouling and vibration properties. An extensive literature study has been carried out in order to map all published research reports written on the topic. The mapping of performed research shows that the available information is limited.

Mathematical correlations for twisted tube thermal-hydraulic characteristics are extracted from the research reports found in the literature study. Correlations for convective heat transfer coefficients and pressure loss for both shell side and tube side are presented. The enhancement of heat transfer by swirl flow in a twisted tube bundle is also discussed.

Measurements on thermal-hydraulic characteristics are collected from a twisted tube heat exchanger installed at the process facility LNG Hammerfest situated at the northern end of Norway. These measurements are then compared to output from the heat exchanger design software HTRI Xchanger Suite. The calculation accuracy of the twisted tube program module is predicted on this basis.

HTRI Xchanger Suite can evaluate heat exchanger design in two different modes. Simulation mode calculates two outlet parameters and thereby the duty, while rating mode calculates only one output parameter where the duty is specified by the user. In rating mode the software has an accuracy of +/-4% for temperature, flow and duty calculations. The overall heat transfer coefficient is miscalculated by approximately +50% and the shell side pressure loss is miscalculated by +40%. In simulation mode the duty is not specified by the user and the program may calculate two output parameters. The predicted accuracy depends on the calculated parameters. Calculation accuracy for two unknown outlet temperatures is +/-7% while calculation accuracy for two unknown mass flow rates is up to +200%. The accuracy on the overall heat transfer coefficient and shell side pressure loss is the same as for rating mode.

The StatoilHydro twisted tube heat exchanger 25-HA-113 design on LNG Hammerfest is evaluated with respect to thermal-hydraulic characteristics. 25-HA-113 is operated with other flows and temperatures than it was designed for. By use of a mathematical method the expected performance in design operation point is predicted. By analysing the measured overall heat transfer coefficient and by use of this mathematical method, it is stated that the heat exchanger has insufficient thermal design. However, investigation of the pressure loss in the same manner shows that the unit performs better than specified in the design basis. The fouling characteristic is examined by evaluation of the overall heat transfer coefficient over a time period. This analysis shows that the fouling tendency is minimal.

By use of the computer program HTRI Xchanger Suite and field measurements a quantitative comparison of a twisted tube, a helix baffled and a single segmental baffled unit is performed for the application of 25-HA-113. The alternatives are compared to each other by evaluation of heat transfer coefficients, pressure loss, fouling characteristics and vibration risks. The conventional and the helix alternative are equipped with low fin tubes which show a somehow higher heat transfer capacity per volume unit. However, the twisted tube provides a higher overall heat transfer coefficient than the two other alternatives. The single segmental baffle concept appears to have the lowest shell side pressure loss, followed closely by the twisted tube. With respect to vibration risk the twisted tube has a superior performance compared the two competing concepts due to a very rigid bundle construction. By considering the thermal hydraulic characteristics and the vibration risk connected to the evaluated application the twisted tube is the recommended alternative.

Sammendrag

Denne masteroppgaven undersøker rørsatsvarmevekslere med såkalte "twisted tubes". Det vil si at rørene har et ovalt tverrsnitt som er vridd om rørets lengdeakse. Denne typen varmevekslere har blitt undersøkt med hovedvekt på termisk-hydrauliske egenskaper, beleggdannelse og risiko for vibrasjonsproblemer. Et omfattende litteraturstudium har blitt gjennomført for å samle mest mulig informasjon om tidligere forskning på dette området. Denne undersøkelsen viser at publisert forskningsarbeid som omfatter slike varmevekslere er av begrenset omfang og tilgjengelighet. Matematiske korrelasjoner for termisk-hydrauliske egenskaper er ekstrahert fra relevante forskningsrapporter funnet i litteraturstudiet. Korrelasjoner for konvektiv varmeovergang og trykktap er presentert for både rør og skall side av veksleren. Økt varmeovergang ved indusering av virvelstrøm er også diskutert.

Målinger av termisk-hydrauliske egenskaper er samlet fra en varmeveksler som er installert ved LNG Hammerfest på Melkøya. Disse målingene er deretter sammenlignet med beregninger fra dataprogrammet HTRI Xchanger Suite. Med bakgrunn i denne sammenligningen er beregningsnøyaktigheten til twisted tube modulen i programmet evaluert.

HTRI Xchanger Suite evaluerer en eksisterende varmeveksler design i to ulike moduser. Simulation modus evner å beregne to ulike prosessparametere og således varmeeffekten til veksleren. I rating modus kan programmet kun beregne en prosessparameter. Varmeeffekten er dermed gitt implisitt av brukeren. Rating modus beregner temperaturer, masserater og varmeeffekt med en nøyaktighet på +/- 4%. Varmeovergangstall og trykktap på skall side blir beregnet for store med henholdsvis +50% og +40% nøyaktighet. I simuleringsmodus avhenger nøyaktigheten av hvilke to parametere som beregnes av programmet. Beregningsnøyaktigheten er lav når begge masseratene er ukjente, med opp mot +200% feilkalkulering. Beregninger gjort med to temperaturer ukjente er derimot høy, med +/- 7%. Nøyaktigheten for beregning av trykktap og varmeovergangstall er den samme i simulation som rating modus.

25-HA-113 twisted tube varmeveksleren installert på LNG Hammerfest er undersøkt med hensyn på termisk-hydraulisk design. Varmeveksleren opereres ved et annet driftspunkt enn det som er spesifisert i design basisen. Ved å bruke en matematisk metode kan den forventede ytelsen i design punkt likevel predikeres. Denne analysen viser at det termiske designet av veksleren ikke er tilstrekkelig. Trykk tap på skall side er undersøkt ved hjelp av den samme metoden. Denne undersøkelsen viser at trykktapet er lavere enn forventet av leverandøren og lavere enn krav spesifisert i design basisen. Beleggdannelsen er også undersøkt. Dette ble gjort ved å evaluere utviklingen av varmeovergangstallet i en gitt tidsperiode. Denne analysen viser at beleggdannelsen i veksleren er minimal.

Ved å bruke dataprogrammet HTRI Xchanger Suite og måledata har en kvantitativ undersøkelse av ytelsen til tre ulike varmevekslerkonsepter blitt gjennomført for anvendelse på 25-HA-113. De tre evaluerte konseptene er twisted tube, heliks bafflet og single segmentelt bafflet varmeveksler. Disse tre løsningene er blitt evaluert med tanke på varmeovergangstall, trykktap, beleggdannelse og vibrasjon risiko. Det konvensjonelle alternativet og helix veksleren er utstyrt med finnedede rør som har en noe høyere varmeoverføringskapasitet. Likevel har twisted tube høyere varmeovergangstall. Den konvensjonelle veksleren med segmentelle baffler viser seg å påføre det laveste trykktapet på skall side, tett fulgt av twisted tube. I forhold til vibrasjonsrisiko viser twisted tube seg overlegen de to andre alternativene på grunn av den stive rørsatskonstruksjonen. Etter vurdering av termisk hydrauliske egenskaper og vibrasjonsrisikoen knyttet til denne anvendelsen anbefales twisted tube i valget mellom de tre alternativene.

Table of contents

FIGURE INDEX	XIII
---------------------	-------------

TABLE INDEX	XIV
--------------------	------------

NOMENCLATURE	XV
---------------------	-----------

ABBREVIATIONS	XVIII
----------------------	--------------

1 INTRODUCTION	1
-----------------------	----------

2 THE TWISTED TUBE HEAT EXCHANGER CONCEPT	2
--	----------

2.1 HISTORY	2
--------------------	----------

2.2 GEOMETRY	2
---------------------	----------

2.3 THERMAL-HYDRAULIC CHARACTERISTICS	5
--	----------

2.3.1 ENHANCEMENT OF HEAT TRANSFER BY INDUCING SWIRL	5
--	---

2.3.2 MATHEMATICAL MODELING OF THE HEAT TRANSFER PERFORMANCE	7
--	---

2.3.3 MATHEMATICAL MODELING OF THE PRESSURE DROP	16
--	----

2.4 FOULING AND DETERMINATION OF FOULING RESISTANCE R_f	18
---	-----------

2.4.1 FOULING IN GENERAL	18
--------------------------	----

2.4.2 FOULING IN TWISTED TUBE HEAT EXCHANGERS	19
---	----

2.4.3 FOULING RESISTANCE R_f	19
--------------------------------	----

2.5 FLOW INDUCED VIBRATION	20
-----------------------------------	-----------

2.5.1 FLOW INDUCED VIBRATION IN HEAT EXCHANGERS	20
---	----

2.5.2 REDUCED RISK FOR FLOW INDUCED VIBRATION IN TWISTED TUBE BUNDLES	21
---	----

2.6 APPLICATIONS	22
-------------------------	-----------

2.7 INDUSTRIAL EXPERIENCE, OPERATION AND MAINTENANCE	23
---	-----------

2.7.1 INDUSTRIAL EXPERIENCE	23
-----------------------------	----

2.7.2 CLEANING	23
----------------	----

3 FIELD MEASUREMENTS ON HA-25-113	24
--	-----------

3.1 BACKGROUND	24
-----------------------	-----------

3.2 KOCH TWISTED TUBE SOLUTION	25
---------------------------------------	-----------

3.3 AUTOMATICALLY LOGGED MEASUREMENTS ON 25-HA-113	27
---	-----------

3.4 MEASUREMENT UNCERTAINTY	29
------------------------------------	-----------

3.4.1 THE ROOT SUM SQUARE FORMULA (RSS)	29
---	----

3.4.2 ABSOLUTE ERROR	30
----------------------	----

3.4.3 RANDOM ERROR	30
--------------------	----

3.4.4 SYSTEMATIC ERROR	31
------------------------	----

3.4.5 TEMPERATURE MEASUREMENT UNCERTAINTY	32
---	----

3.4.6 PRESSURE MEASUREMENT UNCERTAINTY	34
--	----

3.4.7 GAS COMPOSITION MEASUREMENT UNCERTAINTY	34
---	----

3.4.8 FLOW MEASUREMENT UNCERTAINTY	35
------------------------------------	----

3.4.9 DUTY MEASUREMENT UNCERTAINTY	36
------------------------------------	----

3.4.10 OVERALL HEAT TRANSFER COEFFICIENT UNCERTAINTY	37
--	----

4	<u>EVALUATION OF THE HTRI XCHANGER SUITE ACCURACY</u>	38
4.1	INTRODUCTION TO XCHANGER SUITE	38
4.2	METHOD USED TO PREDICT THE HTRI ACCURACY FOR TWISTED TUBE	40
4.3	HTRI CALCULATION ERROR IN RATING MODE	41
4.3.1	TEMPERATURE, MASS FLOW RATE AND DUTY	41
4.3.2	HEAT TRANSFER AND SHELL SIDE PRESSURE LOSS	43
4.4	HTRI CALCULATION ERROR IN SIMULATION MODE	44
4.4.1	TEMPERATURE AND MASS FLOW RATE	44
4.4.2	SHELL SIDE PRESSURE LOSS, HEAT TRANSFER COEFFICIENT AND DUTY	46
5	<u>EVALUATION OF THE TWISTED TUBE DESIGN FOR 25-HA-113</u>	47
5.1	OVERDESIGN AND FOULING RESISTANCE INCLUDED IN DESIGN	47
5.2	HEAT TRANSFER PERFORMANCE	47
5.2.1	MEASURED HEAT TRANSFER COEFFICIENT	47
5.2.2	DESIGN HEAT TRANSFER COEFFICIENT	48
5.2.3	CLEAN HEAT TRANSFER COEFFICIENT	48
5.2.4	CORRECTED HEAT TRANSFER COEFFICIENT FOR OFF DESIGN OPERATION	48
5.2.5	PRESENTATION OF 25-HA-113 THERMAL PERFORMANCE	51
5.3	SHELL SIDE PRESSURE DROP	53
5.3.1	CORRECTED PRESSURE LOSS FOR OFF DESIGN OPERATION	53
5.4	CONSIDERATION OF FOULING ON 25-HA-113	55
6	<u>COMPARISON OF THE TWISTED TUBE SOLUTION TO OTHER HEAT EXCHANGER CONCEPTS</u>	56
6.1	DESCRIPTIONS OF THE DESIGNS FOR 25-HA-113	56
6.1.1	LOW FINNED TUBES WITH SINGLE SEGMENTAL BAFFLES	56
6.1.2	LOW FINNED TUBES WITH HELICAL BAFFLES	59
6.1.3	TWISTED TUBE	60
6.1.4	USED TECHNIQUE TO PERFORM AN ACCURATE COMPARISON	60
6.2	RESULTS	62
6.2.1	SIZE AND WEIGHT	62
6.2.2	THERMAL-HYDRAULIC CHARACTERISTICS	63
6.2.3	THERMAL RESISTANCE DISTRIBUTION	65
6.2.4	SHELL SIDE PRESSURE DROP	67
6.2.5	FOULING	68
6.2.6	VIBRATION	69
6.2.7	QUALITATIVE SUMMERY OF THE DIFFERENCES IN PERFORMANCE	69
7	<u>CONCLUSION</u>	71
8	<u>PROPOSAL FOR FURTHER WORK</u>	73
	<u>REFERENCES</u>	74

<u>APPENDIX A</u>	<u>DESCRIPTION OF THE PERFORMED LITERATURE STUDY</u>
<u>APPENDIX B</u>	<u>MEASUREMENT DATA 25-HA-113 TWISTED TUBE</u>
<u>APPENDIX C</u>	<u>MEASUREMENT DATA 25-HA-113 DOUBLE HELIX</u>
<u>APPENDIX D</u>	<u>DATA SHEETS FOR MEASUREMENT SENSORS</u>
<u>APPENDIX E</u>	<u>TECHNICAL DRAWINGS OF 25-HA-113 TWISTED TUBE</u>
<u>APPENDIX F</u>	<u>TECHNICAL DRAWINGS OF 25-HA-113 DOUBLE HELIX</u>
<u>APPENDIX G</u>	<u>THERMODYNAMIC PROPERTIES OF HC GAS</u>
<u>APPENDIX H</u>	<u>CORRECTION OF THERMODYNAMIC PROPERTIES</u>
<u>APPENDIX I</u>	<u>TEMA SPECIFICATION SHEETS PRINTED FROM HTRI</u>

Figure Index

Figure 2.1: Cross section of a twisted tube	2
Figure 2.2: Illustration of tube alignment[6]	3
Figure 2.3: Twisted tube bundle [3]	4
Figure 2.4: Tube side and shell side flow pattern[3].....	5
Figure 2.5: Illustration of secondary flow when running the cooling fluid on the tube side.....	6
Figure 2.6: Thermal resistance.....	10
Figure 2.7: Illustration of heat transfer in a heat exchanger	10
Figure 2.8: Heat transfer between the two fluids represented by thermal resistances.....	12
Figure 2.9: Shell side flow pattern in a conventional shell and tube.....	19
Figure 2.10: Shell side flow pattern in a twisted tube	19
Figure 3.1: Process diagram of gas liquefaction	24
Figure 3.2: TEMA specification sheet for Koch twisted tube design printed from HTRI	26
Figure 3.3: Process arrangement around 25-HA-113	28
Figure 3.4: Uncertainty classes for temperature measurement, IEC 75 [20]	32
Figure 4.1: The HTRI Xchanger Suite interface	39
Figure 4.2: HTRI calculation error in rating mode for temperatures, flow rates and duty	41
Figure 4.3: HTRI calculation error in rating mode for pressure loss and heat transfer coefficient	43
Figure 4.4: HTRI calculation error in simulation mode for temperature and mass flow rate...	44
Figure 4.5: HTRI calculation error in simulation mode for duty, pressure loss and heat transfer	46
Figure 5.1: Thermal performance of 25-HA-113	51
Figure 5.2: Hydraulic performance of 25-HA-113.....	54
Figure 5.3: Developement of fouling layer on 25-HA-113	55
Figure 6.1: Size and weight to the three heat exchanger designs	62
Figure 6.2:Thermal capacity of the three heat exchanger designs	63
Figure 6.3: The thermal performance of the three alternatives	64
Figure 6.4: Heat transfer capacity to volume ratio.....	64
Figure 6.5: The distribution of thermal resistance for the three concepts	65
Figure 6.6: Shell side pressure drop predicted for the three concepts	67
Figure 6.7: Heat transfer capacity to pressure drop ratio for the three concepts	67

Table index

Table 2.1: List of twisted tube deliveries [1]	22
Table 3.1: List of sensors that collect measurement data used in this report	27
Table 3.2: Temperature measurement uncertainty	33
Table 3.3: Pressure measurement uncertainty	34
Table 3.4: Composition measurement uncertainty	34
Table 3.5: Flow measurement uncertainty	36
Table 3.6: Duty measurement uncertainty	36
Table 3.7: Overall heat transfer coefficient measurement uncertainty	37
Table 4.1: Rating mode – temperature, mass flow and duty	42
Table 4.2: Rating mode – shell side pressure loss and heat transfer coefficient	43
Table 4.3: Rating mode – temperatures and flow rates	44
Table 4.4: Rating mode – duty, pressure loss and heat transfer	46
Table 5.1: Thermal performance in numbers	51
Table 5.2: Hydraulic performance in numbers	54
Table 6.1: conventional alternative run at design point in HTRI	57
Table 6.2: HTRI simulation on averaged operation point for the conventional HE	60
Table 6.3: The origin of performance parameters	61
Table 6.4: Summery of the numbers given in chapter 6	68

Nomenclature

Symbol	Description	Unit
A	area	[m ²]
A _{flow}	cross section area of a flow	[m ²]
B _c	calibration uncertainty	[-]
B _{da}	data-acquisition uncertainty	[-]
B _{dr}	data reduction uncertainty	[-]
B _m	method uncertainty	[-]
B _o	other uncertainties	[-]
B _x	systematic measurement error of x	[-]
C	discharge coefficient	[-]
C _n	frequency constant	[-]
c _p	specific heat capacity	[J/kgK]
D	diameter of venturi tube	[m]
d _e	efficient diameter	[m]
d _h	hydraulic diameter	[m]
d _{max}	maximal diameter of a twisted tube	[m]
d _{min}	minimum diameter of a twisted tube	[m]
ΔF	deviation between the true function F and the measured function	[-]
Δp	pressure loss	[Pa]
ΔT	temperature difference	[K]
ΔT _{lm}	log mean temperature difference	[K]
Δx _n	deviation between the real value and the measured value	[-]
E	modulus of elasticity	[kg/m ²]
ε	wall roughness	[mm]
F	mathematical function	[-]
F _r	dimensionless swirl number	[-]
f _D	Darcy friction factor	[-]
f _n	natural frequency of straight tubes	Hz
f _g	correction factor for heat exchanger geometry	[-]
g	gravitational constant	[m/s ²]

Symbol	Description	Unit
h	convective heat transfer coefficient	[-]
h_e	specific enthalpy	[kJ/kg]
I	sectional moment of inertia	[m ⁴]
k_c	conduction heat transfer coefficient	[W/mK]
L	tube length	[-]
L_t	tube thickness	[m]
L_{un}	tube unsupported span	[m]
\dot{m}	mass flow rate	[kg/s]
μ	dynamic viscosity	[kg/sm]
Nu	nusselt number	[-]
n	sample size	[-]
Pr	prandtl number	[-]
P	perimeter length	[m]
P_x	random measurement error of x	[-]
p	static pressure	[Pa]
q	heat transfer rate	[W]
q''	heat flux	[W/m ²]
Re	reynolds number	[-]
R_{tot}	total heat resistance	[K/W]
R_f	thermal resistance due to fouling	[K/W]
ρ	density	[kg/m ³]
S_x	standard deviation of a sample	[-]
s	twist pitch	[m]
T	temperature	[°C]
t	value from Student's t probability distribution	[-]
U	overall heat transfer coefficient	[W/m ²]
v	fluid velocity	[m/s]
W_e	Effective weight per unit tube length including the weight of the fluid inside tubes	[kg/m]
W_i	absolute measurement error of measurand i	[-]
W_x	absolute measurement error of x	[-]
x	measured parameter	[-]

Subscript	Description
av	averaged
c	cold fluid
d	diameter
h	hot fluid
i	inlet
in	inner
b	evaluated at the bulk
m	metal
o	outlet
ou	outer
s	shell side
t	tube side
w	wall
(x)	evaluated at location x

Superscript	Description
n	temperature ratio exponent
m	viscosity ratio exponent

Abbreviations

ASME	American Society of Mechanical Engineers
PIM	StatioHydro electronic documentation database
HTRI	HTRI Xchanger Suite v5.00 SP2, computer software
Hysys Inc.	Aspen HYSYS process modelling software Incorporated

1 Introduction

Gas is an energy resource of significant importance for the people around the world. It is expected that the importance will continue to grow as the supply of crude oil declines. Gas is found at the same locations as oil. The sources of oil and gas are slowly exhausted and new fields have to be discovered and exploited. New fields are today often found on remote locations with difficult environment conditions. Because of large distances and deep seawater, pipeline transportation to the consumer is a too expensive affair. An alternative to pipeline transportation is liquefaction of the natural gas (LNG). By cooling the product it reduces volume by approximately 600 times. It means that the energy intensity in terms of volume is increased at the same rate. Because of the high energy intensity of the LNG, it is economical and practical to ship the product to the location where it will be used.

Hammerfest LNG plant is located at the island Melkøya at the northern end of Norway. The gas needed at the plant is supplied from the great oil field Snøhvit. The core of the plant is the liquefaction system that cools the natural gas down to $-163\text{ }^{\circ}\text{C}$. This process is done in the following three stages: Pre cooling, liquefaction and sub cooling. Each of the three systems is driven by high capacity compressors through several compressor stages. In between the sub cooling compressor stages the refrigerant is cooled in a heat exchanger by seawater available at the site. The purpose of the installation is to save energy at the downstream compressor stage. This principle is called intercooling.

The intercooler itself is a heat exchanger. When Hammerfest LNG plant was finished in 2007, a helix shell-and-tube heat exchanger was installed in the sub cooling system between the two compressor stages. After approximately one year of operation several tubes inside the helix heat exchanger burst. The component was quickly replaced by a so called twisted tube heat exchanger. The vendor Koch Heat Transfer Incorporated claimed that this was a rigid and almost vibration free design. StatoilHydro has limited experience with the twisted tube heat exchanger. It is therefore preferred to evaluate the design in terms of thermal-hydraulic performance, vibration and fouling characteristics. In addition one wishes to evaluate the software that is used for designing such heat exchangers.

2 The twisted tube heat exchanger concept

An extensive literature study has been carried out in order to collect as much information on the twisted tube heat exchanger as possible. For collecting scientific documentation web based search engines have been used. Complete description of the literature study is given in Appendix A. In addition, information has been gathered from the manufacturers of these heat exchangers by searching their web pages. The information given here are less scientifically reliable, but useful data on applications, operation experience and maintenance where found.

Although some research work has been performed on this type of heat exchanger, the documentation available to public often lacks important details. This appears especially in the presentation of mathematical correlations for pressure drop and heat transfer coefficients. However, by extracting information from multiple sources it was possible to overcome this problem.

2.1 History

Section 2.1 and 2.2 are based on the following references: [1], [2], [3], [4] and [5].

The Twisted tube heat exchanger is not a new design. In fact this type of heat exchangers has been available from the Swedish company Allards (now SiljanAllards AB) since 1984. Allards has provided hundreds of successful twisted tube solutions to the power, chemical and paper industry the last decades. In 1994 Koch Heat Transfer Incorporated (former Brown Fintube Company) took over the responsibility for marketing and manufacturing of the twisted tube outside Scandinavia and has since then delivered twisted tube heat exchangers to the world market.

2.2 Geometry

The twisted tube is a shell-and-tube heat exchanger. It consists of a bundle of tubes fitted inside a cylindrical outer shell. The design differs from a traditional shell-and-tube exchanger by having oval tubes twisted along the longitudinal axis. The number of twists per unit length can vary from design to design. The twist pitch s , is the tube length between each 360 degree twist. Each twisted tube is manufactured with round ends making it possible to fit them into the tube sheets by conventional methods. Every tube is kept in position by contact points to the surrounding tubes. This is achieved by adjusting each tube such that the cross sections are aligned illustrated in Figure 2.2. Such fitting technique results in six contact points per each 360 degree twist. The bundle is strapped firmly by metal belts after installation of the tubes. Such tube configuration results in a very rigid bundle construction.

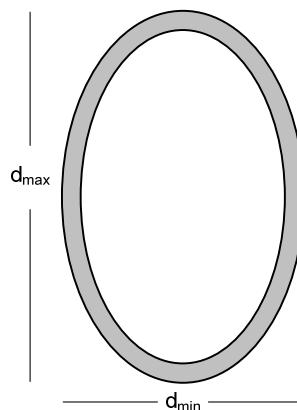


Figure 2.1: Cross section of a twisted tube

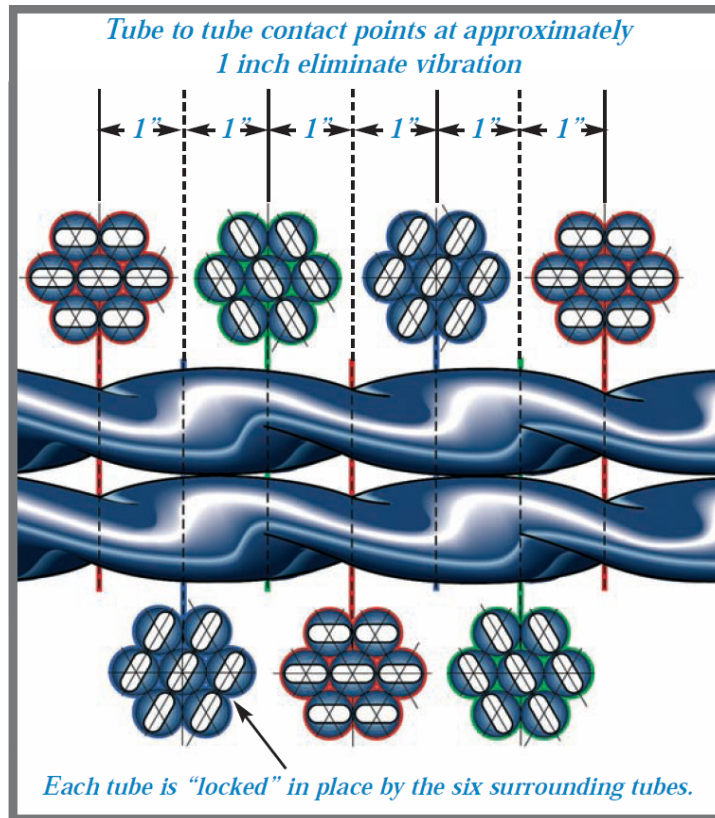


Figure 2.2: Illustration of tube alignment[1]

The tubes are normally manufactured in a one step operation ensuring a constant wall thickness and that the material yield point is not exceeded. The mechanical properties of the used material are therefore retained. Twisted tubes can be manufactured from a full range of materials including carbon steels, stainless steels, titanium, copper and nickel alloys. Arrangement of the tubes can either be done in a triangular or a rectangular pitch and the tube cross-section can be varied. A large deformation will give a small cross-section on the tube side in relation to the shell side, while a small deformation will give the opposite result. Variation of the tube cross section gives flexibility in the design to adapt to the specific application. Twisted tubes and plain tubes may also be combined in the same bundle without losing the tube support function. This may be adequate in certain applications including some condensation duties.

A conventional shell-and-tube heat exchanger is equipped with a certain number of baffles. Baffles are simply metal sheets covering the cross-sectional area of the shell along the longitudinal axis. The sheets have circular holes for the tubes and a cut off opening for the shell side fluid flow. A baffle has two main functions. First, it directs the flow perpendicular to the tubes in order to enhance heat transfer rate. Second, the baffle supports the tubes in order to prevent vibration.



Figure 2.3: Twisted tube bundle [2]

The twisted tube is a baffle free design. One could think that this result in a fragile tube bundle construction making the heat exchanger exposed to fluid induced vibration. In reality the twisted tube design gives a more rigid tube bundle compared to the conventional shell and tube concept. This is a consequence of the fact that each tube is in physical contact with the surrounding tubes along the whole length. These contact points are more frequent per unit length than baffle-to-tube joints in a conventional exchanger. The baffle free design is also claimed to give lower pressure drop (relative to heat transfer rate) because the shell side flow is not forced to do turns and pass sharp edges.

The shell side flow follows a complex pattern which is predominantly axial. To make sure that the shell side flow does not bypass the tubes, the bundle is shrouded. The shroud itself is a metal sheet that covers the bundle. The tube side flow is swirled enhancing heat transfer. The intensity of the swirl depends on the cross sectional shape and the twist pitch to diameter ratio. Why heat transfer is enhanced is discussed in the next section.

2.3 Thermal-hydraulic characteristics

This section is based on the following references: [3], [4], [5] and [6]

Considerable effort has been made the last decades to enhance heat transfer in heat exchanger equipment. Succeeding in this activity resulted in more compact and energy saving solutions which furthermore reduced the installation and operation costs. The twisted-tube heat exchanger is one of the products from this development. The literature study showed that there is a limited amount of published research work on this specific design. Main contributors to the research and documentation are Dzyubenko (Moscow Aviation Institute), Ashmantas (Lithuanian Academy of Sciences) and Ljubicic (Brown Fintube Company, Koch Industries). This chapter makes a summary of the most important research results in terms of empirical data and mathematical models of the twisted-tube thermal-hydraulic characteristics.

2.3.1 Enhancement of heat transfer by inducing swirl

This section is based on [6] and [3].

Heat transfer enhancement is one of the fastest growing areas of heat transfer technology. The technologies are classified into active and passive techniques depending on how the heat transfer performance is improved. A twisted tube is a typical passive technique that uses a specific geometry to induce swirl on the tube side flow.

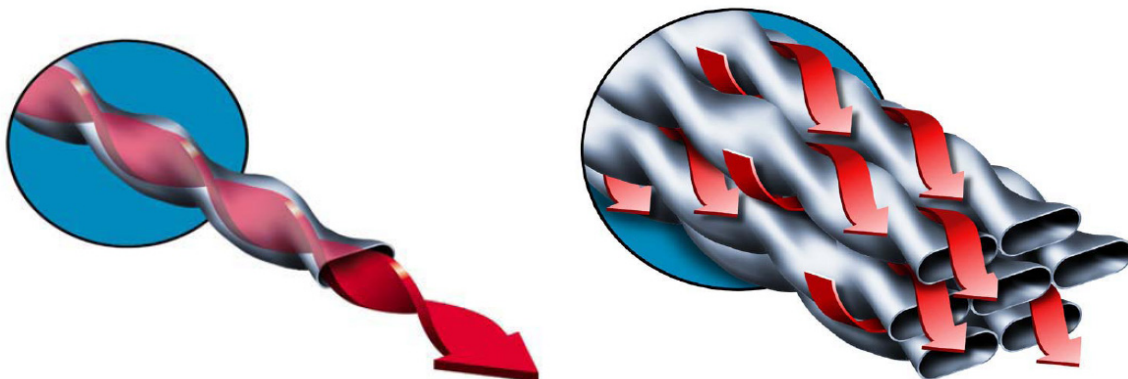


Figure 2.4: Tube side and shell side flow pattern[2]

The helical channel formed in the inter tubular space can be looked upon as series of consecutive short sections of which the build up of a steady velocity profile is interrupted by the constant direction change of the flow. Good transverse mixing is achieved by these interruptions, and the numerous disturbances keep the flow turbulent even at relatively low Reynolds numbers. The turbulent regime offers substantially higher convective heat transfer coefficients compared to laminar flow. By keeping the flow turbulent one secures a high heat transfer performance. These mechanisms contribute to higher heat transfer coefficients on the shell side flow.

For the tube side flow there are several mechanisms that contribute to high thermal performance. In a conventional shell and tube heat exchanger the radial temperature gradient on the tube side can be considerable because the transverse mixing is relatively low. More specifically the core of the tube flow will have a different temperature than the flow near the wall. The heat transfer between the two fluids is then reduced as a result of the lowered temperature difference across the wall. The twisted tube has an important feature that overcomes this problem. Because the swirl flow produces inertial mass forces there will be generated a secondary flow which enhance the tube side mixing.

More practically speaking the following process takes place. By running the cooling fluid inside the tubes one achieve heated fluid at the wall with a lower density compared to the colder core flow. Because of the induced swirl, centrifugal forces tend to move cold high density fluid towards the wall securing as high as possible temperature difference across the tube wall. This situation is illustrated on Figure 2.5. In contrast, if the heating fluid is run inside the tubes, we will have the opposite effect causing lower temperature difference and heat transfer rate.

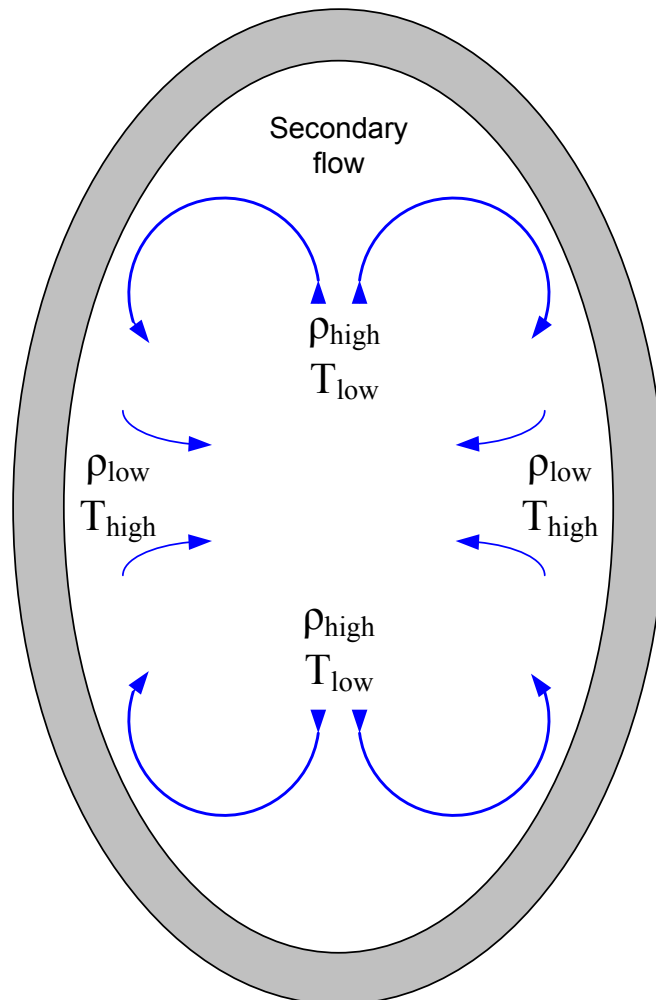


Figure 2.5: Illustration of secondary flow when running the cooling fluid on the tube side

In addition to this mechanism the bulk tube side flow velocity is increased compared to a plain tube. A higher velocity leads to a reduced boundary layer thickness which further leads to lower thermal resistance. This effect also contributes to enhanced heat transfer rate in a twisted tube heat exchanger.

Creating a swirl flow has of course a cost in terms of pressure loss. Pressure losses in the tubes are produced both by friction and by the additional turbulence resulting from swirling. However, experiments show that the increased pressure loss is relatively small compared to the gained heat transfer. Research shows that the use of twisted tubes makes it possible to reduce the volume of the heat exchanger by a factor of 1.25 to 1.4 [5]. It must be emphasized that this is a comparison to plain circular tubes.

2.3.2 Mathematical modeling of the heat transfer performance

One of the major tasks in heat exchanger design is to obtain a large overall heat transfer coefficient. This will reduce the size and furthermore the material and installation costs of the component. One of the basic equations used in heat exchanger thermal analysis underline this fact.

$$q = f_g UA \Delta T_{lm} \quad (2.1)$$

where

- q heat transfer rate
- f_g correction factor for heat exchanger geometry
- U overall heat transfer coefficient
- A heat exchanger area
- ΔT_{lm} Log mean temperature difference

$$\Delta T_{lm} = \frac{T_{h,i} - T_{c,o} - T_{h,o} + T_{c,i}}{\ln[(T_{h,i} - T_{c,o}) / (T_{h,o} + T_{c,i})]} \quad (2.2)$$

The log mean temperature difference is dependent on the four inlet and outlet temperatures. Inlet temperatures and one outlet temperature are given by the application. The latter is the temperature the engineer wants to control and the reason why the exchanger should be installed. The other outlet temperature is given by the chosen flow rate and heat capacity of the actual media. ΔT_{lm} is therefore a rather fixed value of which the designer has low influence. What the designer can affect is the area and the overall heat transfer coefficient. The area is affected by the number of tubes, fitting of fins and so on. The overall heat transfer coefficient can be affected by flow velocity and the type of heat exchanger selected. Mathematical modeling of the twisted tube heat transfer performance is therefore about finding a precise expression for the area and the overall heat transfer coefficient U . Calculation of the area can be done by a mathematical evaluation of the tube geometry. The parameters that decide the area is the shape of the tube cross section and the twist pitch. In the following, formulas for geometrical characteristics and definitions of dimensionless numbers are presented.

Geometrical formulas for twisted tube

Flow area of a twisted tube can be calculated by use of the formula for the area of an ellipse. With our terminology the formula for flow area becomes following.

$$A_{flow} = \frac{\pi}{4} d_{in,max} d_{in,min} \quad (2.3)$$

The perimeter of an ellipse can only be represented exact by a mathematical series. However, the Indian mathematician S. Ramanujan has developed a very accurate formula for determination of perimeter length [7].

$$P = \pi[3(d_{in,max} + d_{in,min}) - \sqrt{(3d_{in,max} + d_{in,min})(d_{in,max} + 3d_{in,min})}] \quad (2.4)$$

By use of the general formula for hydraulic diameter $D_h = 4A/P$ [8], equation (2.3) and (2.4) one arrives at the following expression for the twisted tube hydraulic diameter

$$d_h = \frac{d_{in,max} d_{in,min}}{3(d_{in,max} + d_{in,min}) - \sqrt{(3d_{in,max} + d_{in,min})(d_{in,max} + 3d_{in,min})}} \quad (2.5)$$

Correlations for thermal-hydraulic characteristics are found by the performed literature study. In the correlations an *efficient diameter* d_e is used. None of the sources give a clear definition of this parameter. Some sources [9], which not give the correlations, claim that the hydraulic and the efficient diameter are two different parameters. By investigating known formulas in the sources where the efficient diameter is used, it is concluded that this parameter is equal to the hydraulic diameter.

Dimensionless numbers used in the correlations

Correlations for thermal-hydraulic characteristics are often given as a function of dimensionless numbers. These numbers are presented here starting with the Nusselt number.

$$Nu = \frac{hd_h}{k_c} \quad (2.6)$$

The correlations for Nusselt number are valid for a certain range of Reynolds number defined by

$$Re = \frac{\rho v d_h}{\mu} \quad (2.7)$$

and a function of the Prandtl number

$$Pr = \frac{C_p \mu}{k_c} \quad (2.8)$$

and the dimensionless swirl number

$$Fr = \frac{s^2}{d_{\max} d_h} \quad (2.9)$$

The dimensionless swirl number is a clever way to represent swirl which contain d_{\max} and d_h . By involving both d_{\max} and d_h the dimensionless swirl number not only gives information on degree of twisting, but also the shape of oval cross section. As the difference between d_{\max} and d_h get smaller, the oval cross section will approach a circular shape. The structure of the number also implies that for the same twist pitch s , one can have different values of the dimensionless swirl.

Determination of the heat transfer coefficient U

Here an expression for the local heat transfer coefficient is developed. The case considered below is simplified due to the assumption of equal surface area on shell side and tube side. However, the derivation below shows the idea of the overall heat transfer coefficient.

In thermal analysis an analogy to electricity is often used. The temperature difference has the role as voltage, which is the driving force for exchanging heat. Thus heat has taken the role as current flowing from high temperature (potential) to low temperature (potential). Fluids and materials reduce the heat transfer rate by acting as thermal resistances. The equation and illustration below explains the idea.

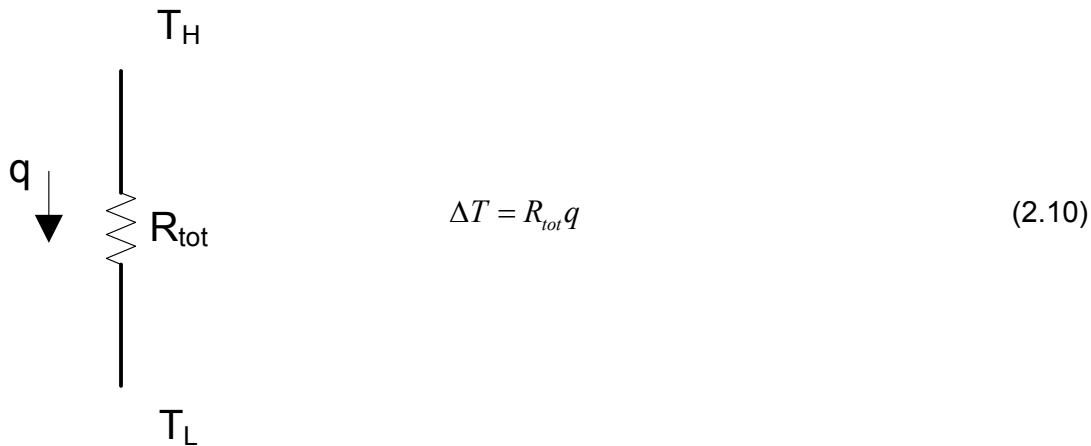


Figure 2.6: Thermal resistance

The illustration below shows the three thermal layers where the heat transfer occurs in the heat exchanger. By use of the figure an expression for the local heat transfer coefficient can be determined.

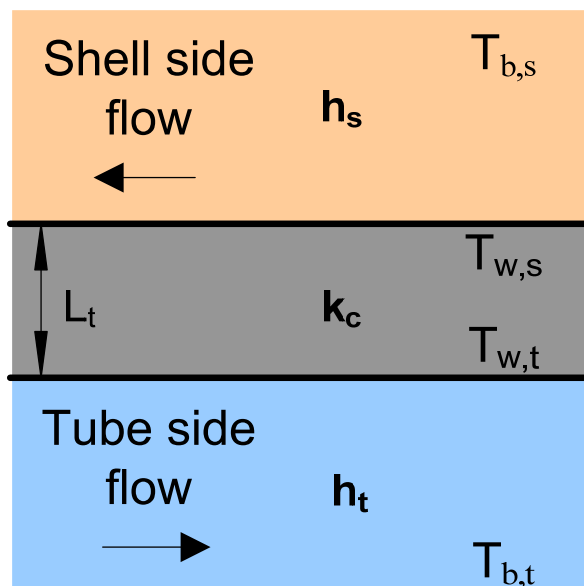


Figure 2.7: Illustration of heat transfer in a heat exchanger

The derivation starts with the following equation describing the total temperature difference over the thermal layers. The temperatures are a function of x along the axial axis of the heat exchanger.

$$T_{b,s(x)} - T_{b,t(x)} = \frac{q''_{(x)}}{U_{(x)}} \quad (2.11)$$

Each layer can be described mathematically by the individual temperature difference. The shell-side convection is modeled by

$$q''_{(x)} = h_s (T_{b,s(x)} - T_{w,s(x)}) \quad (2.12)$$

The conduction through the tube

$$q''_{(x)} = \frac{k_c}{L} (T_{w,s(x)} - T_{w,t(x)}) \quad (2.13)$$

And the tube-side convection

$$q''_{(x)} = h_t (T_{w,t(x)} - T_{b,t(x)}) \quad (2.14)$$

Reorganizing equation (2.12), (2.13) and (2.14) with respect to temperature difference and summing up the left and right hand side give

$$T_{b,s(x)} - T_{b,t(x)} = \left(\frac{1}{h_s} + \frac{L_t}{k_c} + \frac{1}{h_t} \right) q''_{(x)} \quad (2.15)$$

When one compare equation (2.11) to (2.15) it is clear that

$$U_{(x)} = \left(\frac{1}{h_s} + \frac{L_t}{k_c} + \frac{1}{h_t} \right)^{-1} \quad (2.16)$$

The result above is applicable for a clean heat exchanger. In addition one has to take account for fouling on the tube inner and outer surface. This layer will act as a thermal resistant and is accounted for in one parameter R_f despite the fact that fouling may occur on both shell side and tube side. If this parameter is included the following expression for local heat transfer coefficient can be written valid for equal heat transfer area on shell and tube side.

$$U_{(x)} = \left(\frac{1}{h_s} + \frac{L_t}{k_c} + R_f + \frac{1}{h_t} \right)^{-1} \quad (2.17)$$

Figure 2.8 shows how $U_{(x)}$ can be represented by a thermal circuit with resistances.

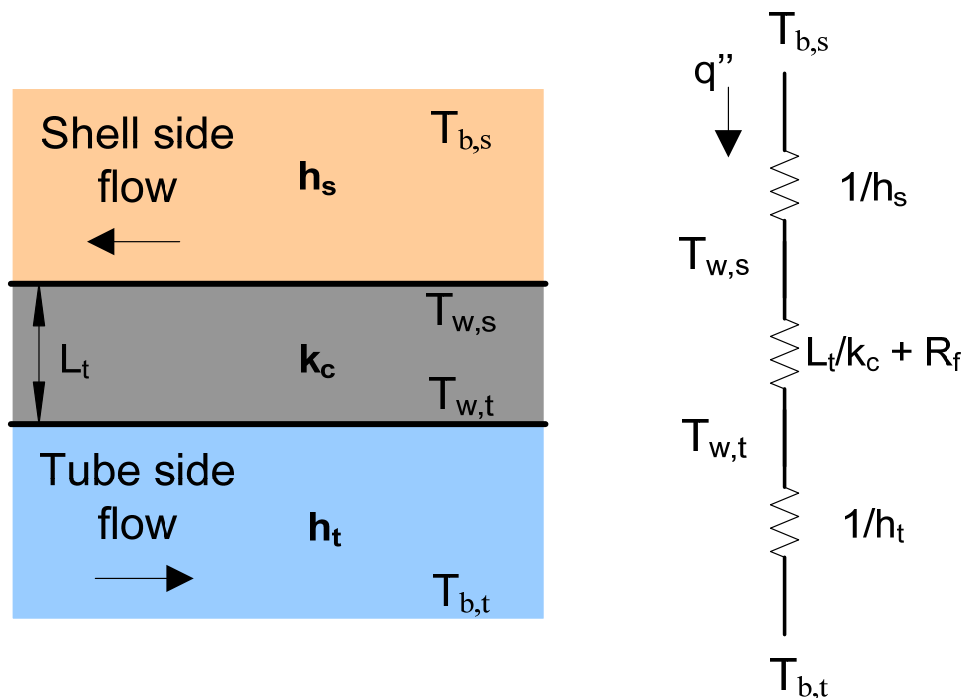


Figure 2.8: Heat transfer between the two fluids represented by thermal resistances.

In the application of heat exchangers the overall heat transfer coefficient U , must be derived on the basis of either the tube side or the shell side surface area. The determination of the twisted tube area is very complex to solve analytically because the perimeter length of an ellipse can only be calculated by mathematical series. Calculation of the area is not performed here. However the area can be determined numerically by a computer program. Computer software for heat exchanger design determines both the area and the overall heat transfer coefficient. In order to achieve accurate heat transfer calculations the software need to use correlations for the convective heat transfer coefficients. Correlations for the shell side and tube side convection coefficients in twisted tube heat exchangers are presented in the following introduced by a section about temperature influence on fluid properties.

Influence of temperature dependent fluid properties

This section is based on [10].

Fluid properties are dependent on temperature to a variable extent. This change of properties must be accounted for when developing correlations for heat transfer rate. The temperature dependent property problem is further complicated by the fact that the properties of different fluids behave differently with temperature. The specific heat of gases is almost constant with temperature, while viscosity and thermal conductivity increase to the 0,8 power of the absolute temperature. Speaking of liquids the thermal conductivity is independent of temperature, while viscosity decreases very markedly with temperature.

There are different approaches for mathematical modeling of these changes. The property ratio scheme involves a correction for both liquids and gases. For liquids where the viscosity variation is responsible for most of the effect, equations of the following form gives a good approximation.

$$\frac{Nu}{Nu_{CP}} = \left(\frac{\mu_w}{\mu_b} \right)^m \quad (2.18)$$

where the subscript CP refers to the appropriate constant-property solution. Petukhov has examined heat-transfer data covering these ranges: Pr=2-140; Re=5000-123000; $\mu_w/\mu_b=0,025-12,5$ and found that appropriate values for m is the following.

$$\mu_w/\mu_b > 1, \quad m = -0,25 \text{ (cooling)}$$

$$\mu_w/\mu_b < 1, \quad m = -0,11 \text{ (heating)}$$

For gases the temperature dependent property effects can be correlated by

$$\frac{Nu}{Nu_{CP}} = \left(\frac{T_w}{T_b} \right)^n \quad (2.19)$$

The following values for n are recommended after evaluation of experiments done for gases.

$$T_w/T_b > 1, \quad n = -0,5 \text{ (heating)}$$

$$T_w/T_b < 1, \quad n = 0,0 \text{ (cooling)}$$

When evaluating the following correlations found for convection coefficients in twisted tube heat exchangers, they are compared to the above temperature and viscosity ratios in order to verify under which conditions the correlations apply. The following correlations for heat transfer coefficients and pressure drop applies for smooth surfaced twisted tube bundles.

Shell side convection coefficient

Correlations for shell side convection coefficient is based on [4].

The following correlations for convection coefficients are found experimentally by the russian researcher B.V Dzyubenko. He used electricity to heat the twisted tubes. The heated fluid was air flowing on the shell side of the test unit. The following correlations are therefore valid for heating of the shell side fluid. For *developed turbulent flow* ($x/d_h > 14$) experiments resulted in the following expressions for the shell side convection coefficient.

$$Nu_{(x),s} = 0,0023 Re^{0,8} Pr^{0,4} [1 + 3,6 Fr^{-0,357}] \left(\frac{T_{w,s}}{T_{b,s}}\right)^{-0,55} \quad (2.20)$$

For $Fr = 232 - 2440$

$$Nu_{(x),s} = 0,0521 Re^{0,8} Pr^{0,4} \left(\frac{T_{w,s}}{T_{b,s}}\right)^{-0,55} \quad (2.21)$$

For $Fr = 64$

For *developing turbulent flow* ($x/d_h < 14$) Dzyubenko came to the following result for shell side convection

$$Nu_{(x),s} = 83,5 Fr^{-1,2} Re^n Pr^{0,4} \left(\frac{T_{w,s}}{T_b}\right)^{-0,55} \left[1 + \frac{3,6}{Fr^{0,357}}\right] \quad (2.22)$$

where the exponent n for

$Fr_M < 924$	$n = 0,212 Fr^{0,194}$
$Fr_M > 924$	$n = 0,8$

It is observed that the temperature ratio exponents in (2.20), (2.21) and (2.22) are in agreement with the value -0,5 recommended for n in equation (2.19). In the scientific article "Testing of Twisted-Tube Exchangers in Transition Flow Regime" by Blazo Ljubicic it is described how experiments are done at the Heat Transfer Research Incorporated testing facility. The experimental set up, a closed loop system, included three twisted-tube exchangers in series. One exchanger operated as a heater, the second as a cooler while the third exchanger operated as an inter-changer. The test fluid circulated on the shell-side in all exchangers, and the service fluids, condensing steam and cooling water, circulated through the tubes. The experiments resulted in the following general correlation for the shell side convective heat transfer coefficient [3].

$$Nu_{(x),s} = C_{h/c} \cdot Re^{m_1} \cdot Pr^{0,4} \Phi^{m_3} \cdot \left(\frac{\mu_b}{\mu_w}\right)^{0,14} \quad (2.23)$$

where

$C_{h/c}$ Two different constants depending if the shell side fluid is heated or cooled
 Φ Swirl flow parameter
 $\mu_{b/w}$ Viscosity in the bulk flow and at the wall respectively

The Reynolds number and swirl flow exponents are unfortunately not given in the article. While Dzyubenko states that his correlation apply for heating of gases, Ljubicic does not specify the application of correlation (2.23). By comparing this equation to the temperature and viscosity ratios in (2.18) and (2.19) it is concluded that the Ljubicic equation applies for heating of liquids on the shell side of twisted tube heat exchangers.

Tube side convection coefficient

The article "Coefficients of Heat Transfer and Hydraulic Drag of a Twisted Oval Tube" by L. A. Asmantas investigates both tube side heat transfer and pressure drop. By analyzing data from tests done on tubes with a twist pitch of 6,2 and 12,2 the researchers ended up with the following tube side heat transfer correlation

$$Nu_{(x),t} = 0,021 Re^{0,8} \cdot Pr^{0,4} [1 + 3,74(s/d_{\max})^{-1}] \left(\frac{T_{w,t}}{T_{b,t}}\right)^n \quad (2.24)$$

where

$$n = -0,17 - 0,27 \cdot 10^{-5} (x/d)^{1,37} [(s/d)^{2,1} - 109,6]$$

and x denotes the distance from the tube entrance. Since the temperature ratio is present in (2.24) it applies for gases and not for liquids. It is not specified in the article whether the correlation holds for heating or cooling.

Equation (2.20), (2.21), (2.22), (2.23) and (2.24) are correlations for the *local* Nusselt number being a function of x. In order to find the average Nusselt number one must both integrate the equation over the tube length L and divide the result with the same parameter. The conversion from local to average Nusselt number can be done by solving the following integral.

$$Nu_{av} = \frac{1}{L} \int_{x=0}^L Nu_{(x)} dx \quad (2.25)$$

For comparison tube side Nusselt number for a *circular* tube is also presented here. The following equation is developed by Sieder and Tate for turbulent tube flow[11].

$$Nu_{(x),t} = 0,027 Re^{4/5} \cdot Pr^{1/3} \left(\frac{\mu_b}{\mu_w}\right)^{0,14} \quad (2.26)$$

valid for

$$\begin{aligned} 0,7 < Pr < 16000 \\ Re_D > 10000 \\ L/D > 10 \end{aligned}$$

2.3.3 Mathematical modeling of the pressure drop

The pressure drop in a heat exchanger is an important concern. In heat exchanger design a high pressure drop result in a higher required pump power leading to increased operation costs. In addition the heat transfer rate can be influenced significantly by the saturation temperature change for a condensing/evaporating fluid if there is a large pressure drop associated with the flow. This is due to the fact that saturation temperature changes with differences in saturation pressure and in turn affects the temperature potential for heat transfer.

There are two main contributions to the pressure drop: pressure drop associated with the core and pressure drop associated with fluid distribution devices such as inlet/outlet headers, manifolders, tanks, nozzles, ducting and so on. The task of the heat exchanger is to transfer heat from one fluid to another. It must be a certain pressure drop present in order to force the fluid past the heat exchanging surface. Therefore most of the pressure drop available should be utilized in the heat exchanger core. The total heat exchanger pressure drop can be described as follows.

$$\Delta p_{total} = \Delta p_{entrance} + \Delta p_{core} + \Delta p_{exit} \quad (2.27)$$

The calculation of entrance and exit pressure drop can be done in the same manner as for a conventional shell and tube heat exchanger. Since this report investigates twisted tube bundles in particular only the core pressure drop will be considered here. The pressure loss in a pipe/duct can be generally described in terms of Darcys friction factor [8].

$$\Delta p_{core} = f_D \frac{L}{2d_h} \rho v^2 \quad (2.28)$$

where

f_D	Darcy friction factor
L	tube length
d_h	hydraulic diameter
ρ	fluid density
v	bulk velocity

The challenge when performing pressure drop predictions is to develop an accurate expression for the friction factor. For circular tubes one can extract f_D from the famous Moody chart when the wall roughness is known. This chart does not apply to the twisted tube or the complex shaped ducts formed in the inter-tubular space. The correlation for the friction factor must therefore be developed on the basis of experiments done on twisted tube bundles.

Shell side friction coefficient

The hydraulic characteristics of twisted tube bundles have been investigated by the researcher B.V. Dzyubenko. Analysis of experimental data show that

$$f_D = \frac{0,3164}{\text{Re}^{0,25}} \left[1 + \frac{3,6}{\text{Fr}^{0,357}} \right] \quad (2.29)$$

For $\text{Fr} > 100$

$$f_D = 0,3164 \text{Re}^{-0,25} (1 + 3,1 \cdot 10^6 \text{Fr}^{-0,38}) \quad (2.30)$$

For $\text{Fr} < 100$

Correlation (2.29) and (2.30) are based on experiments that was performed on bundles with 9 and 37 tubes respectively. Therefore a significant contribution to the friction loss is associated with friction against the shell wall. Of this reason these two correlations apply best to bundles with few tubes were shell wall friction make a considerable contribution to the pressure drop. Based on the same experiments a third expression is developed. This correlation applies for the friction factor in larger bundles containing more tubes. One ends up with the following correlation for the shell wall friction.

$$f_D = 10,5 \text{Fr}^{-1,6181+0,263 \log \text{Fr}} \quad (2.31)$$

For $64 < \text{Fr} < 1052$

Tube side friction coefficient

Tube side pressure loss is investigated by L.A. Asmantas in an article "Coefficients of Heat Transfer and Hydraulic Drag of a Twisted Oval Tube" [5]. By use of his own experiments and analyzing the data a correlation for the tube side pressure loss was found.

$$f_D = 0,92 (s/d_h)^{-0,55} \text{Re}^{-0,18} \quad (2.32)$$

It is emphasized in the article that this friction factor not only includes pressure drop in the heat exchanger core flow, but also pressure losses at the inlet and exit from the twisted oval tube. This loss contribution is estimated to be from 10 to 16 percent. In other words the pressure loss is claimed to be somewhat lower in the heat exchanger core than actually predicted with this correlation. The swirl is here represented by the ratio s/d_h .

For comparison a correlation for turbulent flow in plain circular tubes are also presented here. In 1939 Colebrook combined two pipe flow correlations for smooth and rough wall. This clever combination resulted in an implicit formula that the Moody chart is based on [8].

$$\frac{1}{f_D^{1/2}} = -2,0 \log \left(\frac{\varepsilon/d}{3,7} + \frac{2,51}{\text{Re} f_d^{1/2}} \right) \quad (2.33)$$

2.4 Fouling and determination of fouling resistance R_f

This section is based on [12].

2.4.1 Fouling in general

Fouling is accumulation of unfavorable material on the heat exchanging surface. The layer can consist of crystals, sediments, rust or other substances. Fouling has two effects on the heat exchanger performance. Because the fouling layer acts as a thermal resistant, overall heat transfer coefficient will be reduced. The second effect arise from changes on the heat exchanging surface and the reduced flow area which translate into increased pressure loss. Fouling is also costly. Because it is unpredictable heat exchangers are often oversized in the design process. This means that more material and space is used in the design than necessary. In addition, fouling generates cost from cleaning and the associated loss in production.

The most important parameters that affect fouling are

- The nature of the flowing fluid, clean or dirty
- Flow velocity
- Flow temperature
- Material of construction and surface finish

The nature of the flowing fluid has large influence on an eventual development of a fouling layer. Typically a pollution free, clean fluid like steam will not form a fouling layer while heavy hydrocarbon streams foul readily and affect the thermal hydraulic performance. The choice of fluids is often given by the application and therefore in most cases the designer cannot influence this parameter.

Flow velocity has an important impact on fouling. When the flow velocity is increased the viscous sub layer close to the wall gets thinner resulting in lower resistance to diffusion from the bulk to the wall. This effect of increased velocity will tend to promote fouling. At the same time higher velocity increases the shearing forces that remove the fouled deposit. The net rate of fouling will therefore be a sum of these two opposing effects. Because the shear forces tend to increase more than the diffusion from the bulk to the wall, higher flow velocity invariably result in less fouling.

The rates of chemical reaction are a strong function of temperature. Therefore, for fouling processes caused by chemical reactions, temperature will have an important impact on the extent of fouling. Corrosion is a typical example of a chemical reaction that will be affected by temperature. Bio-fouling is also dependent on the temperature. At higher temperatures, the rates of chemical and enzyme reactions increase due to increased cell growth rate. However, there will be an upper and lower temperature limit in which a specific organism can survive.

The roughness, size, and density of cavities affect crystalline nucleation, sedimentation and the sticking tendency of deposits. Smooth surfaces have properties that make the surface less likely to receive and retain dirt than rough surfaces. Practical experience shows that smooth surfaces tend to foul less.

2.4.2 Fouling in twisted tube heat exchangers

In a conventional shell and tube heat exchanger the fluid is directed perpendicular to the tubes by baffles. The shell side fluid has to make turns around each baffle which is illustrated below. Due to the turning, flow velocity is lower at the outer curve than at the inner curve resulting in an uneven flow distribution. Uneven flow distribution is unfavourable because such flow may contain dead spots where the velocity is very low. As mentioned in the previous section the risk of fouling is increased at locations where the velocity is low and where extreme temperatures arise.

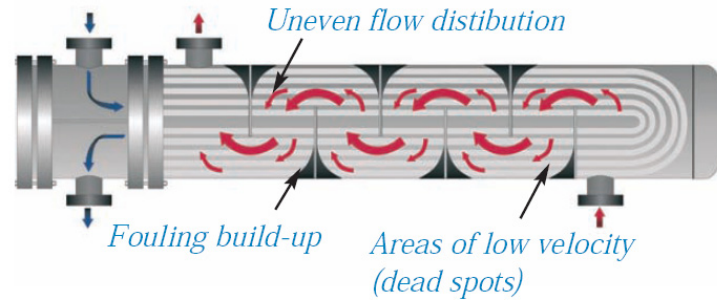


Figure 2.9: Shell side flow pattern in a conventional shell and tube

The illustration below shows the shell side flow pattern on a twisted tube heat exchanger. Because the flow is evenly distributed on the cross section and not forced to do turns, one achieves a uniform flow without dead spots. The twisted tube also has an advantage on tube side fouling. Increased turbulence and absolute velocity result in less risk of fouling inside the twisted tubes compared to plain tubes.

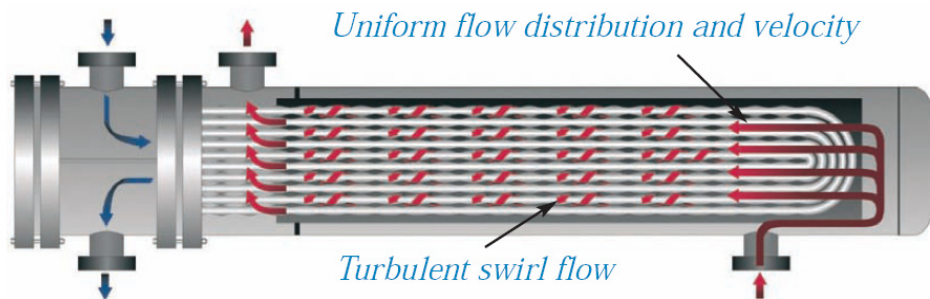


Figure 2.10: Shell side flow pattern in a twisted tube

2.4.3 Fouling resistance R_f

Prediction of the fouling factor R_f is a part of the calculation process for the overall heat transfer coefficient. The thermal resistance caused by fouling can be determined either by mathematical models or empirical data. The vendor uses the discussion presented in section 2.4.2 to explain how the twisted tube is less exposed to fouling compared to the conventional alternative. How a twisted tube heat exchanger performs in terms of fouling can be evaluated by investigation of the overall heat transfer coefficient. In Chapter 5 the fouling tendency is investigated by analyzing measurements performed on a twisted tube heat exchanger in operation. How the twisted tube performs compared to other heat exchanger designs is discussed in Chapter 6.

2.5 Flow induced vibration

2.5.1 Flow induced vibration in heat exchangers

This section is based on [12].

Consideration of tube vibration is an important concern when designing a shell-and-tube heat exchanger. Many exchangers have failed as a result of flow induced vibrations. A good example is the vibration problems that StatoilHydro face on their LNG production facility at Hammerfest, Norway.

Heat exchanger tubes often vibrate, but at such low frequencies that there is no damage. The lowest frequency at which tubes vibrate is the natural frequency. Higher natural frequencies are known as the second mode, third mode, and so on. The natural frequency depends on a number of factors.

- the way they are fixed
- the nature of the intermediate supports
- the length of the unsupported span
- number of spans
- tube material and thickness

The following formula for prediction of the natural frequency is developed by MacDuff and Felgar.

$$f_n = 0,04944C_n \sqrt{\frac{EIg}{W_e L_{un}^4}} \quad (2.34)$$

where

f_n	natural frequency of straight tubes
C_n	frequency constant
E	modulus of elasticity
I	sectional moment of inertia
g	gravitational constant
W_e	effective weight per unit tube length including the weight of the fluid inside tubes
L_{un}	tube unsupported span

Investigating the above equation one observe that some parameters have more influence on the tube natural frequency than others. While the frequency depends on the unsupported span in the power of two, the other equation parameters influence the natural frequency in the power of 0,5. It means that the only parameter left than can be controlled and affect the natural frequency is the unsupported span.

The tube vibration phenomena are vortex shedding, turbulent buffeting, and fluidelastic whirling. These phenomena have in common that they generate pressure variations at certain frequencies. The frequencies depend on parameters such as cross flow velocity and tube diameter. If one of these frequencies is equal to the tube natural frequency there is a high probability for resonance, leading to severe tube vibration. Such vibration will with time lead to a failure in one or several tubes. The most common reasons are rupture caused by interaction between tubes and baffles, but fatigue and tube joint leakage is also frequently experienced.

By prediction of the natural frequency and the vibration frequencies one can prevent failure caused by flow induced vibration. If the vibration frequencies are close to the natural

frequency it is necessary to reduce the unsupported span of the tubes. This will solve the problem because the natural frequency increases more than the vibration frequencies.

2.5.2 Reduced risk for flow induced vibration in twisted tube bundles

Based on the theory for flow induced vibration presented in the previous section, one can qualitatively compare the twisted tube heat exchanger to baffle based designs. The most important point is that the twisted tube bundle is a very rigid construction. Each tube is supported by the adjacent tubes six times per 360 degree twist. Consideration of a twisted tube with a twist pitch to diameter ratio equal to 6 and an outer diameter of 24mm will give an unsupported span of 24mm. A conventional shell and tube exchanger will typically have a baffle spacing of 500mm. By strengthening the bundle with 4 support baffles per baffle set and choosing a no tubes in window configuration result in an unsupported tube span of 100mm. Even by using such design tools to prevent vibration in the conventional design the span is larger than for the twisted tube by a factor of four. Using equation (2.34) this translates into a difference in natural frequency by a factor sixteen in favour of the twisted tube. This example illustrates the stiffness of a twisted tube bundle.

In addition to the reduced unsupported span, the twisted tube design has one more feature that is advantageous with respect to vibrations. All the flow induced vibration phenomena is dependent on a flow velocity perpendicular to the tubes. Since the shell side flow is in the axial direction of the twisted tubes there is no basis for these phenomena to grow in strength and to increase frequency. Summarized the twisted tube is less subject to vibration problems because of the stiffness of the bundle and the flow direction on the shell side. Therefore the vendors of these heat exchangers can claim that the design is vibration free.

2.6 Applications

The twisted-tube exchanger meets the requirements of the design codes TEMA and API 660. It can therefore in most cases be used as a replacement for the conventional shell-and-tube exchanger. In addition the twisted-tube has features this far only found in plate exchangers, and can therefore to some extent replace this type of heat exchangers. Several hundred twisted-tube exchangers have been manufactured since 1984 for various applications. The table below show which industries that have been provided with twisted tube solutions.

Industry	Application
Chemical	Sulphuric acid cooling
	Ammonia preheating
	Hydrogen peroxide cooling/heating
Petroleum	High pressure gas heating/cooling
	Oil heating
	Bitumen heating
	LNG heating
Pulp & paper	Black liquor heating/cooling
	Whit water cooling
	Oil heating/cooling
	Effluent cooling
Power	Turbine steam condensing
	Boiler feedwater heating
	Lube oil cooling
Steel	Quench oil cooling
	Lube oil cooling
	Compressed gas cooling
Mining & mineral processing	Liquor cooling
	Effluent cooling
District heating	Closed loop water heating
	Steam heaters

Table 2.1: List of twisted tube deliveries [13]

2.7 Industrial experience, operation and maintenance

This section is based on reference [14] and [1].

The information is found on Siljan Allards and Koch Heat Transfer web sites respectively. When reading the following one must keep in mind that the text is based on information provided by the vendors of the twisted tube heat exchanger. The statements may be coloured by their incentives to sell this type of equipment.

2.7.1 Industrial experience

The Swedish company Siljan Allards AB has produced twisted tube heat exchangers since the beginning of 1980's. Siljan Allards name their concept Alfatwist. In total 700 exchangers of this type has been delivered to the power, paper, chemical, pharmaceutical and food manufacturing industry. Siljan Allards claim a very high customer satisfactory due to reduction of fouling and elimination of vibration problems.

As an example the Swedes mention a delivery to a large vehicle plant. They had substantial problems with fouling on the tube side of heat exchangers with plain tubes. After installation of twisted tube heat exchangers, the fouling problem was reduced due to intensification of the tube side turbulence. In the same reference list it is mentioned a twisted tube exchanger that replaced a shell and tube heat exchanger in 1983 due to vibration problems. The twisted tube exchanger still operates 24 years later when the reference list was written in December 2007. Siljan Allards has many of these success stories to tell about their Alfatwist concept.

In addition to a vibration free concept the vendors claim that the heat exchanger has higher heat transfer performance and lower pressure drop than a conventional shell and tube. These statements will be investigated by use of measured data and the computer program HTRI in Chapter 6, page 56.

2.7.2 Cleaning

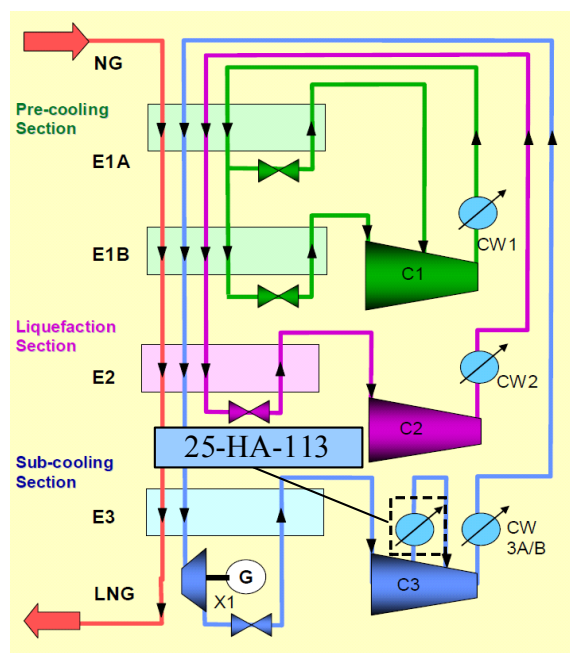
Cleaning may be performed on the heat exchanger in place. Chemical cleaning in place is claimed to be more effective in twisted tube heat exchangers than in conventional shell and tube due to uniform flow distribution and swirl flow. Another way of doing maintenance is by removing the twisted tube bundle from the outer shell. Lanes formed by the tubes allow complete mechanical cleaning by hydro blasting on the shell side. This may be more difficult for a conventional shell and tube because the tubes will form a wall such that the core tubes are not cleaned. The tube side in a twisted tube can also be cleaned effectively by hydro blasting due to the induced swirl flow and high turbulence.

3 Field measurements on HA-25-113

3.1 Background

This section is based on [15].

LNG Hammerfest is a facility for liquefaction of natural gas. The plant is located on the island Melkøya which is situated outside the city of Hammerfest at the northern end of Norway. The facility has been in operation since August 2007 and the production capacity of is about 4,3 million tonnes per year. This corresponds to approximately 5,6 billion m³ of LNG. Natural gas is supplied through pipelines from the gas fields Snøhvit, Albatross and Askeladd in the Barents Sea about 140 km north-west of Hammerfest.



The liquefaction unit is the heart of Hammerfest LNG plant. It consists of three systems that together convert the incoming natural gas at 12 °C to a liquid at a temperature of -163 °C. The system names; Pre-cooling, liquefaction and sub-cooling indicate their roles in the cascade process. Each system is a refrigeration circuit that make use of powerful compressor units to elevate the pressure. This pressure elevation followed by aftercooling and expansion results in very low temperatures. The compression in the *sub-cooling* system is done in two steps. The 25-HA-113 twisted tube heat exchanger is installed in between these two stages as an intercooler (See Figure 3.1). The task of the heat exchanger is to cool the refrigerant in order to save work in the second compressor stage.

Figure 3.1: Process diagram of gas liquefaction

The refrigerant is a mix of methane, ethane, propane and nitrogen gas which is connected to the shell side of the heat exchanger. This hydrocarbon based refrigerant is from now on referred to as HC gas because it is not acting as a refrigerant in the intercooling process. To save as much compressor work as possible it is important that the shell side pressure loss is minimized and that the HC gas is cooled as much as specified in the design. The tube side flow is seawater which is served by the plant cooling water system.

When the plant was finished in August 2007 a helical baffled shell and tube heat exchanger was installed on 25-HA-113. The design was developed by Lummus Technology Heat Transfer B.V. After approximately a year in operation the unit had a broke down as a result of tube vibration. The heat exchanger was replaced in October 2008 by a twisted tube type shell and tube heat exchanger. This heat exchanger was delivered by Koch Heat Transfer Incorporated and the design was promised to be substantially more vibration resistant than the former helical baffled unit. The twisted tube is successfully in operation when this report is written^I. Reliability of the unit is important because a heat exchanger breakdown may be very costly. A shut down of the plant translate into an economic expense of approximately 40 million NOK per day as a result of the lost LNG production^{II}.

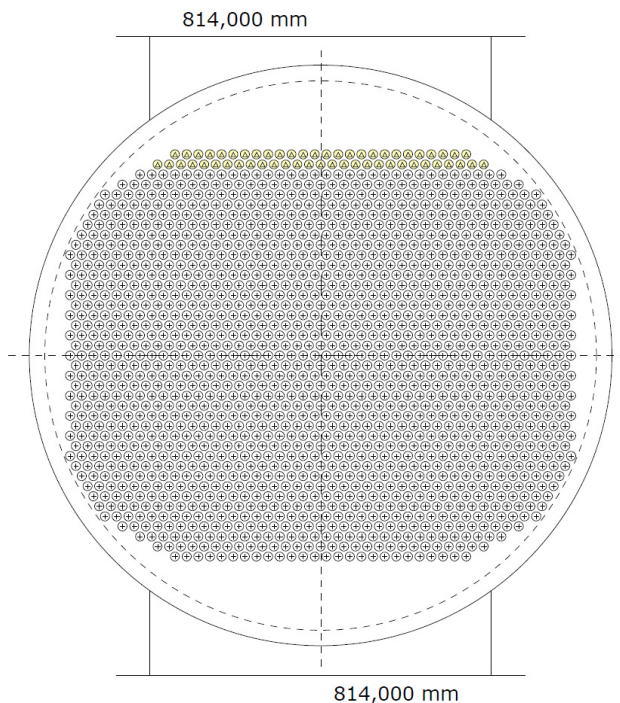
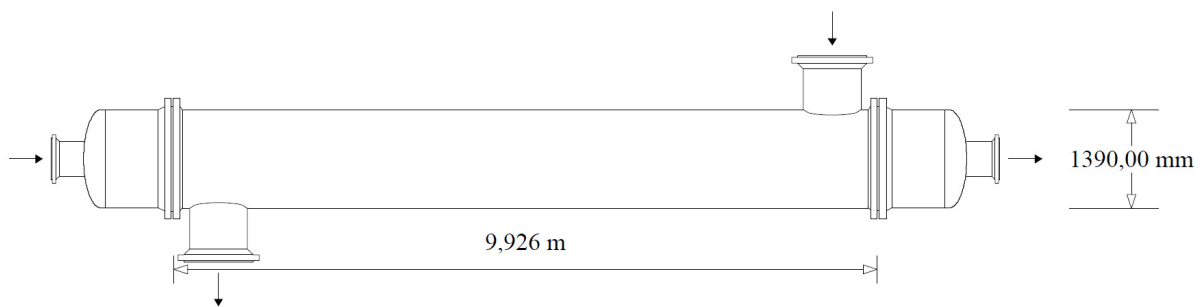
^I June 2009

^{II} Based on a gas price per May 1, 2009

3.2 Koch twisted tube solution

Koch Heat Transfer Inc. has supplied the twisted tube heat exchanger solution. A design basis was handed over to their engineers so they could develop the design. This design basis can be found in PIM^{III} on document number E066-AB-P-DP-2546 [16] and technical drawings of the twisted tube solution can be found in Appendix E. The result of the design process was the heat exchanger described below.

Baffle type: none
 Tube type: twisted
 Twist pitch: unknown
 d_{max}/d_{min} : unknown
 Bundle material: titanium



Item number	25-HA-113
TEMA type	BEM
Shell diameter	1390,00 mm
Outer tube limit	1315,65 mm
Height under inlet nozzle	171,082 mm
Rows of impingement rods	2
Impingement rod diameter	19,050 mm
Height under outlet nozzle	197,276 mm
Tube diameter	22,225 mm
Tube pitch	27,781 mm
Tube layout angle	60
Number of tubes (specified)	1589
Number of tubes (calculated)	1589
Number of tie rods	0
Number of seal strip pairs	0
Number of passes	1
Baffle cut % diameter	0

TUBEPASS DETAILS			
Pass	Rows	Tubes	Plugged
1	39	1589	0

SYMBOL LEGEND	
○	Tube
●	Plugged tube
⊙	Tie rod
⊗	Impingement rod
⊕	Dummy tube
●	Seal rod
□	Seal strip/Skid bar

^{III} See Abbreviations p.xviii

Investigation of a twisted tube type shell-and-tube heat exchanger

HTRI		HEAT EXCHANGER SPECIFICATION SHEET				Page 1	
						SI Units	
Customer		Linde AG for Statoil AS		Job No.			
Address				Reference No.		8422-25HA113-00	
Plant Location		Hammerfest LNG Plant		Proposal No.		8422r/07	
Service of Unit		Subcooling Cycle Compressor Intercooler		Date		05.08.2008 Rev 0	
Size		1390,00 x 9926,00 mm		Type		BEM	
Surf/Unit (Gross/Eff)		1102,64 / 1070,87 m ²		Horz.		Connected In	
				Shell/Unit		1	
				Surf/Shell (Gross/Eff)		1102,64 / 1070,87 m ²	
PERFORMANCE OF ONE UNIT							
Fluid Allocation		Shell Side			Tube Side		
Fluid Name		N2/C1/C2 HC Refrigerant			Sea Water		
Fluid Quantity, Total		kg/hr			500206		
Vapor (In/Out)		500206			500206		
Liquid					1590428		
Steam					1590428		
Water							
Noncondensables							
Temperature (In/Out)		C			61,90 10,00		
Specific Gravity					1,0267 1,0243		
Viscosity		mN-s/m ²			0,0120 0,0110		
Molecular Weight, Vapor							
Molecular Weight, Noncondensables							
Specific Heat		kJ/kg-C			2,1000 2,0400		
Thermal Conductivity		W/m-C			0,0350 0,0282		
Latent Heat		kJ/kg					
Inlet Pressure		kPa			1884,03 610,009		
Velocity		m/s			13,54 1,26		
Pressure Drop, Allow/Calc		kPa			70,001 81,352		
Fouling Resistance (min)		m ² -K/W			0,000180		
Heat Exchanged W		14917752			MTD (Corrected) 17,7 C		
Transfer Rate, Service		787,18 W/m ² -K			Clean 1176,56 W/m ² -K		
					Actual 940,55 W/m ² -K		
CONSTRUCTION OF ONE SHELL				Sketch (Bundle/Nozzle Orientation)			
		Shell Side		Tube Side			
Design/Test Pressure		kPaG		2500,04 / 1750,03 /			
Design Temperature		C		140,00 50,00			
No Passes per Shell		1		1			
Corrosion Allowance		mm					
Connections		In mm		1 @ 814,000 1 @ 488,000			
Size & Rating		Out mm		1 @ 814,000 1 @ 488,000			
		Intermediate		@ @			
Tube No.		1591		OD 22,225 mm		Thk(Avg) 1,734 mm	
Tube Type		Twisted		Length 9,926 m		Pitch 27,781 mm	
Shell		ID 1390,00 mm		Material		TITANIUM-GRADE 2	
Channel or Bonnet		Shell Cover		Channel Cover			
Tubesheet-Stationary		Tubesheet-Floating		Impingement Plate		Rods	
Baffles-Cross		Type NONE		%Cut (Diam)		Spacing(c/c) 9640,02	
Baffles-Long		Seal Type		Inlet mm			
Supports-Tube		U-Bend		Type			
Bypass Seal Arrangement		Tube-Tubesheet Joint		Expansion Joint		Type	
Rho-V2-Inlet Nozzle		4555,05 kg/m-s ²		Bundle Entrance		Bundle Exit kg/m-s ²	
Gaskets-Shell Side		Tube Side		-Floating Head			
Code Requirements		TEMA Class					
Weight/Shell		26877,8		Filled with Water 45059,5		Bundle 10074,7 kg	
Remarks: Case 03							
Note: Reported duty and flow rates include a user-specified multiplier of 1.05. Reprinted with Permission (v5 SP2)							

Figure 3.2: TEMA specification sheet for Koch twisted tube design printed from HTRI

3.3 Automatically logged measurements on 25-HA-113

The LNG Hammerfest plant is monitored continuously from the control room at the site. Hundreds of installed thermometers, pressure transducers and flow meters make sure that the operators are well informed about the state in the process at all times. Each unit perform measurements at a certain frequency that is saved electronically in a database. In this way the entire plant process history is available for evaluation and analysis.

On 25-HA-113 there are several thermometers installed at the HC gas inlet and outlet. Pressure of the HC gas is measured by two pressure transducers on the inlet and outlet respectively while HC gas flow is measured by a flow meter based on the venturi principle. In order to determine the heat exchanger duty it is also necessary to know the gas composition. This is measured by gas chromatography. Physical properties of the HC gas are then calculated by use of the GERG08 which is a highly accurate equation of state. Heat exchanger duty can then be determined by the calculated enthalpy and the measured flow.

The seawater temperatures are also logged, but no flow meter is installed on this side. However, seawater flow can be determined by the other measured quantities. This is simply done by a heat balance calculation dividing the duty by seawater temperature difference and specific heat capacity. It is important to keep in mind that the seawater flow is only a result of GERG08 property calculations and is not measured directly. Measurements used for the analysis of 25-HA-113 are performed from 26.october 2008 to 2.february 2009 and can be found in Appendix B. The table below show the installed equipment that collected data for the analysis performed in this master thesis.

Tag number	Property	Manufacturer	Position
25-TI-1799A	Temperature	ABB	HC gas inlet
25-TI-1799B	Temperature	ABB	HC gas inlet
25-TI-1799C	Temperature	ABB	HC gas inlet
25-TI-1573	Temperature	ABB	HC gas inlet
25-TI-1330	Temperature	ABB	HC gas outlet
25-TI-1431	Temperature	ABB	HC gas outlet
25-TI-1039	Temperature	ABB	HC gas outlet
55-TI-1049A	Temperature	ABB	Seawater inlet
85-TI-2011	Temperature	ABB	Seawater outlet
85-PI-2013	Pressure	ABB	HC gas inlet
85-PI-2014	Pressure	ABB	HC gas outlet
25-FI-1416	Flow	Dosch	HC gas outlet
25-FI-1308	Flow	Dosch	HC gas outlet
25-AI-1387A1	CH ₄ content	ABB	HC gas closed loop
25-AI-1387B1	C ₂ H ₆ content	ABB	HC gas closed loop
25-AI-1387C1	C ₃ H ₈ content	ABB	HC gas closed loop
25-AI-1387D1	N ₂ content	ABB	HC gas closed loop
25-AI-1868A1	CH ₄ content	ABB	HC gas closed loop
25-AI-1868B1	C ₂ H ₆ content	ABB	HC gas closed loop
25-AI-1868C1	C ₃ H ₈ content	ABB	HC gas closed loop
25-AI-1868D1	N ₂ content	ABB	HC gas closed loop

Table 3.1: List of sensors that collect measurement data used in this report

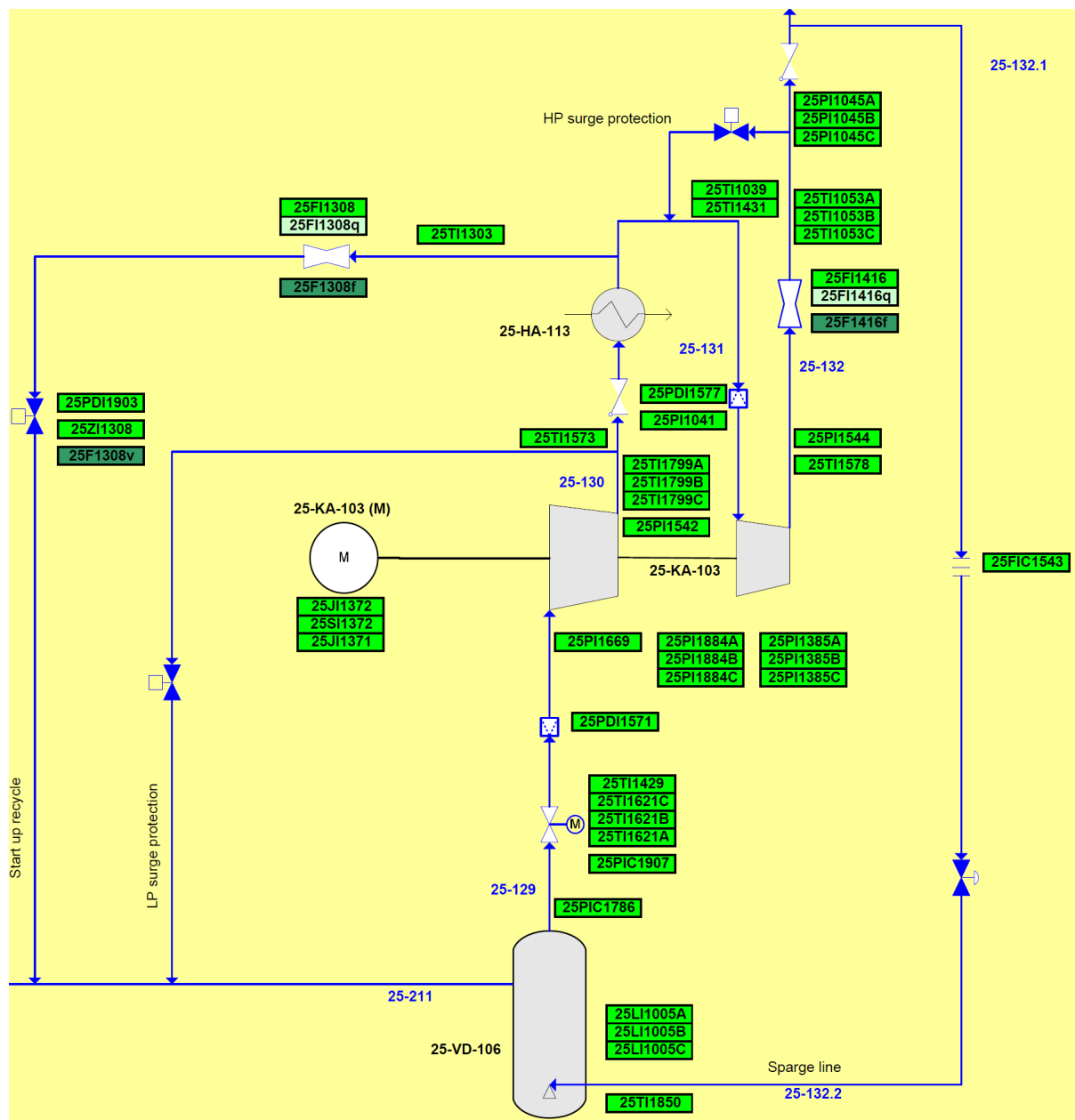


Figure 3.3: Process arrangement around 25-HA-113

The illustration above shows the process arrangement around the twisted tube heat exchanger 25-HA-113. Flow measurements are performed at 25FI1416 down stream of compressor stage two. In some operation modes valve 25ZI1308 is open. The flow through 25-HA-113 is then equal to the sum of measured flows in both 25FI1416 and 25FI1308.

StatoilHydro has performed an analysis on the energy balance by use of the computer program Hysys. It turns out that there is a deviation between the delivered compressor work from 25-KA-103 calculated by Hysys and the compressor work measured on the site. The flow measurement of HC gas is as already mentioned performed downstream of compressor stage two. StatoilHydro believe that a possible leakage in the closed valve 25ZI1308 may be the reason why the calculated work is not in agreement with measurements. A leakage here means that the flow of HC gas is actually larger through the first compressor stage and heat exchanger 25-HA-113 than measured by the flow meter. If such leakage flow is discovered it

means that the heat exchanger duty is larger in reality than indicated by measured data. This is an additional uncertainty to the measurements. Analysis performed by Tor Erling Sandvik at StatoilHydro show that the leakage is 5-15 tonnes/hr. Considering an average flow measured through 25F11416 of 524 tonnes/hr this leakage will result in a increased real flow and duty by maximum 2,9%.

3.4 Measurement uncertainty

This section is based on [17] and [18].

Measurement of a physical quantity involves consideration of the associated uncertainty. Prediction of the uncertainty requires that a certain confidence interval is specified. The confidence interval depicts the probability of a measured value to be within an upper and a lower limit. Normally a confidence level of 95% is used in uncertainty analysis. Therefore this level of confidence is also chosen in the following evaluation.

3.4.1 The root sum square formula (RSS)

A formula that is very often used in uncertainty analysis is the Root-Sum-Square (RSS). The derivation of this formula will be shortly presented here. We initiate the derivation by defining a general known mathematical function

$$F = f(x_1, x_2, \dots, x_n) \quad (3.1)$$

F is a function of the independent variables $x_1, x_2, x_3, \dots, x_n$. These variables are the measured values. Because of uncertainties associated with the measurements there will be a deviation between the real value and the measured value denoted by Δx . These deviations will lead to a change in F denoted by ΔF . This can be mathematically described by

$$F + \Delta F = f(x_1 \pm \Delta x_1, x_2 \pm \Delta x_2, \dots, x_n \pm \Delta x_n) \quad (3.2)$$

The right hand expression above can be developed by a Taylor series. Terms of higher order than one are neglected. Equation (3.2) can therefore be written as

$$F + \Delta F = f(x_1, x_2, \dots, x_n) + \frac{\partial f}{\partial x_1} \cdot \Delta x_1 + \frac{\partial f}{\partial x_2} \cdot \Delta x_2 + \dots + \frac{\partial f}{\partial x_n} \cdot \Delta x_n \quad (3.3)$$

By subtraction of (3.3) by (3.1) one obtain

$$\Delta F = \left| \frac{\partial f}{\partial x_1} \cdot \Delta x_1 \right| + \left| \frac{\partial f}{\partial x_2} \cdot \Delta x_2 \right| + \dots + \left| \frac{\partial f}{\partial x_n} \cdot \Delta x_n \right| \quad (3.4)$$

The above expression will calculate the largest possible ΔF for the given measured parameters $x_1, x_2, x_3, \dots, x_n$. This expression anticipates that all the measured values will contribute to either an increase or a decrease of ΔF . In reality the measurements will both give a positive and a negative contribution and thereby to some extent cancel each other. It has been shown that the right way to express ΔF as a function of Δx is the following.

$$\Delta F = \pm \sqrt{\left(\frac{\partial f}{\partial x_1} \cdot \Delta x_1 \right)^2 + \left(\frac{\partial f}{\partial x_2} \cdot \Delta x_2 \right)^2 + \dots + \left(\frac{\partial f}{\partial x_n} \cdot \Delta x_n \right)^2} \quad (3.5)$$

This is called the Root-Sum-Square formula and is a widely used in error analysis.

3.4.2 Absolute error

In measurement theory it is common to divide the measurement error into systematic and random error. The systematic error is the constant deviation from the true value for a repeated measurement done by the same operator under the same environmental conditions. The random error is by nature random and unpredictable. Typically random errors are round-off errors, operator errors and errors caused by small changes in environmental conditions. While determination of the systematic error requires analysis of the calibration procedure and equipment, calculation of the random error is a matter of statistical analysis. Absolute error is the true error that depends on both systematic and random error. Mathematically the relation between absolute, systematic and random error can be presented in the following way.

$$w_x = \sqrt{B_x^2 + P_x^2} \quad (3.6)$$

where

W_x absolute uncertainty
 B_x systematic uncertainty
 P_x random uncertainty

3.4.3 Random error

The random uncertainty is dependent on the standard deviation of the measurements, number of readings in the sample and the statistical Student's t-distribution. Compared to the Normal distribution the Student's t is a wide probability function that includes the uncertainty associated with small sample sizes. Because the sample sizes considered here are less than 30 the Student's t is an appropriate probability distribution. The random error can be calculated with the following equation.

$$P_x = \pm t \frac{S_x}{\sqrt{n}} \quad (3.7)$$

where

t value of Student's t for 95% confidence interval and a certain sample size
n sample size
 S_x standard deviation of the sample

$$S_x = \left(\frac{\sum_{i=1}^n (x_i - \bar{x})^2}{(n-1)} \right)^{1/2} \quad (3.8)$$

3.4.4 Systematic error

The systematic uncertainty remains constant if the test is repeated under the same conditions. From a statistical point of view the systematic error is the constant deviation between the true value and the population mean. The population mean is the mean of an infinite sample size from the actual measurement set up. Systematic uncertainties include errors which are known or can be estimated but have not been eliminated through calibration or the measurement process itself.

The most practical method of systematic error determination is by combining elemental uncertainties. Different types of elemental errors can be generated in each component in a measurement system. ASME^{IV} suggests grouping the elemental errors into five categories: calibration uncertainties, data-acquisition uncertainties, data-reduction uncertainties, uncertainties due to methods, and other uncertainties. Data-acquisition uncertainties need further explanation. This kind of uncertainty arises when a specific measurement is made. Among the errors produced is random variation of the measurand, installation effects such as measurand loading, analog-to-digital converter uncertainties and uncertainties in recording or indicating devices.

By using the elemental error approach the systematic error can be estimated by the following formula.

$$B_x = \sqrt{B_c^2 + B_{da}^2 + B_{dr}^2 + B_m^2 + B_o^2} \quad (3.9)$$

where

B_c	calibration uncertainty
B_{da}	data-acquisition uncertainty
B_{dr}	data reduction uncertainty
B_m	method uncertainty
B_o	other uncertainties

Manufacturers of the measuring equipment often provide information on the uncertainty, but not always in the desired form. It is common for manufacturers to supply the uncertainty descriptor called accuracy. This parameter normally includes error due to hysteresis, linearity and repeatability in addition to the assumption that the calibration is still valid. When this parameter is given it can be considered the systematic accuracy. This approach is conservative for two reasons. The accuracy is often based on a confidence higher than 95% and the repeatability error is included twice in the calculation. In the following analysis accuracy informed by the manufacturer is considered as the systematic accuracy.

^{IV} See
Abbreviation page xviii

3.4.5 Temperature measurement uncertainty

The systematic uncertainty associated with the temperature measurements can be found by use of the information provided in PIM^V. According to document E066-AB-J-DT-0001 all temperature sensors have an accuracy which agrees with IEC 751 class A. This standard specifies a tolerance for absolute deviation depending on the measured temperature. Figure 3.4 show how the tolerance is determined.

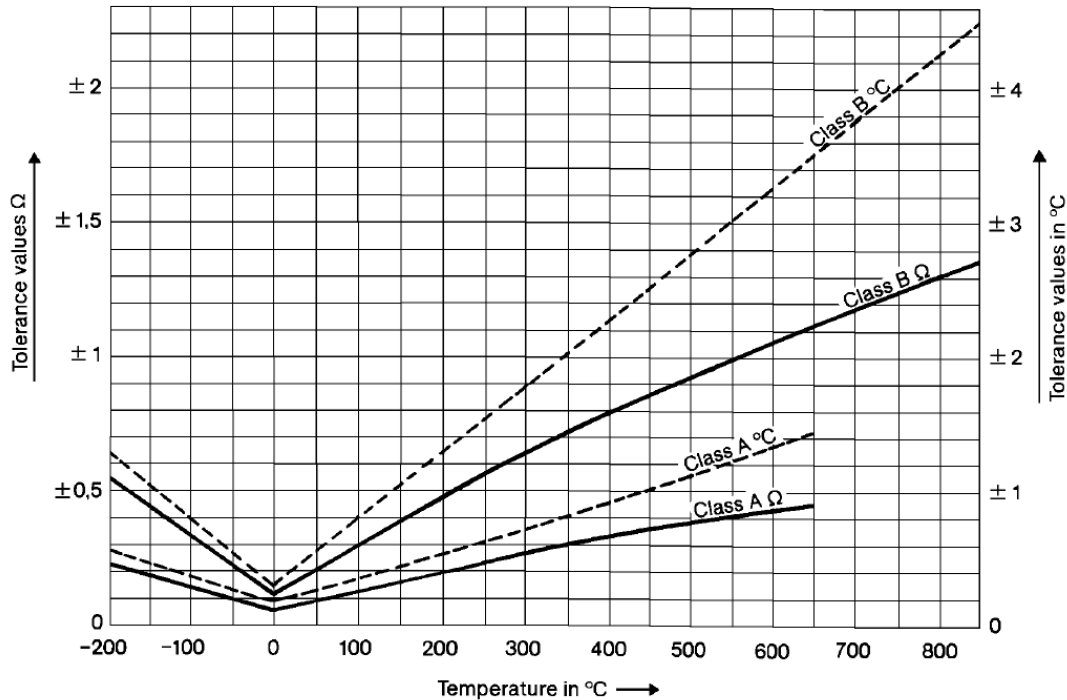


Figure 3.4: Uncertainty classes for temperature measurement, IEC 75 [19]

Using the diagram one can see that the tolerance is low for class A. One has to distinguish between the HC gas outlet/seawater temperature (10 °C) and the HC gas inlet temperature (60 °C) measurement. The diagram gives the following values for the systematic uncertainty.

$$B_x(T_{h,o}/T_c) = +/-0,20 \text{ } ^\circ\text{C}$$

$$B_x(T_{h,i}) = +/-0,30 \text{ } ^\circ\text{C}$$

The random uncertainty must also be determined in order to predict an absolute uncertainty value for temperature measurements. This is done by using equation (3.7) which includes the determination of standard deviation and student's t distribution value. The measurand, in this case the temperature, will vary with time because the operation point is not completely stable. However, a reasonable assumption is that the operation point does not change within one minute. The standard deviation is calculated based on this assumption. Some sensors transmit measurements at a higher rate than others to the electronic database. Therefore the standard deviation will also vary among the temperature sensors. Investigation of the standard deviation to three different temperature sensors resulted in the following conservative value.

$$S_x = 0,30 \text{ } ^\circ\text{C}$$

^V See Abbreviations p.xviii

The sensors register at least six temperature readings per minute. These registrations result in five degrees of freedom. For a 95% confidence interval this translates into a specific value from the student's t distribution[18].

$$t = 2,571$$

Using (3.7) one arrives at the following value for temperature random uncertainty.

$$P_x = \pm 0,31 \text{ } ^\circ\text{C}$$

Now one can determine the absolute uncertainty W_x by putting the values for systematic and random uncertainty into equation (3.6). Two different values are calculated as the systematic uncertainty varies with the measured temperature. The calculated absolute uncertainties and other key parameters are presented in Table 3.2 below.

Parameter	Value
S_x	0,30 $^\circ\text{C}$
n	6
t	2,57
B_x 10 $^\circ\text{C}$	0,20 $^\circ\text{C}$
B_x 60 $^\circ\text{C}$	0,30 $^\circ\text{C}$
P_x	0,31 $^\circ\text{C}$
W_x 10 $^\circ\text{C}$ (+/-)	0,37 $^\circ\text{C}$
W_x 60 $^\circ\text{C}$ (+/-)	0,43 $^\circ\text{C}$

Table 3.2: Temperature measurement uncertainty

As indicated in Table 3.1 there are several sensors that measure the HC gas inlet/outlet temperatures. An average of these values is used. This will lower the systematic uncertainty from the values presented here. Because it is desirable to calculate the uncertainty in a conservative way it is decided to keep the numbers presented above.

3.4.6 Pressure measurement uncertainty

The pressure sensors are of the type 2600T and manufactured by ABB. The data sheet found in PIM claims an accuracy of 0,075% of the span. Using this information and a 24 bar span one can predict the systematic uncertainty.

The random uncertainty is predicted by investigating the measurement frequency and standard deviation in the same way as for the temperature measurements. Calculated uncertainties for pressure measurement are presented in Table 3.3.

Parameter	Value
Span	24 bar
Accuracy in % of span	0,075 %
S_x	0,020 bar
n	11
t	2,228
B_x	0,018 bar
P_x	0,013 bar
$W_x (+/-)$	0,022 bar

Table 3.3: Pressure measurement uncertainty

3.4.7 Gas composition measurement uncertainty

The composition of HC gas is determined by gas chromatography at two locations in the closed circuit. No documentation on the systematic accuracy of the sensors was found in PIM. The accuracy is therefore assumed $\pm 1\%$. Investigation of the measurement frequency and standard deviation together with this assumption gave the following results.

Parameter	Value
S_x	0,13 %
n	3
t	4,303
B_x	1,00 %
P_x	0,32 %
$W_x (+/-)$	1,05 %

Table 3.4: Composition measurement uncertainty

3.4.8 Flow measurement uncertainty

Flow measurement of HC gas is performed by use of a venturi tube. Dosch messtechnik GmbH has manufactured this equipment which uses the principle of conserved energy to predict the flow rate. The tube has a narrow passage that accelerates the flow. Pressure measurements are performed at the inlet and in the constriction. Knowing the cross sectional areas at both locations the flow can be calculated. The uncertainty associated with the flow measurement must therefore be based on investigation of the pressure sensors used and how the flow is calculated from these values. Flow of HC gas is determined using the Bernoulli, continuity and area of circle equation.

$$p_1 + \frac{1}{2} \rho v_1^2 + \rho g h_1 = p_2 + \frac{1}{2} \rho v_2^2 + \rho g h_2 \quad (3.10)$$

$$\rho A_1 v_1 = \rho A_2 v_2 \quad (3.11)$$

$$A = \frac{\pi}{4} D^2 \quad (3.12)$$

By using these three equations one can express the mass flow as a function of the pressure change from inlet to the narrow passage [20].

$$\dot{m}_h = C \frac{\pi}{4} D_2^2 \sqrt{\frac{2\rho(p_1 - p_2)}{1 - D_2^4 / D_1^4}} \quad (3.13)$$

where

- C discharge coefficient
- D_1 diameter at inlet
- D_2 diameter at narrow passage

The discharge coefficient C is dependent on the geometry and the material of the venturi tube. Therefore it will be an associated uncertainty to this coefficient in addition to the pressure measurement and prediction of gas density. Until now evaluation of single measurand uncertainty is discussed. In this case the quantity we are interested in is dependent on multiple measurands. The total uncertainty can be predicted by the derived RSS formula, equation (3.5).

$$W_{m_h} = \pm \sqrt{\left(\frac{\partial \dot{m}_h}{\partial C} \cdot \Delta C \right)^2 + \left(\frac{\partial \dot{m}_h}{\partial (p_1 - p_2)} \cdot \Delta(p_1 - p_2) \right)^2 + \left(\frac{\partial \dot{m}_h}{\partial \rho} \cdot \Delta \rho \right)^2} \quad (3.14)$$

The differentiation terms in the equation (3.14) can be found by differentiation of the expression for m_h in equation (3.13) and gathering of operational values for C, $p_1 - p_2$, D_1 , D_2 and ρ . In addition one must determine the Δ -terms by investigation of uncertainty connected

to C , ρ and p_1-p_2 to find the systematic uncertainty of the flow measurement. By using PIM and information on the operation point of the heat exchanger all necessary input were found. The results are presented in the table below.

Parameter	Value
Accuracy C	0,05
Accuracy p	375 Pa
Accuracy ρ	0,22 kg/m ³
Differential C	145,60 kg/s
Differential p	0,00054 kg/sPa
Differential ρ	3,80 m ³ /s
W_x (+/-)	7,33 kg/s

Table 3.5: Flow measurement uncertainty

3.4.9 Duty measurement uncertainty

The duty of the heat exchanger is not measured directly. It is determined by the mass flow rate of HC gas and the enthalpy which is calculated by GERG08 equation of state.

$$q_h = \dot{m}_h (h_{h,i} - h_{h,o}) \quad (3.15)$$

The enthalpy is a function of temperature, pressure and gas composition. Using this information one can write the total uncertainty for the duty in the same manner as in equation (3.14)

$$W_{q_h} = \pm \sqrt{\left(\frac{\partial q_h}{\partial \dot{m}_h} \cdot \Delta \dot{m}_h \right)^2 + \left(\frac{\partial q_h}{\partial p_h} \cdot \Delta p \right)^2 + \left(\frac{\partial q_h}{\partial T_h} \cdot \Delta T_h \right)^2 + \left(\frac{\partial q_h}{\partial C_{omp}} \cdot \Delta C_{omp} \right)^2} \quad (3.16)$$

By using the thermodynamic properties in Appendix G one can calculate how enthalpy is affected by a change of pressure, temperature and composition. The term for HC gas mass flow rate can be determined by differentiating the duty with respect to mass flow rate.

Parameter	Value
Accuracy \dot{m}_h	7,33 kg/s
Accuracy p	2246 Pa
Accuracy T	0,43 °C
Differential \dot{m}_h	110,09 kJ/kg
Differential p	0,01283 J/kgPa
Differential T_h	1948,92 J/kgK
W_x (+/-)	807,04 kW

Table 3.6: Duty measurement uncertainty

3.4.10 Overall heat transfer coefficient uncertainty

The overall heat transfer coefficient is calculated by the duty, the heat transfer area and the log mean temperature difference. The geometry factor f_g is assumed 1 for all calculations performed in this report. This may lead to a marginal error especially in Chapter 6, but the assumption is still used due to simplicity and to keep consistency in the calculations. The overall heat transfer coefficient is calculated by the following formula.

$$U = \frac{q}{f_g A \Delta T_{lm}} \quad (3.17)$$

Using (3.5) one arrives at the below expression for absolute uncertainty.

$$W_U = \pm \sqrt{\left(\frac{\partial U}{\partial q} \cdot \Delta q\right)^2 + \left(\frac{\partial U}{\partial f} \cdot \Delta f\right)^2 + \left(\frac{\partial U}{\partial A} \cdot \Delta A\right)^2 + \left(\frac{\partial U}{\partial \Delta T_{lm}} \cdot \Delta T_{lm}\right)^2} \quad (3.18)$$

By using this formula one arrive at the uncertainty presented in the table below.

Parameter	Value
Accuracy q	817,44 kW
Accuracy f	0,05
Accuracy A	10,00 m ²
Accuracy ΔT_{lm}	1,00 °C
Differential q	0,00 1/m ² K
Differential f	-741,27 W/m ² K
Differential A	-0,69 W/m ⁴ K
Differential ΔT_{lm}	-36,68 W/m ² K ²
$W_x (+/-)$	64,50 W/m ² K

Table 3.7: Overall heat transfer coefficient measurement uncertainty

4 Evaluation of the HTRI Xchanger Suite accuracy

4.1 Introduction to Xchanger Suite

Heat Transfer Research Incorporated is a company that do research on heat transfer equipment. They also develop methods and software for the thermal design and analysis of heat exchangers. HTRI Xchanger Suite v5.00 SP2 is a heat exchanger simulation program provided by Heat Transfer Research Incorporated. From now on this software will be referred to as HTRI.

The program is very useful in the design process of a heat exchanger system but also for investigating and post processing of existing designs. HTRI supports all types of conventional heat exchangers. The user simply specifies the heat exchanger geometry and working fluids that will be used. When the program has received all the necessary input data a calculation can be run. The program then predicts heat transfer coefficients, pressure loss and other useful parameters for the specified heat exchanger system.

The twisted tube is not considered as a conventional type of heat exchanger. Heat Transfer Research Incorporated has this far not implemented the twisted tube in HTRI. A vendor of such type of heat exchangers, Koch Heat Transfer Incorporated, has therefore developed their own twisted tube add-on module to the simulation program. By using this module it is possible to do simulations of twisted tube heat exchanger in HTRI.

When using HTRI one has to choose among three different calculation modes: rating, simulation or design. As the names indicate rating and simulation are suitable modes for investigating an existing design, while design mode is suitable for design development. The only difference between rating and simulation is that in rating mode the user can only leave one process parameter unknown among the six temperatures and flow rates. This means that the duty of the heat exchanger is specified by the user before the calculations are run. In simulation mode it is possible to leave two parameters unknown. The program then uses the geometry input to predict the heat transfer coefficients, duty and the other parameters on the heat exchanger. The HTRI interface is shown in Figure 4.1 on the next page.

The Koch twisted tube add-on has been used in this master thesis to compare its output with field measurements done on a twisted tube heat exchanger in operation. By doing such comparison it is possible to estimate the calculation accuracy and reliability of the computer program. HTRI has also been used to quantitatively compare the twisted tube concept to other relevant heat exchanger concepts for compressor intercooling (25-HA-113) application. The results from this analysis are presented in chapter 6.

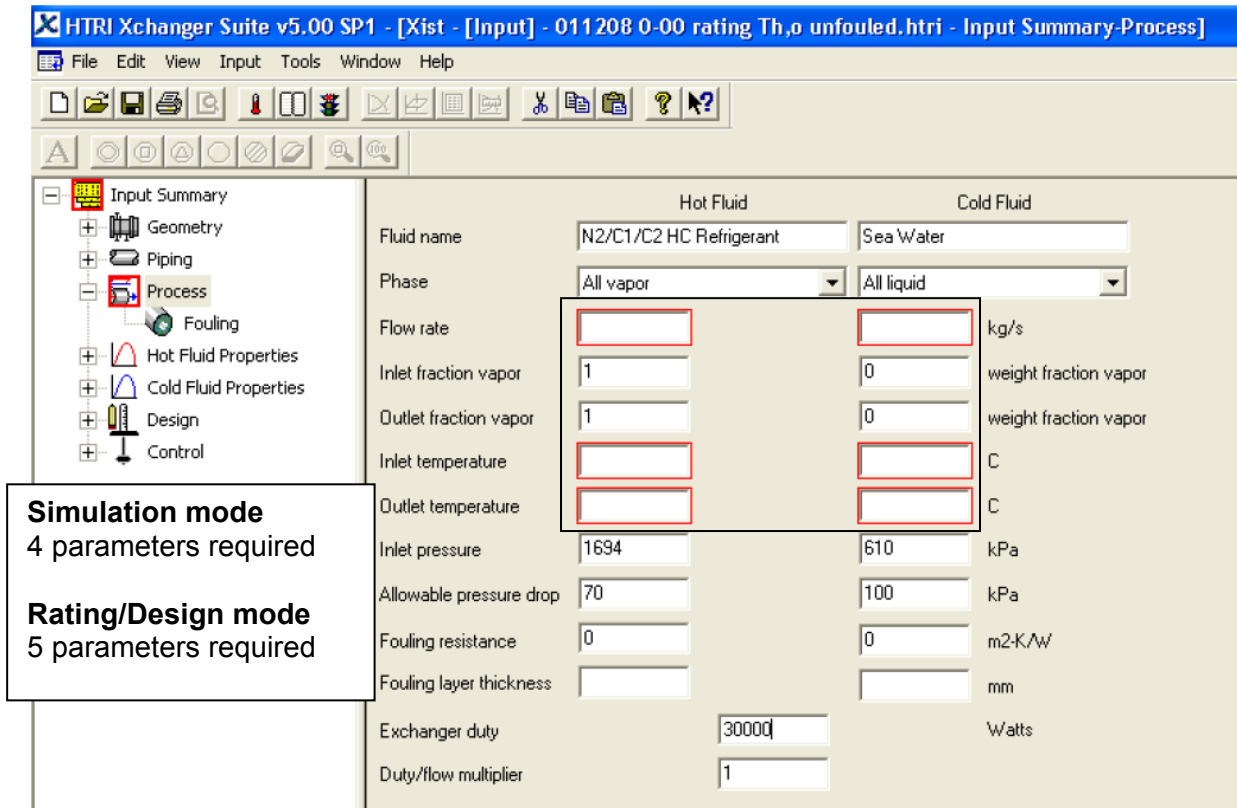


Figure 4.1: The HTRI Xchanger Suite interface

4.2 Method used to predict the HTRI accuracy for twisted tube

For the future use of twisted tube module in HTRI it is very useful to know the strengths and weaknesses of the program. Therefore it is here performed an analysis of the calculation accuracy using the twisted tube add-on provided by Koch. Measured data on 25-HA-113 described in Chapter 3 are compared to calculated values by HTRI. It must be emphasized that this analysis is comparing HTRI calculations to measurements from one specific twisted tube heat exchanger. These results can therefore be used only as an indication on the calculation accuracy. The method used to predict HTRI calculation accuracy can be described by the following five steps

- Establishment of the 25-HA-113 geometry in twenty five HTRI files
- Reading of twenty five measured operation points into the HTRI files
- HTRI calculations in rating mode – one parameter calculated
- HTRI calculations in simulation mode – two parameters calculated
- Comparison of HTRI calculated parameters to measured values

The procedure starts with establishment of a geometry in HTRI that is identical to the 25-HA-113 twisted tube heat exchanger installed at LNG Hammerfest. The vendor Koch Heat Transfer Incorporated has provided an “as built” HTRI file which is the file their design is based on. This file is used as a basis for the HTRI analysis. It is very important that the geometry in HTRI is exactly the same as the heat exchanger that are subject to measurements. Therefore the “as built” HTRI file was checked by comparing the geometry with technical drawings of the design. The drawings can be found in Appendix E. When the geometry input in HTRI was identical to the real twisted tube heat exchanger, the procedure could move on to the next step.

The HTRI accuracy is checked against twenty five field measurements performed on 25-HA-113 from October 26, 2008 to February 2, 2009. Each of the twenty five measurements is done at a certain point in time and therefore represents a unique operation point. The pressures, temperatures, flow rates and gas compositions for each operation point were read into a HTRI file. This procedure resulted in twenty five HTRI files representing the measurements. All files were saved with the verified twisted tube geometry.

Now we have twenty five HTRI files with all process input. The accuracy in rating mode was first tested. In rating mode only one process parameter is allowed to be unknown. Each file was run with outlet temperatures and mass flow rates open. It means that four rating simulations per HTRI file were run. The output parameter from HTRI was then compared to the measured value. This information is presented graphically in the next section.

The accuracy in simulation mode was then checked. This mode allows two process parameters to remain unknown. Four simulations were run on each HTRI-file; the mass flow rates were both left open, the outlet temperatures and the two combinations of one outlet temperature and one mass flow rate. The results are presented in the diagram in section 4.4.

4.3 HTRI calculation error in rating mode

4.3.1 Temperature, mass flow rate and duty

Figure 4.2 and Table 4.1 show the calculation accuracy in rating mode. The bar diagram present the deviation between the measured and calculated values while the table give additional information on standard deviation and uncertainty. Note that all numbers are given in percent with the measured value as reference. The temperature deviation has measured ΔT from outlet to inlet as reference. In rating mode only one of the temperatures or mass flow rates can be left unknown. This means that the duty is specified by the user through the heat capacity values generated by the program. When a data parameter is unknown on the HC gas side, the duty is specified by the water flow, inlet/outlet temperatures and the heat capacity of the water. When a parameter is left unknown on the water side, in the same way the duty is specified by the heat capacity of the HC gas.

One cannot measure duty directly. The measured duty is determined by the flow and temperature measurements done on the HC gas and by use of GERG08, while HTRI use Peng-Robinson equation of state. The duty calculated in HTRI is, as explained above, dependent on which process parameter that is left unknown. To indicate this, two bars for the duty are presented in the chart below. The duty calculated when $T_{h,o}$ was unknown is slightly overestimated while duty calculated by HTRI when $T_{c,o}$ was unknown is underestimated. In the first case the duty is given by the heat capacity of the sea water. The Peng-Robinson equation of state slightly overestimates the heat capacity of water compared to GERG08. In the second case HTRI underestimates the heat capacity of HC gas when one compare to the GERG08 equation. This analysis can be used to explain why the deviation on temperatures and mass flow rates are as shown in Figure 4.2.

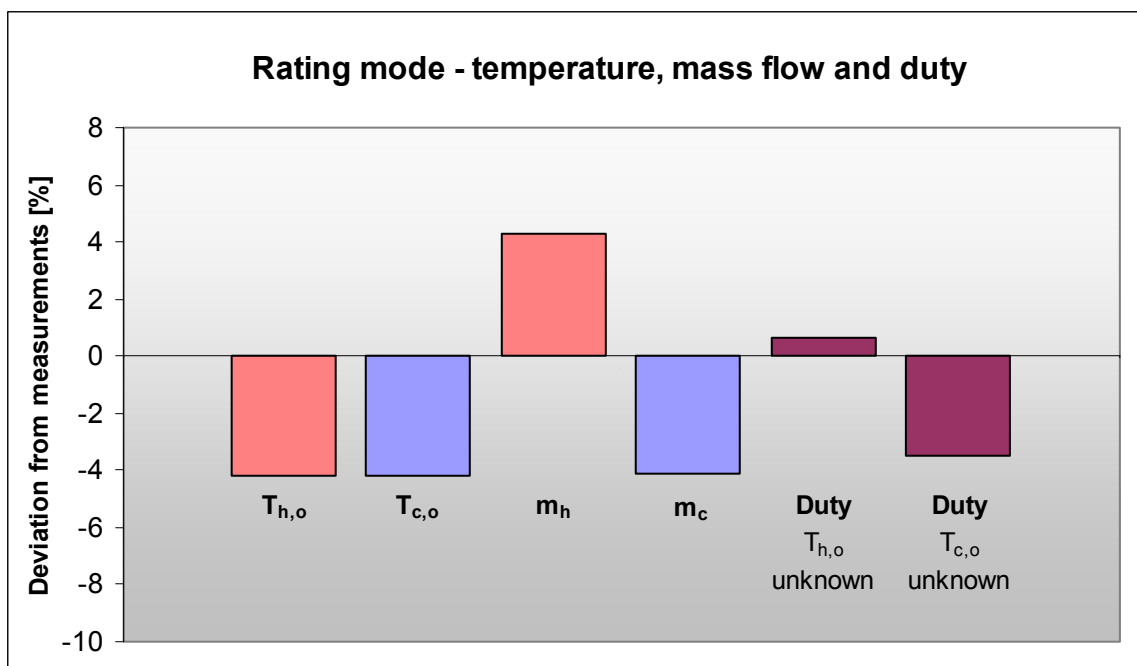


Figure 4.2: HTRI calculation error in rating mode for temperatures, flow rates and duty

Parameter	Mean error [%]	Standard deviation [%]	Uncertainty [%]
$T_{h,o}$	-4,2	2	+/- 0,7
$T_{c,o}$	-4,2	1,3	+/- 4,1
\dot{m}_h	4,3	1,3	+/- 5,0
\dot{m}_c	-4,1	1,4	+/- 5,0
Duty $T_{h,o}$ open	0,7	1,2	+/- 5,0
Duty $T_{c,o}$ open	-3,5	0,2	+/- 5,0

Table 4.1: Rating mode – temperature, mass flow and duty

The temperature and mass flow rate bars, denoted by T and M respectively, indicate whether they are overestimated or underestimated by HTRI compared to measured values. $T_{h,o}$ is underestimated of about 4 percent compared to measured values. In this case the duty is given by the water side input. We know that the duty is slightly overestimated and the heat capacity of the HC gas is underestimated. These two miscalculations will both contribute to a lower HC gas outlet temperature $T_{h,o}$, when the heat balance is calculated by HTRI. It is easily seen that these two contributions pull in the same direction when one consider the equation below. ΔT must compensate that q is larger and the heat capacity is lower. This is achieved by increasing ΔT and thereby lowering the HC gas outlet temperature.

$$q = \underbrace{Cp_{av} \Delta T}_{\Delta h_e} \dot{m} \quad (4.1)$$

$T_{c,o}$ is also underestimated by approximately 4 percent. In this case the duty is given by the HC gas side and thereby underestimated. Lower duty leads to lower temperature rise in the cooling water and therefore this result is also expected. The same explanation can be used on the mass flow rates. HC gas mass flow rate \dot{m}_h is overestimated. In this case the duty is given by the water heat capacity. Since the heat capacity of HC gas is underestimated by HTRI, the program will arrive at a higher mass flow rate in order to compensate the low heat capacity.

The conclusion is that HTRI miscalculates temperatures and flow rates with up to 4 % when run in rating mode. It is very important to emphasize that this deviation is most probably due to differences between the Peng-Robinson and GERG08 equation. One must also comment on the uncertainty. Considering the mass flow rates and the two duties we see that the uncertainty is actually larger than the mean deviation between measured values and HTRI values. Inaccurate measurements can therefore also be a reason for the deviations.

4.3.2 Heat transfer and shell side pressure loss

Figure 4.3 shows how accurate the shell side pressure loss is calculated in rating mode. The presentation of the pressure drop accuracy is based on rating simulations performed with $T_{c,o}$ unknown. In these simulations the shell side mass flow rate is given. This is case is chosen because the pressure drop depends very much on the HC gas mass flow rate. Compared to the measured pressure loss, HTRI overestimate this parameter with a mean of approximately 40%. In other words HTRI calculate the pressure drop in a very conservative way.

The graph below also shows how accurate the overall heat transfer coefficient is predicted in rating mode. The heat transfer coefficient U has an average error of +50%. It means that HTRI overestimates the twisted tube capability of transferring heat by a factor of 1,5 in this particular application and operation point. The heat transfer correlations that HTRI uses for determination of U are in general not conservative, but the other way around.

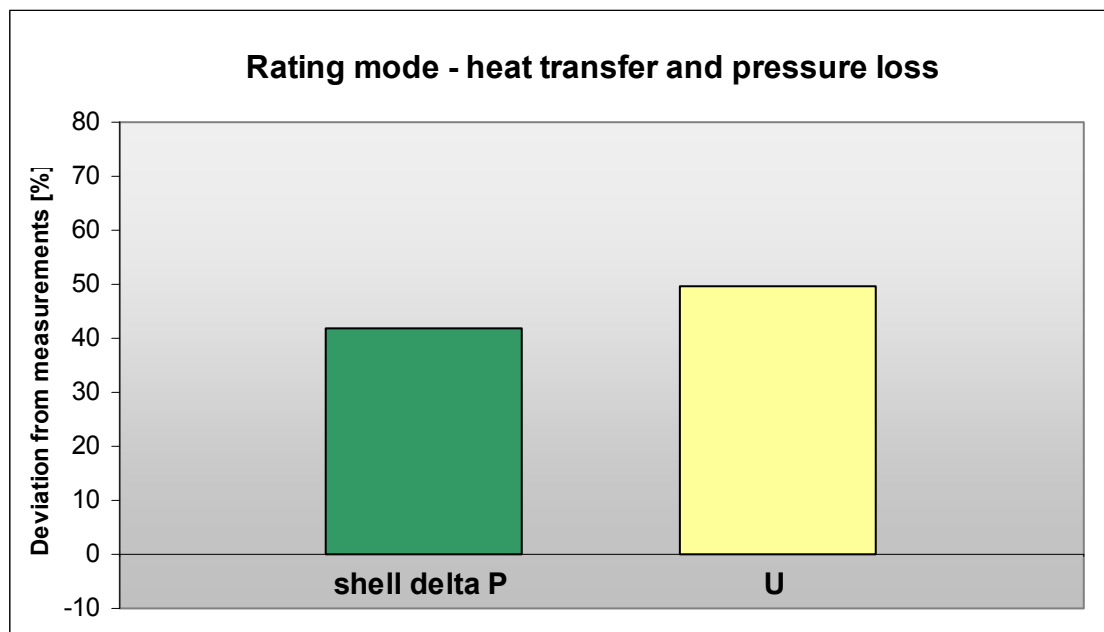


Figure 4.3: HTRI calculation error in rating mode for pressure loss and heat transfer coefficient

Parameter	Mean error [%]	Standard deviation [%]	Uncertainty [%]
Delta P	41,7	3,5	+/- 3,2
U	49,5	3,1	+/- 8,6

Table 4.2: Rating mode – shell side pressure loss and heat transfer coefficient

Since mass flow rates have an impact on U , the mean value from HTRI is found by using the rating runs where both mass flow rates were given from measurements. The rating simulations used are therefore when $T_{h,o}$ was kept unknown. In addition, the duty is most accurate in this case. One must also comment on how the measured U value has been predicted. Obviously this parameter can not be measured directly. However, it can be determined from measurements of other physical parameters. Measured U is found by dividing the duty on shell side (HC gas) by heat transfer area and log mean temperature difference. It means that measured U is a result of GERG08 prediction of the heat capacity of HC gas. If the measured U had been calculated by use of Peng-Robinson it had been reduced by 3,5%^{VI} and thereby the calculation accuracy would have looked slightly better.

^{VI} See Table 4.1

4.4 HTRI calculation error in simulation mode

4.4.1 Temperature and mass flow rate

In simulation mode HTRI has the capability to calculate with two process parameters unknown. When running in simulation mode the duty of the heat exchanger is not given by the user but calculated by HTRI. Four different combinations of unknowns were tested; both outlet temperatures, both mass flow rates and the two combinations of one temperature and one flow rate.

Examining Figure 4.4 below one can observe that there is a huge difference in calculation accuracy depending on which parameters that are unknown. Keeping both outlet temperatures unknown give a relatively low deviation compared to measurements, while keeping both mass flow rates unknown result in a deviation reaching almost 200%. Without investigation of the HTRI programme code it is difficult to point out what makes the error huge in some specific cases. One explanation could be the following.

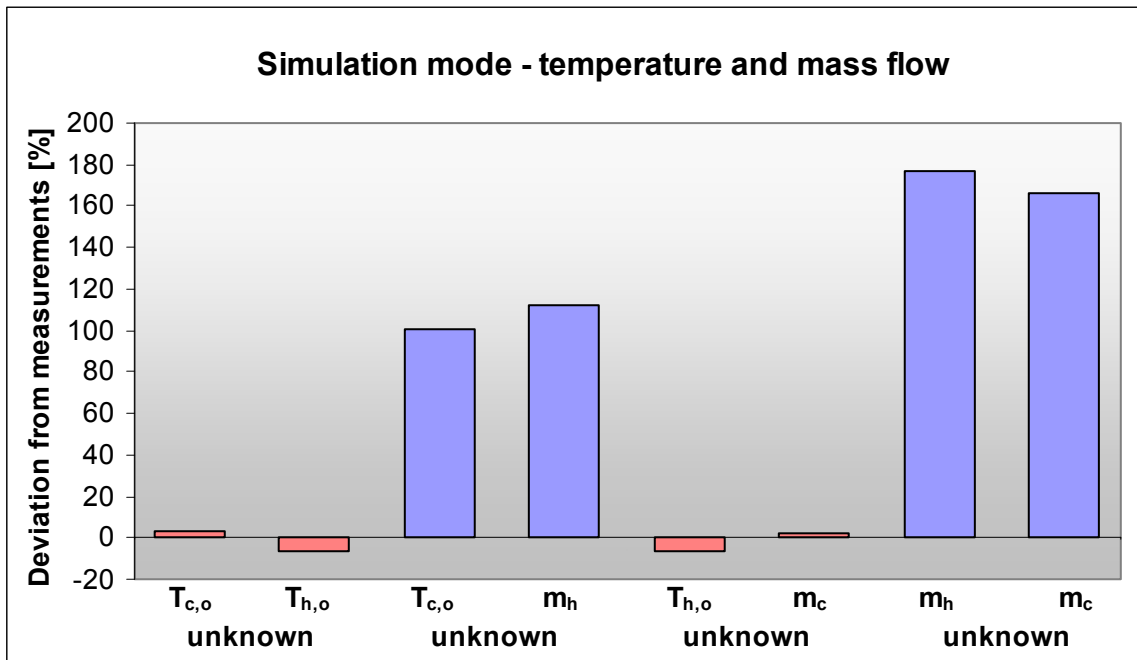


Figure 4.4: HTRI calculation error in simulation mode for temperature and mass flow rate

Parameter	Mean error [%]	Standard deviation [%]	Uncertainty [%]
$T_{c,o}$	1,9	1,4	+/- 4,1
$T_{h,o}$	-6,6	0,6	+/- 0,7
$T_{c,o}$	100,9	3,7	+/- 4,1
\dot{m}_h	112,4	5,5	+/- 5,0
$T_{h,o}$	-6,7	0,6	+/- 0,7
\dot{m}_c	2	1,4	+/- 5,0
\dot{m}_h	176,6	10,1	+/- 5,0
\dot{m}_c	166,4	10,8	+/- 5,0

Table 4.3: Rating mode – temperatures and flow rates

It is known from Chapter 2 that the overall heat transfer coefficient has a strong dependency on the flow rates, expressed in Reynolds number. The iteration process in HTRI uses the

local heat transfer coefficient to predict how much heat is transferred between the two fluids. It is also known from the tests in rating mode that HTRI overestimates heat transfer coefficient by a factor of 1,5. When both flow rates are unknown HTRI will start to iterate with low flow rates. Because the heat transfer coefficient is too high, the heat exchanger appears to be more efficient than in reality, and the outlet temperature will be too low for HC gas and too high for seawater respectively. In order to get the specified outlet temperatures HTRI must increase both flow rates. When the flow rate increase, the heat transfer coefficient will also increase in the power of 0,8^{VII}. These two mechanisms will pull the temperatures in opposite directions. Therefore the program must increase the flow rate substantially in order to get the right outlet temperatures. One can illustrate the mechanism by investigating the following equations.

$$UA(\Delta T_{lm}) = Cp_h(T_{h,o} - T_{c,i}) \dot{m}_h \quad (4.2)$$

$$T_{h,o} = T_{h,i} - \frac{UA}{Cp_h \dot{m}_h} (\bar{T}_h - \bar{T}_c) \quad (4.3)$$

Investigating equation (4.3) one observe that increasing the shell side mass flow rate will at first sight lead to an increased $T_{h,o}$. But as mentioned the overall heat transfer coefficient increase at almost the same rate and therefore HTRI end up with a way too high mass flow rate. This explanation can also be used in the case were $T_{c,o}$ and m_h are unknown.

The cases with both T_c/T_h and $T_{h,o}/m_c$ unknown are much more accurate. These cases have in common that m_h is known. Because m_h is known the heat transfer coefficient will approach a constant behaviour. Despite the fact that the heat transfer coefficient is too high, the program will reach a solution earlier at a value closer to the reality. One can conclude that the twisted tube add on in HTRI is unpredictable in simulation mode. Use of simulation mode should be done with caution and both mass flow rates should be input.

^{VII} See section 2.3 p.5

4.4.2 Shell side pressure loss, heat transfer coefficient and duty

In the previous section accuracy for temperature and flow rate values were tested. The HTRI calculations appeared to be very unpredictable. In order to show the best side of HTRI the pressure loss, heat transfer and duty values are in this section based on simulation performed with $T_{c,o}/T_{h,o}$ unknown. The results are presented in Figure 4.5 below.

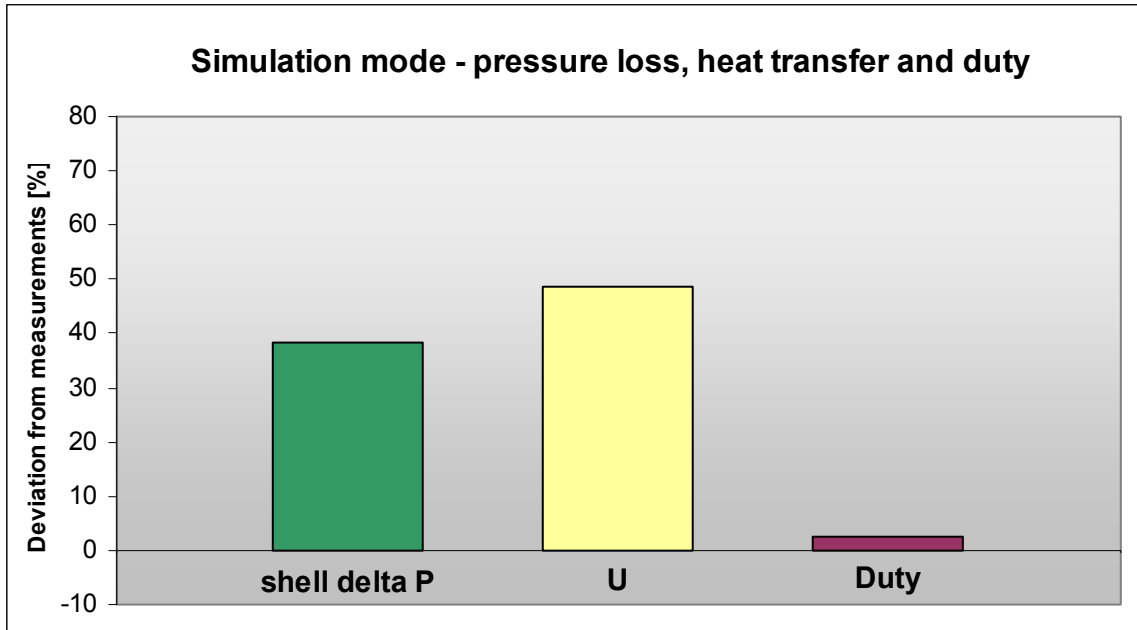


Figure 4.5: HTRI calculation error in simulation mode for duty, pressure loss and heat transfer

Parameter	Mean error [%]	Standard deviation [%]	Uncertainty [%]
Delta P	38,4	3,4	+/- 3,2
U	48,6	2,6	+/- 8,6
Duty	2,4	0,6	+/- 5,0

Table 4.4: Rating mode – duty, pressure loss and heat transfer

Here one should expect deviations that are about the same as in rating mode. Comparison of the pressure loss and heat transfer coefficient to the values calculated in rating mode show that the calculations are in agreement.

Rating mode and simulation mode overestimate the pressure loss of about 40%. This means that the twisted tube heat exchanger perform better in reality than calculated in HTRI. The overall heat transfer coefficient is overestimated by approximately 50%. In this case the heat exchanger performs worse than predicted by HTRI. When it comes to temperatures and flow rates, rating mode calculates these values by an accuracy of +/-4%. The main reason for the deviation is the use of Peng-Robinson equation of state which is not in agreement with GERG08 equation. In simulation mode the calculation accuracy depends very much on the input. If both mass flow rates were left unknown the error is up to 200% compared to measured values. The reason for this is probably a combination of the overestimation of U and the fact that U is dependent on both flow rates. It is therefore preferable to do simulations where both flow rates are known. The accuracy on temperatures and flow rates are then at +/- 7%.

5 Evaluation of the twisted tube design for 25-HA-113

In this chapter the twisted tube heat exchanger installed on tag number 25-HA-113, LNG Hammerfest is investigated with respect to thermal-hydraulic performance. The design is developed by the company Koch Heat Transfer Incorporated. Calculations done in the design process were based on the design basis E066-AB-P-DP-2546. In this document information about the operational gas physical properties, inlet temperatures and mass flow rates are given. The performance of the heat exchanger is therefore designed to be in agreement with these input values. 25-HA-113 is run at a different operation point than specified in the design basis. In order to compare the performance expected by Koch with measured performance data, one must take into account that there is a deviation between given operation point in the design basis and the real operation point.

5.1 Overdesign and fouling resistance included in design

Overdesign is the extra margin incorporated in a design. It is important to do so in order to cover uncertainties in flow rates, temperatures, physical properties and the software used in the design process. In this case the overdesign is set to 5%. The overdesign is included in the HTRI model by adding 5 percent to the HC gas mass flow rate. The increased mass flow rate results in a heat exchanger design that is able to handle a 5% higher duty than the design operation point.

In addition to the input uncertainties one has taken fouling into account. Fouling will increase the thermal resistance at the wall and thereby lower the overall heat transfer coefficient over time. StatoilHydro has requested a fouling resistance of 1,8 E-4 m²K/W to be included in the design.

5.2 Heat transfer performance

The thermal performance of the twisted tube design will be investigated in this section. A convenient parameter to examine for this matter is the overall heat transfer coefficient, U. In the following different variations of U will be explained and derived. At the section end, these parameters are plotted in a diagram showing the thermal performance of the heat exchanger. The first explained parameter is the measured heat transfer coefficient U_{measured} .

5.2.1 Measured heat transfer coefficient

Measured heat transfer coefficient are predicted by using the duty of the heat exchanger. The duty is calculated by a GERG08 equation of state which returns the enthalpy for a known pressure and temperature. The enthalpy difference of the refrigerant from inlet to outlet is then multiplied by the measured mass flow rate. f_g is assumed equal to 1 and the shell side area, A_s is extracted from TEMA specification sheet in Appendix I.

$$Q_h = \dot{m}_h (h_{e, h,i} - h_{e, h,o}) \quad (4.4)$$

$$U = Q_h / (f_g \cdot \Delta T_{lm} \cdot A_s) \quad (4.5)$$

5.2.2 Design heat transfer coefficient

The design U is here defined as the overall heat transfer coefficient required to cool the gas as specified in the design basis, operating at design point in fouled condition. The heat transfer area must be specified to determine this parameter. Here the calculated efficient area from HTRI is used.

$$U_d = \frac{Q_{design}}{\Delta T_{lm,design} A_{HTRI}} \quad (4.6)$$

5.2.3 Clean heat transfer coefficient

Clean U is found by subtracting the expected fouling resistance R_f from the design U. This parameter represents the expected heat transfer coefficient when the exchanger is new and clean

$$U_{clean} = \left(\frac{1}{U_{design}} - R_f \right)^{-1} \quad (4.7)$$

5.2.4 Corrected heat transfer coefficient for off design operation

It is interesting to compare design U with U measured. However, the heat exchanger was operating away from design point when the measurements were performed. It is therefore not fair to compare these two values directly. Operation away from design point will affect U measured which makes a comparison less valuable. A technique is developed to make U measured and design U comparable. This is done by normalizing U measured with the heat correlations presented in section 2.3.2. By mathematical manipulation it is possible to obtain a corrected heat transfer coefficient. *U corrected is the thermal performance one would expect if the heat exchanger was run at design conditions.* In order to predict U corrected the following mathematical method has been used.

The heat transfer coefficient must always be evaluated for a certain area. For simplicity U corrected is developed for a circular tube area, not for the twisted tube. A circular tube that has the same cross sectional flow area as the twisted tube is chosen in the mathematical analysis. By using this assumption one can calculate a circular equivalent diameter d_{ce} . This is the diameter that corresponds to a circular tube with the same cross sectional area as the twisted tube.

The circular equivalent d_{ce} can be calculated by use of equation (2.3) for twisted tube cross sectional area, assumption of $d_{t,max}/d_{t,min}$ (tube side diameters) = 2 and the area formula for a circular cross section. Combination of these three equations result in the following expression for the circular equivalent tube side diameter $d_{t,ce}$ for the circular tube.

$$d_{t,ce} = \frac{d_{t,max}}{\sqrt{2}} \quad (4.8)$$

By using the wall thickness $L_t = 1,734\text{mm}$ and $d_{s,max} = 22,225\text{ mm}$ (see Appendix I for design specification), one can calculate the corresponding circle diameters $d_{t,ce}$ and $d_{s,ce}$. The following correlation for U is expressed based on the shell side area considering a clean unit without fouling layer [11].

$$U_{t,corrected} = \frac{1}{\frac{1}{h_{s,corrected}} + \frac{\ln(d_{s,ce}/d_{t,ce})d_{s,ce}}{2k_c} + \frac{d_{s,ce}}{d_{t,ce}h_{t,corrected}}} \quad (4.9)$$

By simplification of equation (2.20) and considering that the application is cooling on the shell side where the temperature ratio exponent $n=0$, $h_{s,corrected}$ can be written

$$h_{s,corrected} = K Re_{design}^{0,8} Pr_{design}^{0,4} \quad (4.10)$$

Here K is unknown. In order to get an expression for $h_{s,corrected}$ that can be calculated, the above equation is expanded in the following way

$$h_{s,corrected} = \underbrace{K Re^{0,8} Pr^{0,4}}_{h_{s,measured}} \underbrace{\left(\frac{Re_{design}}{Re^{0,8}}\right)^{0,8} \left(\frac{Pr_{design}}{Pr^{0,4}}\right)^{0,4}}_{correction \ terms} \quad (4.11)$$

Observed from HTRI calculations it turns out that the thermal resistance distribution is 75% for shell side convection, 15% for tube side convection and 10% for tube conduction for a clean unit. All terms in equation (4.11) can be determined by use of measured data, design specifications and the information on thermal resistance. To find $h_{s,measured}$ the following relation is used.

$$h_{s,measured} = \frac{U_{measured}}{0,75} \quad (4.12)$$

The correction terms are calculated by using the below formulas for Reynolds number and Prandtl number

$$\left(\frac{Re_{design}}{Re^{0,8}}\right)^{0,8} = \left\{ \left(\frac{\mu}{\mu_{design}}\right) \left(\frac{A_{flow}}{\dot{m}}\right) \left(\frac{\dot{m}}{A_{flow}}\right)_{design} \right\}^{0,8} =$$

$$\left(\frac{\dot{m}_{design} \mu}{\dot{m} \mu_{design}}\right)^{0,8} = \left(\frac{\dot{m}_{design}}{\dot{m}} \underbrace{[1 + 0,00186(T_{h,i} - T_{h,i \ design})]}_{change \ in \ viscosity \ from \ design}\right)^{0,8} \quad (4.13)$$

The change in viscosity term is found by use of the Peng-Robinson equation of state in HTRI. Small pressure differences have negligible influence on the viscosity while variations in temperature are correlated linearly as showed in the above equation. See Appendix H for details. In the following formula for Prandtl number, Peng-Robinson has been used additionally to correlate the heat capacity with pressure and temperature. The conduction terms will cancel each other.

$$\left(\frac{\text{Pr}_{design}}{\text{Pr}^{0,4}}\right)^{0,4} = \left(\frac{c_{p,design} \mu_{design} k_c}{k_{c,design} c_p \mu}\right)^{0,4} = \left(\frac{1}{[1 + 0,00186(T_{h,i} - T_{h,i design})] + [1 + 0,0035(p_{h,i} - p_{h,i design})]}\right)^{0,4} \quad (4.14)$$

Now $h_{s,corrected}$ can be determined knowing all the terms in (4.11). A similar approach as the one presented above is used to find the corrected tube side convection coefficient $h_{t,corrected}$ by using equation (2.24). Since the application is heating of liquid the temperature ratio is replaced by the viscosity ratio with an exponent $m=-0,11$.

$$h_{t,corrected} = K \text{Re}^{0,8} \cdot \text{Pr}^{0,4} \left(\frac{\mu_w}{\mu_b}\right)^{-0,11} \quad (4.15)$$

The procedure from here is exactly the same expanding (4.15) with correction terms.

$$h_{t,corrected} = \underbrace{K \text{Re}^{0,8} \text{Pr}^{0,4} \left(\frac{\mu_w}{\mu_b}\right)^{-0,11}}_{h_{t,measured}} \underbrace{\left(\frac{\text{Re}_{design}}{\text{Re}^{0,8}}\right)^{0,8} \left(\frac{\text{Pr}_{design}}{\text{Pr}^{0,4}}\right)^{0,4} \left(\frac{\mu_w}{\mu_b}\right)^{-0,11} \left(\frac{\mu_b}{\mu_w}\right)^{-0,11}}_{\text{correction terms}} \quad (4.16)$$

The viscosity and Prandtl number ratios is assumed one since these properties have negligible variations for the actual pressure and temperature deviations. Correction terms for Reynolds number is presented below. In prediction of $h_{t,measured}$ one must also correct for the area that U is based on by using d_{ce} .

$$h_{t,measured} = \frac{d_{s,ce} U_{measured}}{d_{t,ce} 0,15} \quad (4.17)$$

$$\left(\frac{\text{Re}_{design}}{\text{Re}^{0,8}}\right)^{0,8} = \left(\frac{\dot{m}^{design}}{\dot{m}} \underbrace{(1 + 0,0478(T_{c,i design} - T_{c,i}))}_{\text{change in viscosity from design}}\right)^{0,8} \quad (4.18)$$

Now we have all the terms required to calculate $h_{t,corrected}$. By use of the information on thermal resistance distribution it is also possible to calculate the conduction term in (4.9). This term will not change with operation and can therefore be calculated from $U_{measured}$.

$$\frac{d_{s,ce} \ln(d_{s,ce} / d_{t,ce})}{k_c} = \frac{0,10}{U_{measured}} \quad (4.19)$$

All terms in equation (4.16) are now determined and the corrected heat transfer coefficient $U_{corrected}$ can be calculated. In the next section the results from this analysis are presented.

5.2.5 Presentation of 25-HA-113 thermal performance

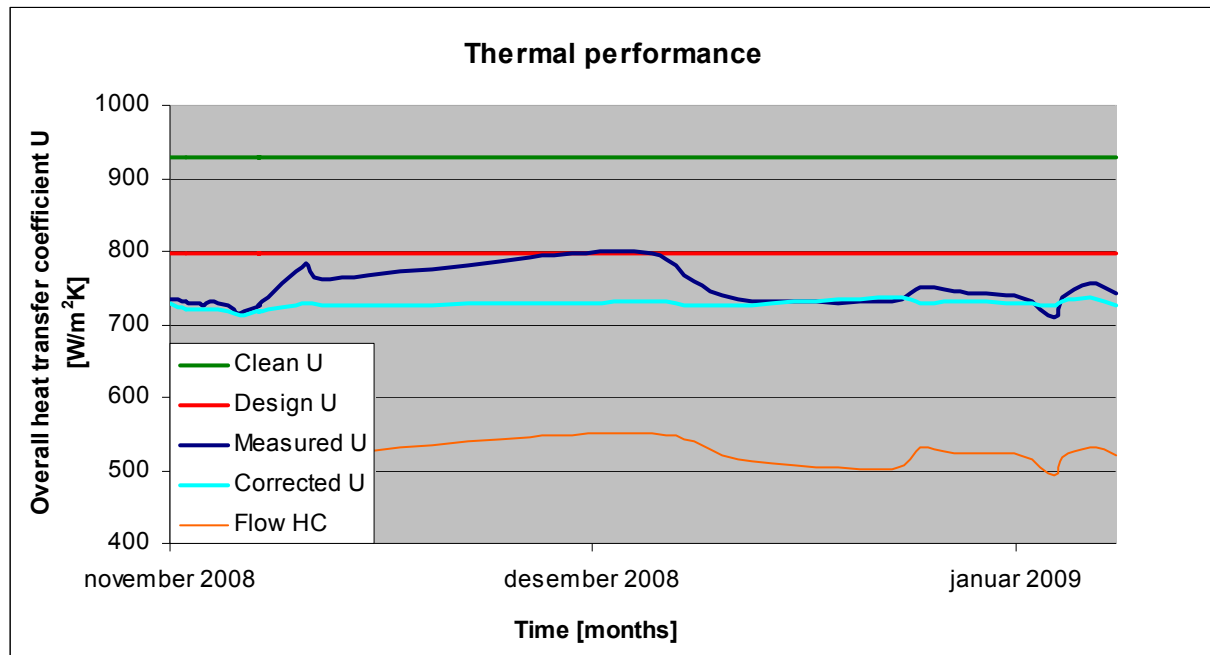


Figure 5.1: Thermal performance of 25-HA-113

Parameter	Mean	Standard deviation	Uncertainty	Unit
Clean U	929,6	-	-	W/m ² K
Design U	796,4	-	-	W/m ² K
Measured	744,0	23,3	+/- 64	W/m ² K
Corrected	725,7	7,2	+/- 64	W/m ² K

Table 5.1: Thermal performance in numbers

Figure 5.1 presents the thermal performance of the twisted tube heat exchanger. The diagram is based on 25 measurements performed on 25-HA-113 from 26.october 2008 to 2.february 2009. In other words the heat exchanger is expected to be in new and clean condition.

It is observed that the measured U is lower than both design U and clean U in the actual time period. One explanation could be that the heat exchanger is run at off design conditions. If these conditions are unfavourable for the heat transfer coefficient the measured value will be lower than the actual value at design point. However, when one corrects the measured U for the operation point (indicated by Corrected U) it is seen that the true thermal performance is even lower than measured. The heat exchanger is operated with higher flow rates than specified in the design. Higher flow rates contribute to better thermal performance. This is emphasized by also showing flow rate of HC gas in the same diagram indicated by a brown curve. One can clearly observe that the measured U follows the same pattern as the shell side mass flow rate. Because the heat exchanger is run at a favourable operation point in terms of heat transfer coefficient, the corrected U will be lower than the measured U. Corrected U has an average value of 726 W/m²K while measured U has an average value of 744 W/m²K.

The expected heat transfer coefficient by the vendor, design U, has an average of 796 W/m²K. This is considerably higher than the mean measured value, 744 W/m²K. If one compare with the corrected U, which reflects the true performance at design operation point, the gap between design and measured values are even larger. This underlines the fact that the heat exchanger is not able to transfer the amount of heat that was specified in the design. In other words the vendor has overestimated its thermal performance. It was shown in Chapter 4 that the software HTRI Xchanger Suite predicts the heat transfer 50% higher than the real value in the case of 25-HA-113. When Koch Heat Transfer Incorporated uses this software as a design tool it may result in an insufficient thermal designs.

5.3 Shell side pressure drop

The hydraulic performance of the twisted tube design will be investigated in this section. In the intercooling application of 25-HA-113 the pressure drop of HC gas on shell side is the concern. Therefore only the shell side pressure drop is investigated here. A convenient parameter to examine for this matter is obviously the pressure drop Δp from shell inlet to shell outlet. In the following Δp corrected will be explained and derived. At the section end, the parameter is plotted with measured Δp in a diagram showing the hydraulic performance of the heat exchanger.

5.3.1 Corrected pressure loss for off design operation

In the same manner as for the overall heat transfer coefficient it is interesting to determine a corrected Δp in order to compare the result with the design pressure drop. By using correlations from section 2.3.3 one can correct the measured values. The method is initiated by inserting equation (2.29) for f_D in equation (2.28).

$$\Delta P = \frac{0,3164}{Re^{0,25}} \left[1 + \frac{3,6}{Fr^{0,357}} \right] \frac{L}{2d_h} \rho v^2 \quad (4.20)$$

By including constant parameters into K one can simplify to

$$\Delta P = K Re^{-0,25} \rho v^2 \quad (4.21)$$

Expanding the above equation with correction terms for off design operation one obtain the corrected pressure loss, $\Delta p_{corrected}$

$$\Delta p_{corrected} = K Re^{-0,25} \rho v^2 \left(\frac{Re_{design}}{Re} \right)^{-0,25} \left(\frac{\rho_{design}}{\rho} \right) \left(\frac{v_{design}}{v} \right)^2 =$$

$$\underbrace{K Re^{-0,25} \rho v^2}_{\text{measured pressure loss}} \underbrace{\left(\frac{Re_{design}}{Re} \right)^{-0,25} \left(\frac{\rho_{design}}{\rho} \right) \left(\frac{v_{design}}{v} \right)^2}_{\text{correction terms}} = \quad (4.22)$$

The first correction term can be calculated directly from measurements and design specifications. A correlation for the last term is developed by using Peng-Robinson property generator in HTRI.

$$\frac{\rho}{\rho_{design}} = [1 + 0,0566(p_{h,i} - p_{h,i \text{ design}})] \quad (4.23)$$

Using the above correlations it is possible to calculate a corrected pressure drop, $\Delta p_{corrected}$. This parameter reflects the pressure drop one would expect if 25-HA-113 were run at design operation point. In addition, it is interesting to investigate the measured pressure loss $\Delta p_{measured}$ in comparison to the design value Δp_{design} . Measured pressure loss is extracted directly from the measurement data while design pressure loss is the pressure loss predicted by Koch when they developed the design. The results on hydraulic performance are presented in the following.

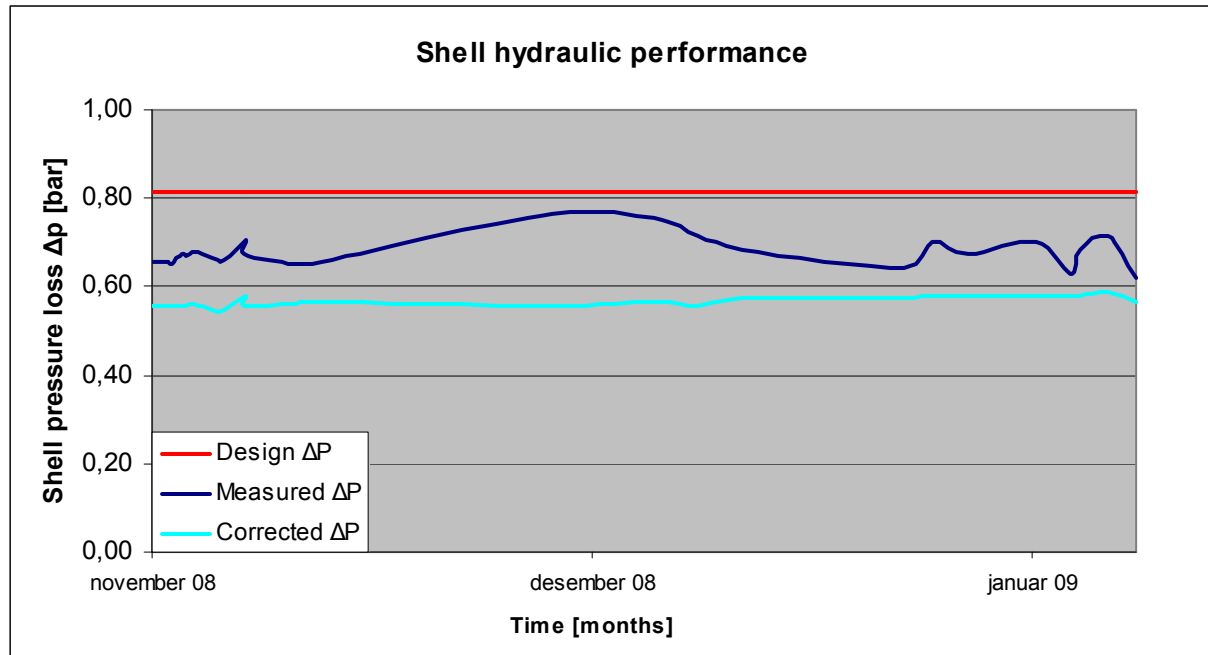


Figure 5.2: Hydraulic performance of 25-HA-113

Parameter	Mean	Standard deviation	Uncertainty	Unit
Design Δp	0,81	-	-	bar
Measured Δp	0,68	0,03	+/- 0,022	bar
Corrected Δp	0,57	0,01	+/- 0,022	bar

Table 5.2: Hydraulic performance in numbers

Figure 5.2 show how the measured pressure drop vary with time indicated by the blue line. The straight red line is the expected pressure loss by the vendor at design operation point. A corrected pressure loss for operation away from design condition is also plotted, indicated by a turquoise line.

Because the heat exchanger is operated with a higher flow rate of HC gas than specified in the design one would expect higher measured pressure loss. Despite 25-HA-113 is operated unfavourable with respect to pressure loss, the shell hydraulic performance is good. The measured pressure loss is lower at all measured operational conditions compared to the design pressure loss. Investigating the corrected pressure loss for off design conditions, the picture is even clearer. 25-HA-113 performs better than expected with respect to shell side pressure loss. As with the thermal performance this may have a connection with the software used to develop the design. In chapter 4 it was shown that HTRI do a conservative calculation of the shell side pressure drop. Use of this software will result in a design that performs better than predicted with respect to pressure drop.

5.4 Consideration of fouling on 25-HA-113

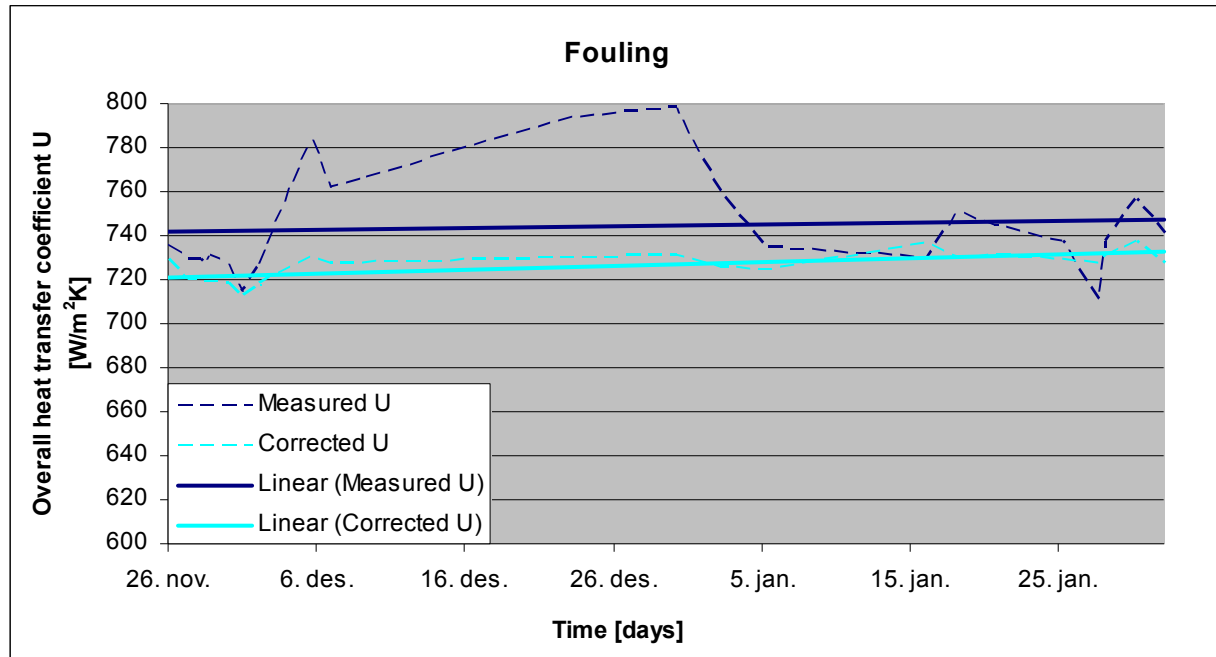


Figure 5.3: Development of fouling layer on 25-HA-113

The diagram above shows the development of the heat transfer coefficient with time. Both measured U and corrected U are plotted. In addition each curve has a linear regression line that visualizes the trend with respect to time. As the heat exchanger was recently installed 26.november 2008 one can consider the unit in clean condition.

One would expect the overall heat transfer coefficient to decrease with time as a result of a growing fouling layer. Both linear trend lines show the opposite effect by a minimal increase of heat transfer coefficient with time. The increasing measured U could be explained by a change to more favourable operation conditions with respect to heat transfer, but the linear regression of the corrected U also shows an increasing trend. This line is not affected by changing operation conditions. The increasing trends are therefore most probably due to uncertainty in measurement and the correlations used for calculating the corrected U.

Investigation of Figure 5.3 shows that the corrected U has a clear decreasing trend from 26.november to approximately 1.december. The corrected U is then increasing until 6.december. When the heat exchanger was installed there may have been a process where a fouling layer first developed and then has fallen off as result of shear forces exerted by the seawater flow.

By observing the development of the measured and corrected heat transfer coefficient one can conclude that the thermal performance is unaffected in the time period considered. Therefore the development of a fouling layer is most probably minimal on 25-HA-113.

6 Comparison of the twisted tube solution to other heat exchanger concepts

As a part of the comparison between twisted tube heat exchangers and competing heat exchanger solutions the simulation program HTRI has been used. By using this software and specifying a certain application it is possible to compare the heat exchanger types not only qualitatively but also quantitatively.

The application investigated in this analysis is the seawater cooled intercooler 25-HA-113 described in section 3.1 p.24. The design basis for this application can be found in StatoilHydro's PIM system at document number E066-AB-P-DP-2546 [16]. Chosen heat exchanger concepts evaluated for this application are a twisted tube, a helix baffled and a single segmental baffled heat exchanger. The twisted tube is the present installed unit on 25-HA-113^{VIII}, while the helix heat exchanger is the previously installed unit at the same tag number. Measurement data from both units are available.

The conventional shell and tube solution has been designed in HTRI for the application 25-HA-113 corresponding to the design basis. This heat exchanger is only a HTRI design performed for this investigation and has never been in operation. In addition HTRI files for both the twisted tube and the helix configuration is used in some parts of the analysis. The helix baffled heat exchanger has been reconstructed in HTRI by using technical drawings (can be found in Appendix F), while the twisted tube design was reconstructed by using the "as built" HTRI file provided by Koch Heat Transfer Inc.

By using HTRI the conventional design is compared to the former installed helix baffled and the present twisted tube heat exchanger. It must be emphasized that the comparison of thermal hydraulic performance is based on field measurements from the twisted tube and helical baffled heat exchangers, while the conventional thermal-hydraulic performance is extracted from HTRI calculations. This is done in order to increase the reliability of the analysis. Other parameters such as size and weight will also be presented. In addition, their properties in terms of fouling and vibration will be discussed qualitatively.

6.1 Descriptions of the designs for 25-HA-113

6.1.1 Low finned tubes with single segmental baffles

It was decided to develop a standard shell and tube heat exchanger design with single segmental baffles. The application is cooling of gas by seawater. Gases exhibit low heat transfer coefficients due to their low thermal conductivity and low density, while liquids in general exhibit high heat transfer coefficients [12]. To compensate for this property it is advantageous to increase the gas side heat transfer area. In order to be competitive compared to the other more sophisticated designs, the tubes are therefore chosen to be low finned on the shell side. Normally low finned tubes give a relatively high heat transfer to pressure drop ratio. In addition, designing the heat exchanger with low finned tubes result in a compact unit due to the high heat transfer surface achieved. This is the simplest design among the three alternatives. In the design process some parameters have been fixed such that the solution is a true alternative to the two other designs. The parameters that are fixed include the following.

^{VIII} June 2009

Tube length	9,93 m
Tube OD	22,225 mm
Tube avg.thickness	1,734 mm
Tube material	titanium grade-2
TEMA	BEM
Inlet ID	814/488mm (shell/tube)
Outlet ID	814/488mm (shell/tube)

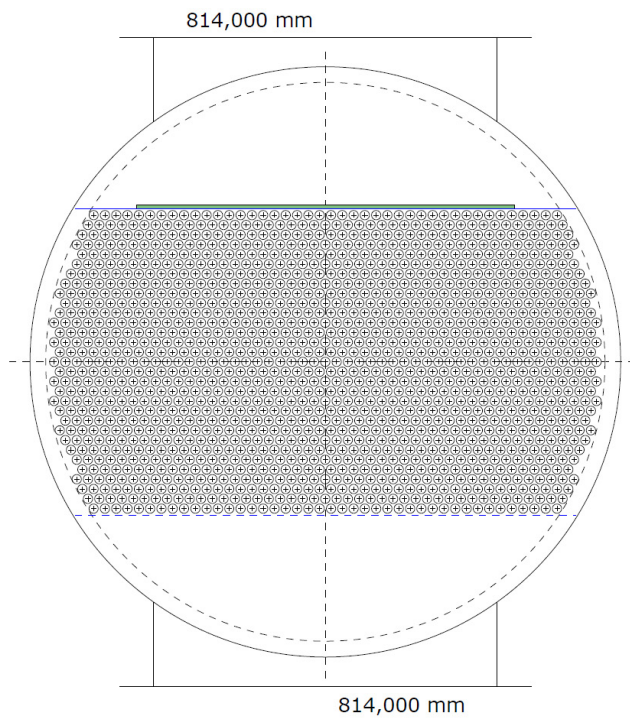
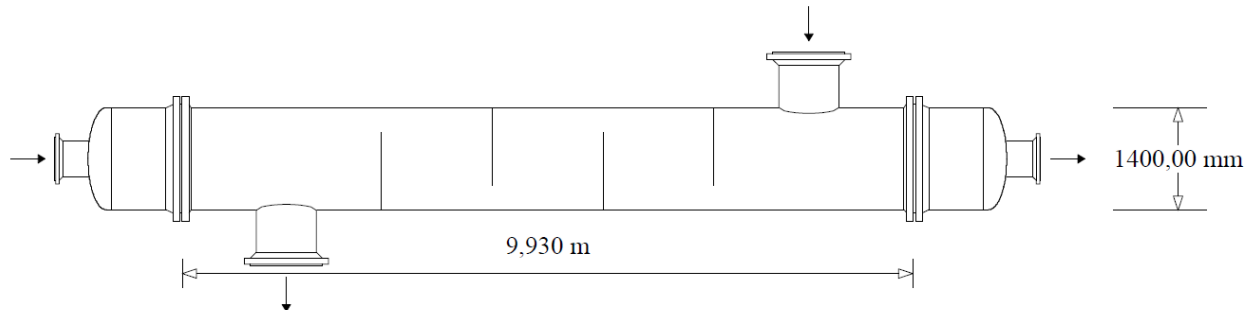
The conventional shell-and-tube design process was initiated with a shell inner diameter of 1400 mm. A single segmental baffle configuration and 30% cut resulted in an HTRI output with a satisfactory thermal performance. The pressure drop turned out to be higher than the requirements and the vibration report indicated a substantial risk of vibration problems. To solve the vibration issue and to reduce the shell side pressure drop the baffle configuration was changed to “no tubes in window”. This means that all the tubes that pass through a baffle cut window will be removed. Between each sets of baffles four support plates were installed strengthening the bundle. In order to compensate for the lost heat transfer area when tubes were removed, the cut was reduced to 24%. These modifications eliminated the vibration problem and the pressure drop was reduced substantially. The chosen design was then optimized by finding the best tube lay out and pitch ratio with respect to the thermal-hydraulic performance. The optimization process resulted in a low pressure drop and a compact design. In the following an illustration of the design is shown including key parameters. The full design specification can be found in Appendix I. The below table show input and output parameters from a HTRI simulation operating at design conditions. Bold values are calculated by HTRI.

Parameter	Value	Unit
unit	conventional	
mode	simulation	
$T_{h,i}$	61,9	[°C]
$T_{h,o}$	9,9	[°C]
$T_{c,i}$	6,1	[°C]
$T_{c,o}$	14,1	[°C]
\dot{m}_h	476,4	[tonn/hr]
\dot{m}_c	1514,7	[tonn/hr]
$p_{h,i}$	18,8	[bar]
$p_{h,o}$	18,4	[bar]
$p_{c,i}$	6,1	[bar]
$p_{c,o}$	5,1	[bar]
Rf	0,00018	[m ² K/W]
flow multiplier	1,05	
HC composition	design	

Table 6.1: conventional alternative run at design point in HTRI

Investigation of a twisted tube type shell-and-tube heat exchanger

Baffle type: single segmental, no tubes in window
 Support baffles: 4 per baffle set
 Tube type: low finned
 Bundle material: titanium



Item number	25-HA-113
TEMA type	BEM
Shell diameter	1400,00 mm
Outer tube limit	1325,45 mm
Height under inlet nozzle	328,291 mm
Height under outlet nozzle	340,991 mm
Tube diameter	22,225 mm
Tube pitch	26,781 mm
Tube layout angle	30
Number of tubes (specified)	1435
Number of tubes (calculated)	1435
Number of tie rods	0
Number of seal strip pairs	0
Number of passes	1
Baffle cut % diameter	24

TUBEPASS DETAILS			
Pass	Rows	Tubes	Plugged
1	31	1435	0

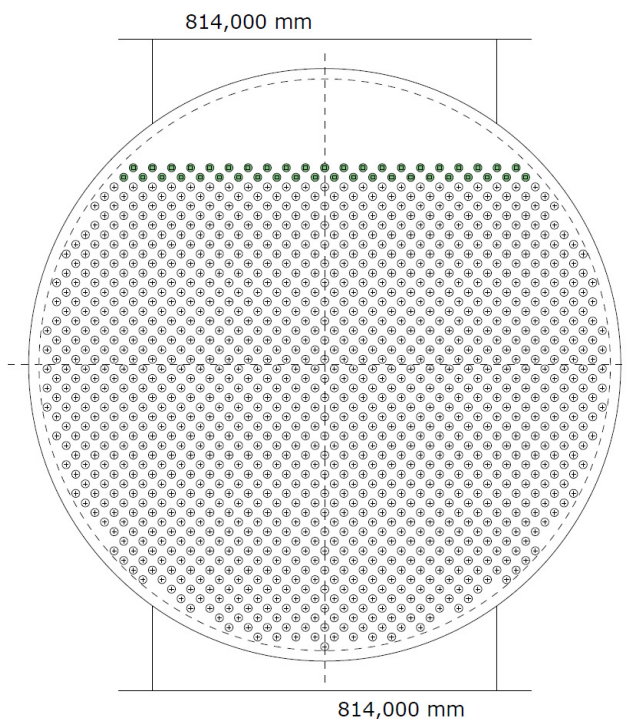
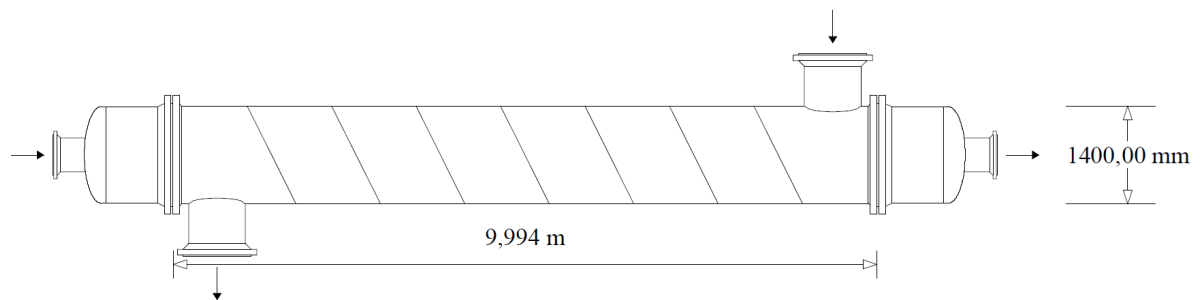
SYMBOL LEGEND	
○	Tube
⊗	Plugged tube
●	Tie rod
⊙	Impingement rod
⊕	Dummy tube
●	Seal rod
□	Seal strip/Skid bar



6.1.2 Low finned tubes with helical baffles

When Hammerfest LNG plant was built a helical baffled heat exchanger was chosen for 25-HA-113. The design was developed by Lummus Technology Heat Transfer B.V. Autumn 2008 the equipment had a break down and was replaced by a twisted tube heat exchanger. The design of the former helix exchanger is reproduced in HTRI by using data from technical drawings found in StatoilHydros electronic document storage system PIM. The drawings can be found in Appendix F. Geometrical data presented in this chapter such as size and weight is extracted from the HTRI model, while thermal-hydraulic characteristics are based on field measurements. Key parameters and an illustration of the heat exchanger are given below. See Appendix G for complete design description.

Baffle type: Double helix
 Helix angle: 30 degrees
 Tube type: low finned
 Bundle material: Titanium



Item number	25-HA-113
TEMA type	BEM
Shell diameter	1400,00 mm
Outer tube limit	1350,80 mm
Height under inlet nozzle	224,986 mm
Rows of impingement rods	2
Impingement rod diameter	19,050 mm
Height under outlet nozzle	24,600 mm
Tube diameter	19,050 mm
Tube pitch	32,000 mm
Tube layout angle	45
Number of tubes (specified)	1078
Number of tubes (calculated)	1201
Number of tie rods	0
Number of seal strip pairs	0
Number of passes	1
Baffle cut % diameter	0

TUBEPASS DETAILS			
Pass	Rows	Tubes	Plugged
1	49	1201	0

SYMBOL LEGEND

○	Tube
⊗	Plugged tube
⊙	Tie rod
⊕	Impingement rod
⊘	Dummy tube
●	Seal rod
□	Seal strip/Skid bar

6.1.3 Twisted tube

The twisted tube design developed by Koch Heat Transfer Inc. for 25-HA-113 is described in section 3.2 p25.

6.1.4 Used technique to perform an accurate comparison

A goal of the presented analysis is to compare the thermal-hydraulic performance of the conventional, helix and twisted tube heat exchanger. The determined thermal-hydraulic performance for twisted tube and helix heat exchanger is based on measurements while for the conventional shell and tube alternative HTRI output is used. By using measurement data for helix and twisted tube the uncertainty in the analysis is reduced considerably.

When one investigates the heat exchanger designs it is important that their performance can be compared on the same premises. The twisted tube and the helix units were run at various operation conditions when the used measurements were performed. In order to get a comparable output from HTRI, the conventional shell and tube heat exchanger is run at an average of these different operation conditions. At this averaged operation point HTRI will calculate one specific value for overall heat transfer and pressure drop while there are many measured values for helix and twisted tube. In order to get one comparable number from the measurements, they are averaged. By using this method the three alternatives are operated virtually at the same conditions.

The size, weight and the thermal resistance distribution of the heat exchangers are also compared. In this case values from all heat exchangers are calculated by HTRI. All three HTRI files have been run at an averaged operation point specified in Table 6.2 while Table 6.3 gives an overview of the origin to the different calculated parameters.

Parameter	Value	Unit
unit	conventional	
mode	simulation	
$T_{h,i}$	65,6	[°C]
$T_{h,o}$	10,5	[°C]
$T_{c,i}$	calculated	
$T_{c,o}$	calculated	
\dot{m}_h	535,9	[tonn/hr]
\dot{m}_c	1620,8	[tonn/hr]
$p_{h,i}$	17,1	[bar]
$p_{h,o}$	15,9	[bar]
$p_{c,i}$	6,1	[bar]
$p_{c,o}$	5,1	[bar]
CH ₄	57,5	%
C ₂ H ₆	28,0	%
C ₃ H ₈	0,2	%
N ₂	14,2	%
Rf	0,00018	m ² K/W
flow multiplier	1,0	

Table 6.2: HTRI simulation on averaged operation point for the conventional HE

Parameter	Conventional	Helix	Twisted tube
Size and weight	HTRI	HTRI	HTRI
UA	HTRI	measurement	measurement
U	HTRI	combination	combination
UA/body volume	HTRI	combination	combination
Resistance distribution	HTRI	HTRI	HTRI
Shell ΔP	HTRI	measurement	measurement
UA/shell ΔP	HTRI	combination	combination

Table 6.3: The origin of performance parameters

6.2 Results

6.2.1 Size and weight

The diagram below are based on values from HTRI calculations

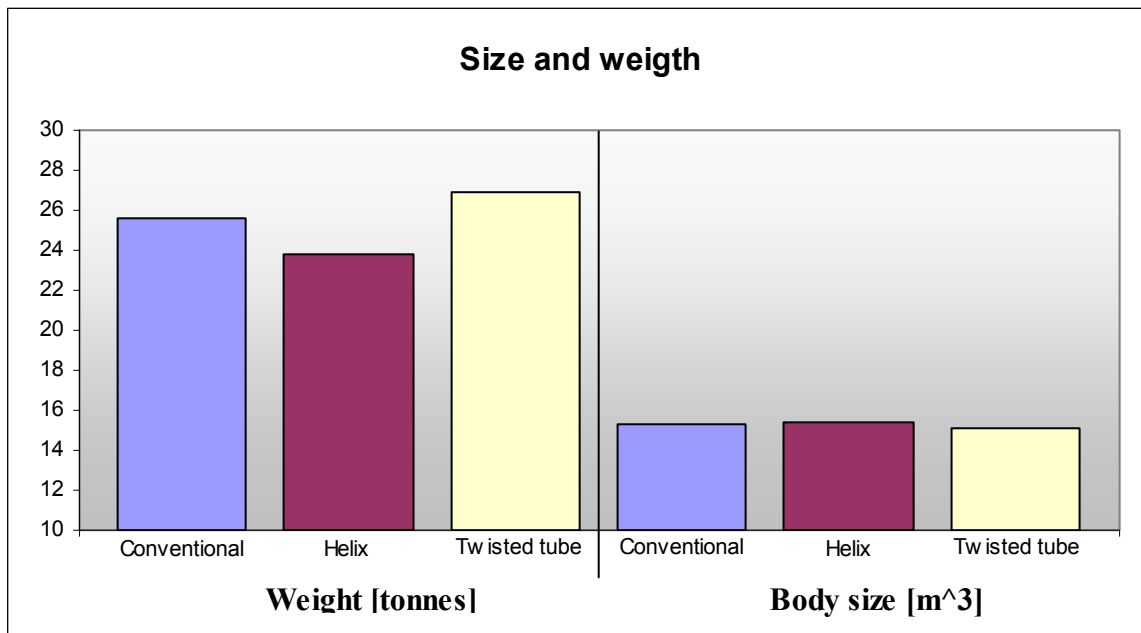


Figure 6.1: Size and weight to the three heat exchanger designs

Size and weight are important aspects of heat exchanger design. Both these parameters translate into costs and should therefore be minimized. Especially for off shore applications the volume displaced by the unit will have a substantial influence on the associated investment cost. The weight reflects the material use in the heat exchanger. In this case it is directly comparable because all three bundles are made in Titanium. Increased weight will also require additional foundation which also generates costs.

The diagram above show the three alternatives compared to each other. Their size is identical, while the weight differs. One may conclude that the use of material is more efficient in both the helix and the conventional alternative compared to twisted tube.

6.2.2 Thermal-hydraulic characteristics

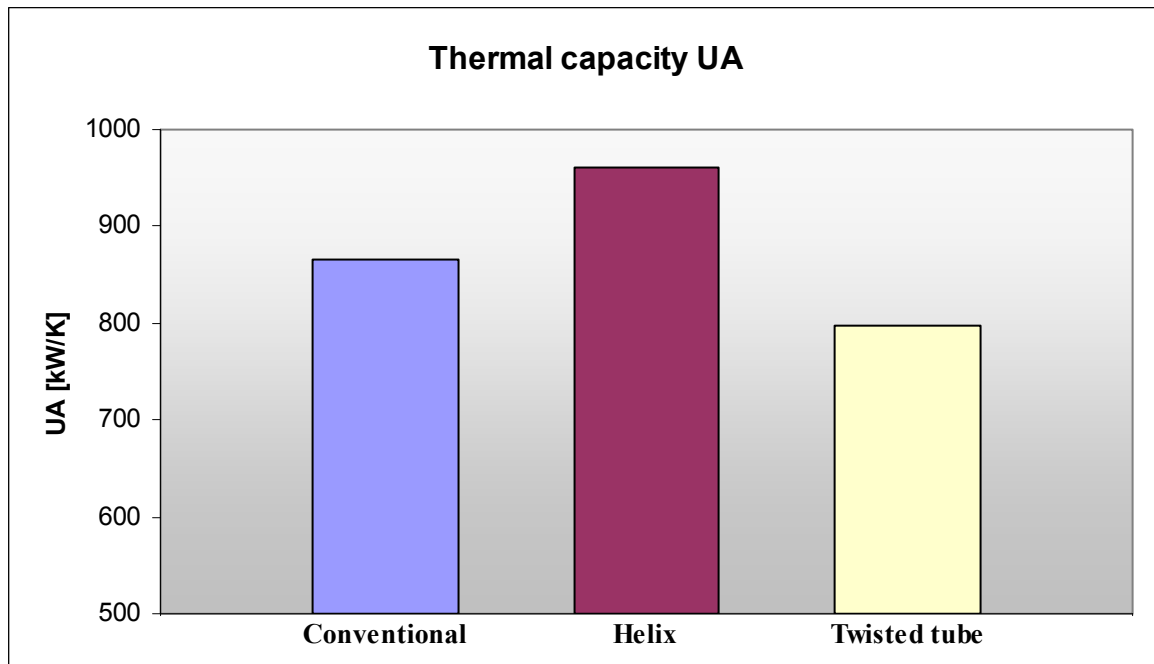


Figure 6.2: Thermal capacity of the three heat exchanger designs

The UA product reflects the heat exchanger ability to transfer heat between the working fluids. As seen in the design specification on the conventional and helix heat exchangers they have a low finned tube configuration. Their heat transfer area will therefore be larger than for the twisted tube. However, the twisted tube design should have compensated for less area by having a higher overall heat transfer coefficient U . Since these designs are developed for the same application, the UA product should be about the same in order to cool the gas stated in the design specification. The diagram shows clearly that this is not the case. This emphasizes the fact stated in Chapter 5. The twisted tube heat exchanger is under designed for the application of 25-HA-113.

The UA product is specified by the designer who can adjust the heat transfer area for the application. Therefore this parameter is not a good indicator on the thermal performance. However, if the overall heat transfer coefficient is high the area can be reduced and thereby the size of the heat exchanger. It is therefore desirable to achieve as high heat transfer coefficient as possible. Some heat exchanger concepts offers higher heat transfer coefficient than others. For this reason the overall heat transfer coefficient to the three alternatives is plotted in Figure 6.3. The coefficient is calculated by the assumption of geometry correction factor $f_g=1$. This assumption leads to a lower calculated value for helix and the conventional alternative, than the true value.

The twisted tube geometry has a very high overall heat transfer coefficient when one compare to the other alternatives. Concepts that provide high heat transfer coefficients often lead to smaller designs. Therefore one should think that the twisted tube heat exchanger could be designed smaller than the helix and conventional alternative. Figure 6.1 show that this is not the case. In this analysis the twisted tube is competing with low finned tube configurations. Heat transfer enhancement with such fins is very efficient because a large area is achieved. The advantage with fins is that a large heat transfer area can be packed into a relatively small volume. Compared to the helix and conventional heat exchanger with low fins, the twisted tube has a marginally lower heat transfer capacity to size ratio. This is shown in Figure 6.4

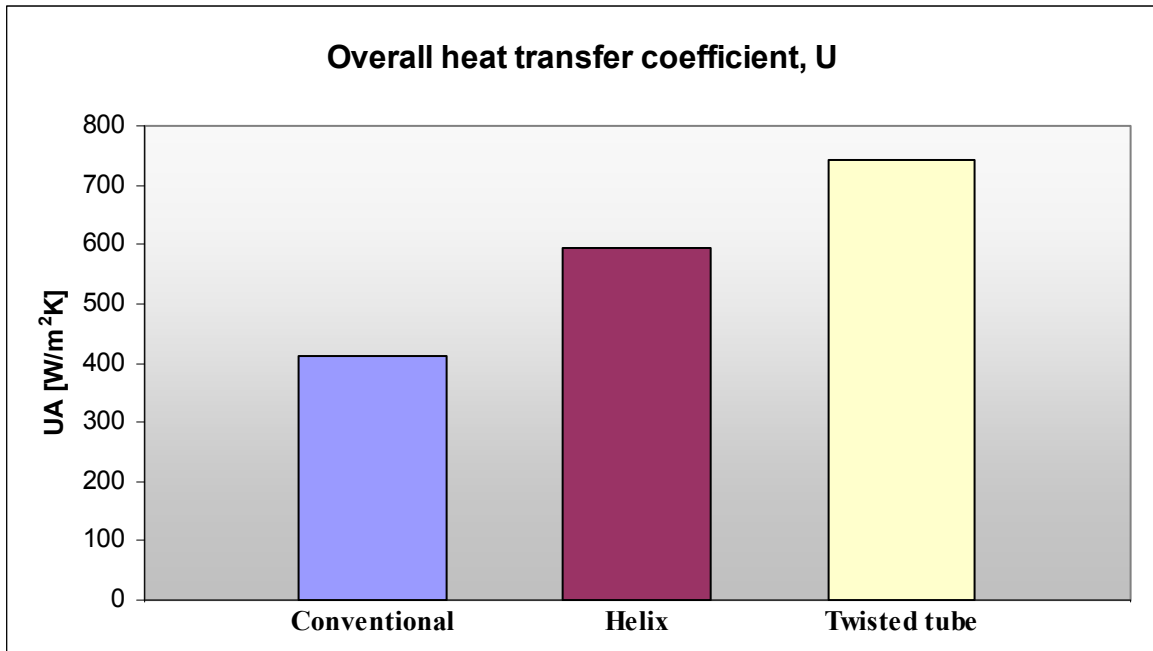


Figure 6.3: The thermal performance of the three alternatives

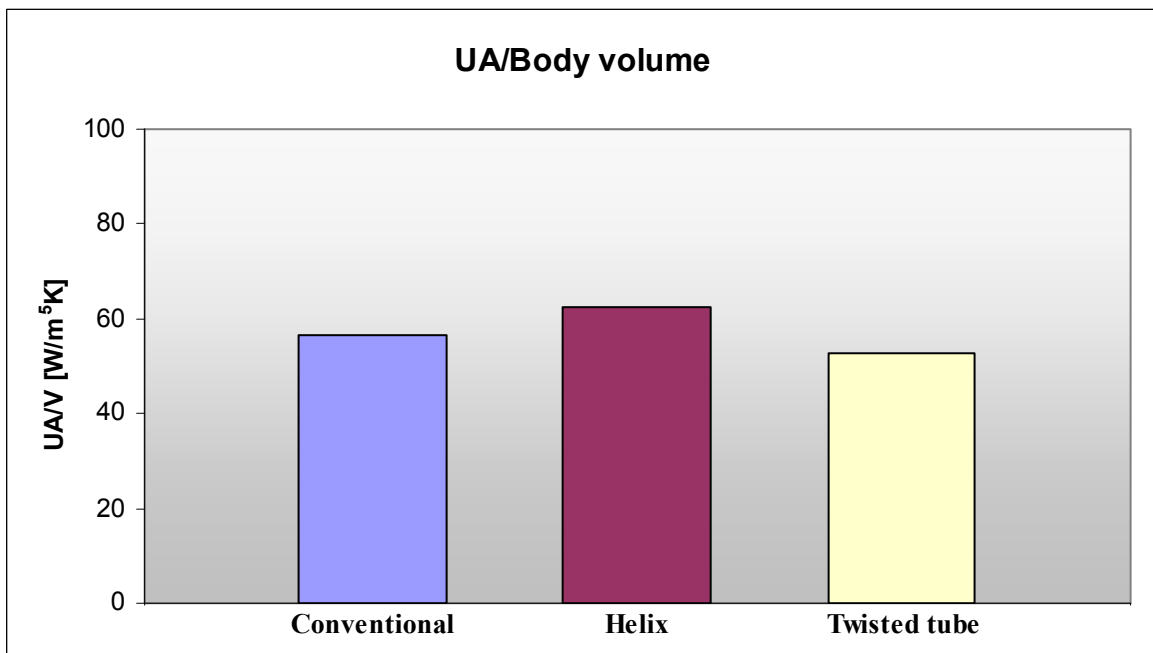


Figure 6.4: Heat transfer capacity to volume ratio

6.2.3 Thermal resistance distribution

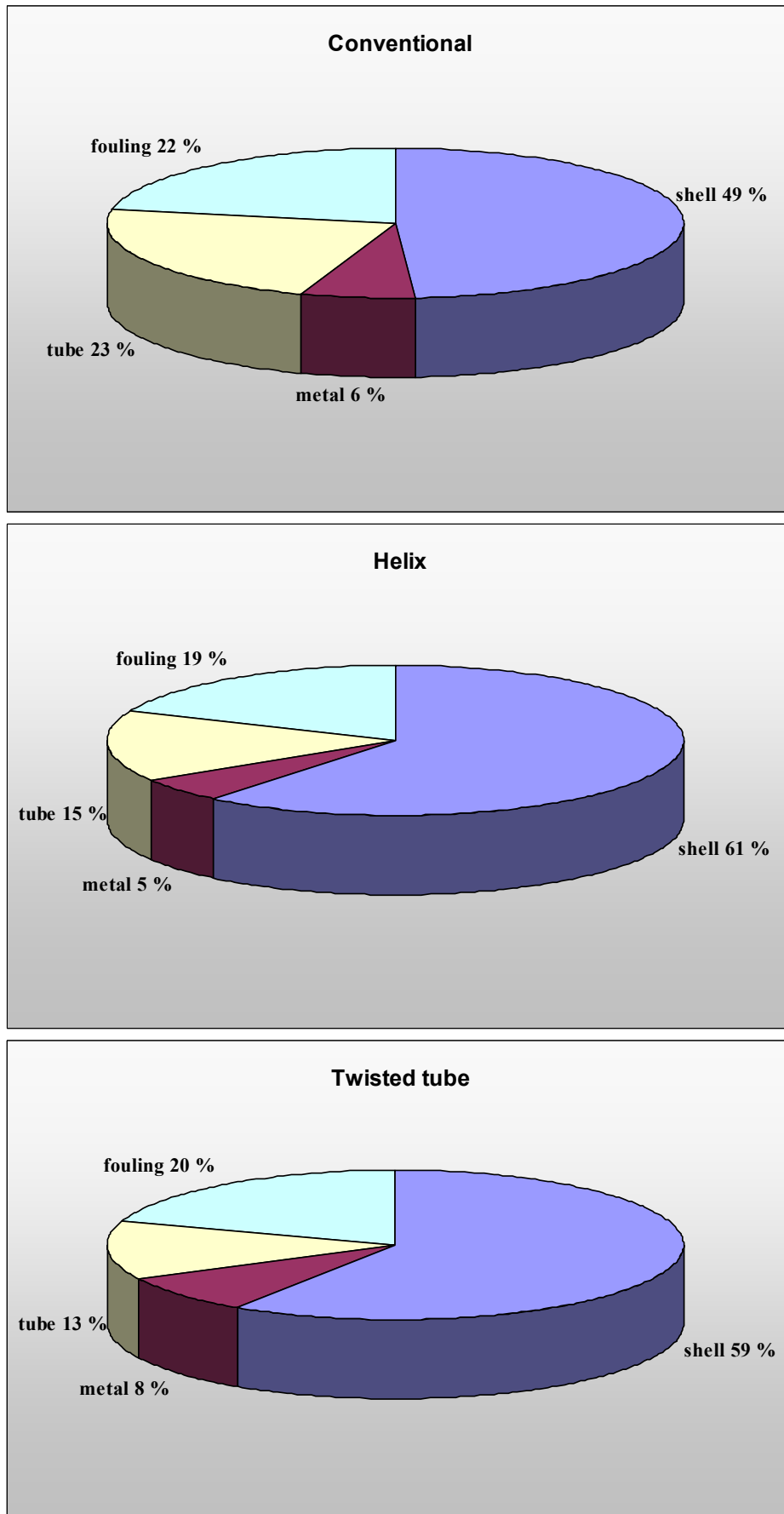


Figure 6.5: The distribution of thermal resistance for the three concepts

Figure 6.5 shows the distribution of the thermal resistance on tube side, shell side and through the metal for the three heat exchanger concepts. The numbers are based on HTRI simulations at the averaged operation point.

In the application of 25-HA-113 the shell side fluid is a hydrocarbon based gas. Gases exhibit extremely low heat transfer coefficients due to their low thermal conductivity and low density. The tube side fluid is seawater which provides higher heat transfer coefficients. Therefore it is favourable to enhance the heat transfer capacity on the shell side. This is done by using low finned tubes in the conventional and helix concept. The twisted tube has no expanded area on the shell side that will increase the heat transfer capacity. One should therefore expect that the thermal resistance on the shell side is high for twisted tube compared to the two other alternatives. The sector diagram show that this is the case to some extent, but it is not a clear pattern. The twisted tube has a shell side heat transfer area of 1071m^2 , while helix and the conventional heat exchanger have 2109m^2 and 1619m^2 respectively. It appears that the twisted tube to some extent compensate the small area by having a higher convective heat transfer coefficient on shell side relative to the other concepts.

Consideration of the tube side thermal resistance for the twisted tube show that it is very low compared to the shell side. This has obviously to do with the fact that seawater exhibits a high convective heat transfer coefficient. When one compare with the other alternatives the thermal resistance show the same tendency on the tube side. But the tube side resistance is of higher importance for helix and the conventional concepts. In these two configurations the tube side flow is inside a plain tube, in contrast to the twisted tube. As explained in section 2.3.1 the twisted shape will enhance the tube side heat transfer compared to a plain tube. This may be the reason why the thermal resistance distribution looks the way Figure 6.5 illustrates.

6.2.4 Shell side pressure drop

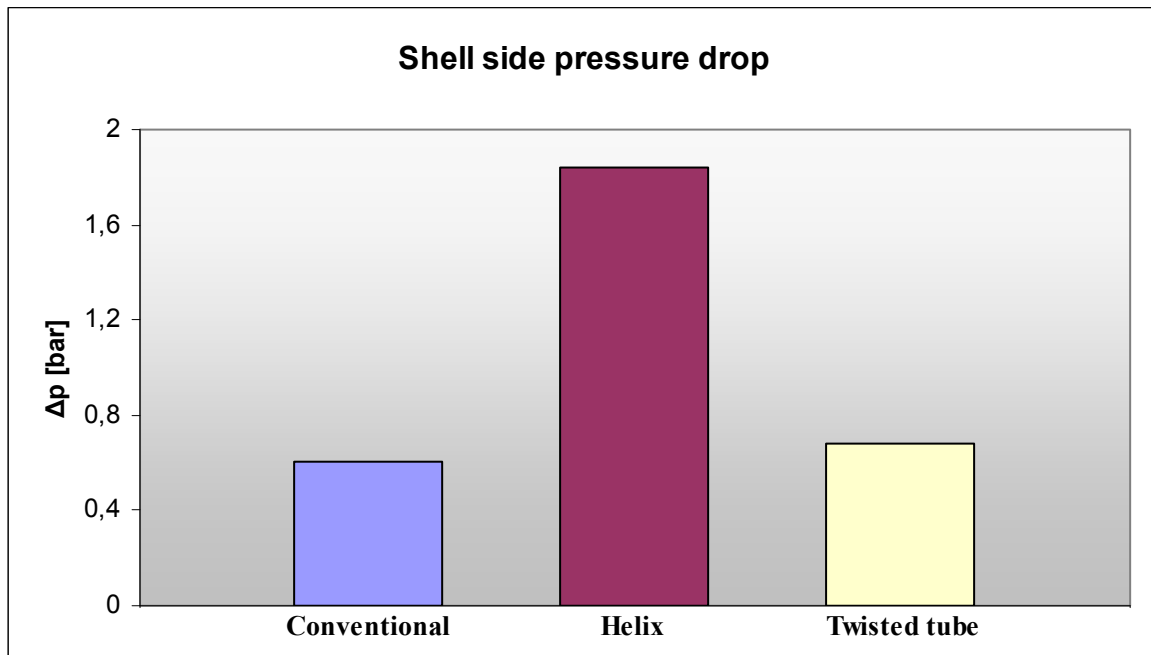


Figure 6.6: Shell side pressure drop predicted for the three concepts

The diagram above shows the shell side pressure drop for the three competing concepts. The helical baffled configuration contributes to a pressure drop on the hydrocarbon gas by almost 200 kPa. Considering that 70 kPa is specified in the design basis, this is a very high value. The twisted tube and the conventional heat exchanger perform much better with respect to pressure drop. Both designs are within the limits specified in the design basis.

When designing a heat exchanger a trade off between heat transfer and pressure loss must be considered. The ratio of these two parameters gives a good indication on the thermal-hydraulic performance of the different concepts. This ratio is presented in Figure 6.7

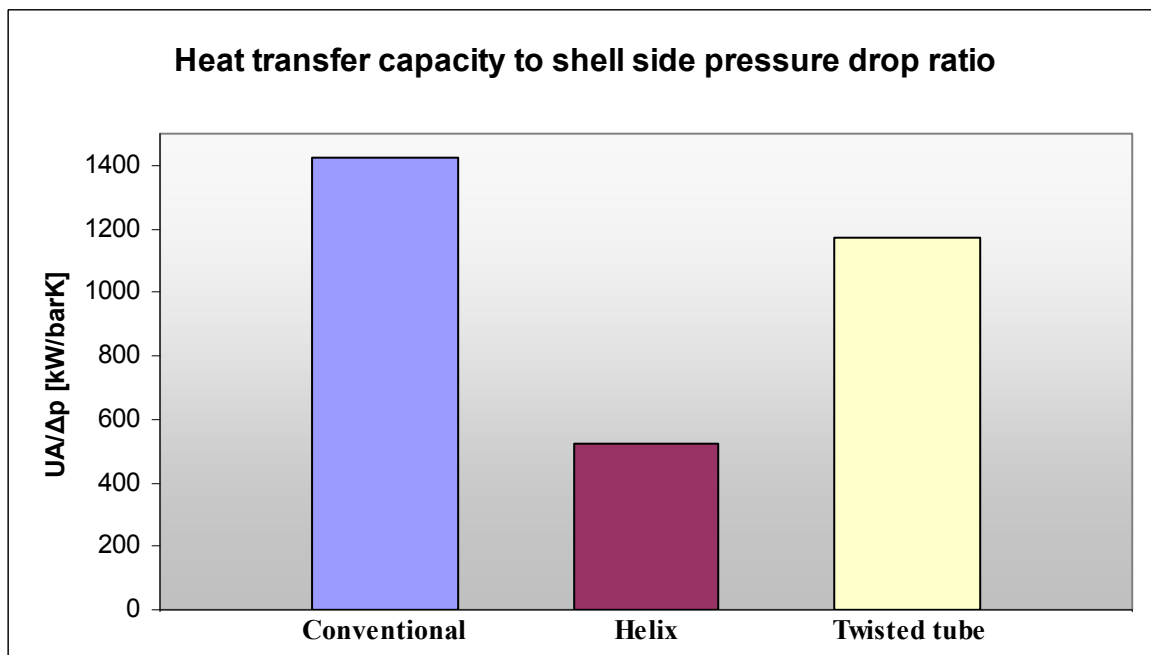


Figure 6.7: Heat transfer capacity to pressure drop ratio for the three concepts

The conventional heat exchanger achieves the highest heat transfer capacity to pressure drop ratio followed by the twisted tube. As a result of the substantial shell side pressure loss in the helix concept this unit has a low thermal-hydraulic performance. All the results presented in this chapter are summed up in the table below.

	Conventional	Helix	Twisted tube
ID	1400	1400	1390 mm
Tube Length	9,93	9,994	9,926 m
Tube OD	22,225	19,05	22,225 mm
Tube thickness	1,734	1,25	1,734 mm
Number of tubes	1435	1078	1591
Pitch	26,78	32	27,781
Lay out	30	45	60 degrees
Effective area	2109,03	1618,85	1070,87 m ²
Weigth dry	25,648	23,797	26,878 kg
U fouled	410	593	744 W/m ² K
Shell Δp	0,60692	1,84	0,68 bar
Body volume	15,29	15,38	15,06 m ³
Area/volume	137,97	105,23	71,10 1/m
UA	865,38	959,98	796,73 W/K
UA/volume	56,61	62,40	52,90 W/m ³ K
UA/ Δp shellside	1425,85	521,73	1171,66 kW/barK
U/ Δp shellside	676,07	322,28	1094,12 W/m ² barK

Table 6.4: Summery of the numbers given in chapter 6

6.2.5 Fouling

Dead spot is a location in the heat exchanger where the flow has low velocity relative to the bulk velocity. This may result in extreme temperatures in the actual regions. At such locations the risk for development of a fouling layer is increased. The twisted tube geometry provoke circulation and mixing on both tube and shell side. This not only improves the heat transfer coefficient but also avoid the risk for dead spots in the heat exchanger. How the 25-HA-113 twisted tube unit performs with respect to fouling is presented in section 5.4. The helical baffled exchanger has the same properties on this issue. Such baffle configuration ensures a smooth flow path lowering the risk for dead spots.

In the segmental baffled heat exchanger the flow is turned vertically by the baffles. Such flow pattern will have an uneven velocity distribution in the turns. At these locations the flow has low velocity close to the shell wall. This makes the segmental baffled design most exposed to fouling.

6.2.6 Vibration

Vibration has been the cause of many heat exchanger break downs. These vibrations arise when fluid is passing the tubes on the shell side. There are two ways to overcome the vibration problem. One can strengthen the bundle construction by installing more baffles. The other solution is to change the flow direction to a more favourable one such that the flow induced vibration is reduced. The twisted tube uses both solutions. This is done by directing the flow along the tubes and by supporting each tube six times to the adjacent tubes per 360 degree twist. Such design gives a very rigid construction that is so to speak vibration free. Why the twisted tube is not exposed to flow induced vibration is discussed in more detail in section 2.5.

In contrast the segmental baffled heat exchanger has two unfavourable design properties that make it vulnerable to vibrations. The flow is passing perpendicular to the tubes inducing severe vibration. In addition there is a large distance (relative to the twisted tube) between each location where the tube is supported by the baffle. The tubes will therefore have a relatively low eigen frequency making them more exposed to flow induced vibration. The helical baffled heat exchanger is also vulnerable to vibration in the same way as the segmental baffled configuration. This can be solved to some extent by installing two helix baffles and thereby give additional support to the tubes. However it must be emphasized that the helical baffled design presented in this analysis had a broke down due to vibrations. This underlines the fact that the double helix can be exposed to a vibration problem if the design is unfavourable.

6.2.7 Qualitative summery of the differences in performance

The twisted tube design is an alternative to more traditional designs like a conventional shell and tube exchanger with single segmental baffles or helical baffles. In the present analysis the twisted tube is compared to these two designs equipped with low finned tubes. Only one application where gas is cooled by seawater is considered here. A comparison may be different for other applications.

The thermal performance of the twisted tube is very good compared to the two alternatives. On the other hand the heat transfer area on the shell side is small on shell side were the heat transfer coefficient is limited. The twisted tube is not able to fully compensate the small area with higher overall heat transfer coefficient. This problem could be solved by designing the heat exchanger with more tubes providing a larger area. But then the concept is no longer competitive in terms of size and weight.

The hydraulic performance of the twisted tube is good, but the conventional alternative perform even better for this application. The double helix baffled heat exchanger has a poor hydraulic performance. It may be a design error rather than a general pattern for this type of units that cause the high pressure drop.

Fouling is an unpredictable phenomenon. Investigation of the development of the overall heat transfer coefficient for 25-HA-113 in section 5.4 shows that the fouling tendency is minimal or may even be negligible. In addition to this analysis the flow pattern in the twisted tube is most probably uniform and free of dead spots due to the geometry. A helical baffled unit will also have a continuous flow pattern which prevents fouling. The conventional unit with single segmental baffles will have a higher risk of developing a fouling layer. This is due to its baffle geometry and the resulting uneven velocity distribution.

The twisted tube concept is a practically speaking vibration free concept as a result of how the bundle is designed. Both the helix alternative and conventional alternative will be more exposed to vibration problems even if the bundles are strengthened with shorter baffle spacing.

The twisted tube alternative will be recommended for the application of 25-HA-113. Considering that the application has shown potential for vibration issues, the selection of this unit is rational. In addition to superior vibration properties this type has show acceptable thermal performance and good hydraulic performance. Also with respect to fouling the twisted tube shows very promising characteristics.

7 Conclusion

This thesis investigates twisted tube type shell-and-tube heat exchangers in general. It is emphasized on the thermal-hydraulic characteristics, fouling and vibration properties. In order to gather information on performed research on this type of heat exchangers an extensive literature study has been carried out. In addition, measurements done by StatoilHydro on a twisted tube unit installed at LNG Hammerfest, have been analysed and discussed. The heat exchanger design software HTRI Xist Xchanger has been used as a tool for the analysis and the accuracy of the program is evaluated.

The performed literature study returned a limited amount of information on the twisted tube heat exchanger. It appears that research work performed on heat transfer enhancement by inducing swirl flow is mainly directed towards the application of twisted tape inserts in plain tubes. However, useful information and mathematical correlations for heat transfer and pressure loss were collected.

The literature study forms the basis for the heat transfer correlations presented in this report. It is a challenging task due to the varieties of correlations for heating, cooling, gas and liquid applications. By extracting correlations from multiple sources it was possible to present reliable formulas for heat transfer in twisted tubes.

Koch Heat Transfer Incorporated has developed a special program module that can be added to the ordinary HTRI Xchanger Suite software. The reliability of this program module has been investigated by comparison with field measurements performed on a twisted tube heat exchanger in operation. Xist Xchanger Suite can evaluate heat exchanger designs in two different modes: rating and simulation mode. In rating mode Xist Xchanger Suite calculate only one output parameter. Since the duty is specified by the user calculation accuracy is very high for temperatures and mass flow rates. However, the overall heat transfer coefficient is overestimated by a factor of 1,5, while the shell side pressure loss is overestimated by a factor of 1,4.

In simulation mode the user is allowed to calculate two output parameters with the program. This implies that the duty of the specified unit is not given. The program uses heat transfer correlations and the geometry to calculate the output values. It appears that the accuracy of these calculations depends very much on which two parameters that is determined by the software. Calculation of both mass flow rates resulted in a calculation error reaching almost +200% while calculation of both outlet temperatures had an accuracy of +/- 7%. The same tendency was found in simulation mode as for rating mode with respect to thermal-hydraulic calculations. Overall heat transfer coefficient is overestimated by approximately 1,5 and the pressure drop is overestimated by a factor of 1,4. It means that Xist Xchanger Suite calculates the shell side pressure drop conservatively, but the heat transfer coefficient is overestimated.

An evaluation of StatoilHydro 25-HA-113 twisted tube heat exchanger design has been carried out. Analysis of measurement data performed on the unit show that the thermal performance is too low compared to the specifications in design basis E066-AB-P-DP-2546. However, the shell side pressure loss is lower than specified in the design. Fouling has been investigated by considering the overall heat transfer coefficient over time. The analysis shows that the fouling effect is minimal.

The twisted tube concept has been compared quantitatively with a conventional and a helix baffled shell-and-tube heat exchanger. The specified application was LNG Hammerfest 25-HA-113 intercooler. With respect to thermal characteristic the twisted tube has the highest

overall heat transfer coefficient. However, the two other alternatives have higher thermal capacity for the same unit size. This is due to the low finned tubes in the conventional and helix unit that provide large heat transfer area per volume unit.

The conventional alternative has a somewhat lower shell side pressure loss than twisted tube, but both units are within the design specification. The helix heat exchanger has a very poor hydraulic performance. This may be a result of a design error on the specific unit that is considered.

Twisted tube has an advantage with respect to fouling and vibration issues. Fouling is low due to the flow pattern in this type of unit. The helix alternative is also expected to have small risk of fouling. The conventional concept is more exposed to fouling due to flow pattern and the resulting uneven velocity distributions.

Twisted tube has superior properties with respect to the vibration issue due to a very rigid bundle construction. Process history has show that both competing alternatives may be subject to a vibration problem. Considering the bundle rigidness, fouling characteristics and good thermal-hydraulic properties, the twisted tube heat exchanger was recommended for the application of 25-HA-113.

8 Proposal for further work

The topic in this thesis has been investigation of a twisted tube type shell-and-tube heat exchanger, with the following focus.

1. Presenting reliable correlations for convective heat transfer coefficients
2. Consideration of the calculation accuracy for twisted tube in HTRI Xchanger Suite v5.00
3. Investigation of a particular twisted tube design for a gas to liquid application by use of measurement data.
4. Benchmarking of a twisted tube, a helix baffled and a conventional baffled unit for the same gas to liquid application by use of HTRI Xchanger Suite and measurement data.

The correlations found for heat transfer coefficients and pressure loss are only presented and used to investigate a particular twisted tube design. It would have been interesting to plot these correlations and compared them to traditional correlations for conventional shell-and-tube heat exchangers. Such plots would more clearly show the strengths and weaknesses of the twisted tube concept.

Heat transfer correlations vary for different applications. Therefore one should have heat transfer correlations available for shell side, tube side, heating, cooling, gas and liquid applications. Correlations for all this applications were not found in the literature study. In order to verify the found correlations and to complete the set of equations it would have been desirable to put up a complete twisted tube test rig in the laboratory.

It was stated in this thesis that the calculation accuracy for twisted tube in HTRI Xchanger Suite is low for pressure drop and heat transfer coefficient calculations. These accuracy predictions rely on measurement from one single unit. To verify this statement it is recommended to collect measurement data from more twisted tube units and to compare them with HTRI output. It had also been very interesting to determine what kind of correlations this software rely on. This can either be done by a communication with Koch Heat Transfer who has developed the program or by running numerous simulations were the right parameters are varied. With right parameters is meant the parameters that pressure loss and heat transfer depend on. On this basis one can come up with suggestions on how the program correlations can be changed and thereby increase the calculation accuracy.

In this thesis only a gas to liquid application is investigated for the twisted tube concept. It is desirable to examine how the twisted tube design performs in other applications including liquid to liquid, gas to gas and applications were the fluid is changing phase. The proposal for further work can be summed up in the following points.

1. Evaluation of present heat transfer correlations for twisted tube compared to correlations for a conventional shell and tube heat exchanger
2. Establishment of a complete test rig for verification of existing heat and pressure correlations and for completion of the set of equations.
3. Collection of measurement data from more twisted tube units and verification of the calculation accuracy in HTRI for more applications. In addition, it is interesting to determine the pressure and heat correlations that are implemented in the program. On this basis one can suggest how the accuracy can be improved.
4. Evaluation of the twisted tube performance for liquid to liquid, gas to gas and applications were the fluid is changing phase.

References

1. Koch, H.t.c., *Twisted tube heat exchangers*.
2. Morgan, R.D., *Twisted tube heat exchanger technology*.
3. Ljubicic, B., *Testing of Twisted-Tube Exchangers in Transition Flow Regime*.
4. Dzyubenko, B.V., *Modeling and Design of Twisted Tube Heat Exchangers*. 2000: Begell House Inc. Publishers. 203.
5. Asmantas, L.A., *Coefficients of Heat Transfer and Hydraulic Drag of a Twisted Oval Tube*. HEAT TRANSFER-Soviet Research, 1985. 17.
6. Ljubicic, B., *Twisted Tube Heat Exchangers: Technology and Application*.
7. Numericana. *Perimeter of an Ellipse*. [Web page] 2009; Available from: www.numericana.com/answer/ellipse.htm.
8. White, F.M., *Fluid mechanics*. 2003, Boston, Mass.: McGraw-Hill. XIII, 866 s.
9. Engineeringtoolbox. *Equivalent diameter*. [Web page] 2005; Available from: <http://www.engineeringtoolbox.com/>.
10. Kays, W.M., M.E. Crawford, and B. Weigand, *Convective heat and mass transfer*. 2005, Boston: McGraw-Hill. XXX, 546 s.
11. Incropera, F.P. and D.P. DeWitt, *Fundamentals of heat and mass transfer*. 2002, New York: Wiley. XIX, 981 s.
12. Mukherjee, R., *Practical thermal design of shell-and-tube heat exchangers*. 2004, New York: Begell House. XI, 228 s.
13. D. Butterworth, A.R.G., J. J. Welkey, *Design and application of twisted-tube exchangers*.
14. Allards, S., *The Twisted Tube Heat Exchanger AlfaTwist*. 2007.
15. Hydrocarbons-technology.com. *Snohvit LNG Export Terminal, Melkoya Island, Hammerfest, Norway*. 2009; Available from: <http://www.hydrocarbons-technology.com>.
16. Gwinner, M., *25-HA-113 Process data sheet*. 2002.
17. Gertsbakh, I., *Measurement theory for engineers*. 2003, Berlin: Springer. XIII, 150 s.
18. Wheeler, A.J. and A.R. Ganji, *Introduction to engineering experimentation*. 2004, Upper Saddle River, N.J.: Pearson/Prentice Hall. XI, 452 s.
19. Cryotronics, L. *DIN IEC 751 Temperature/Resistance Table for Platinum Sensors* 2007; Available from: <http://www.lakeshore.com/>.
20. LMNO Engineering, R.a.S.L. *Venturi flowmeter calculation of liquid flow*. 2005; Available from: <http://www.lmnoeng.com>.

Appendix A Description of the performed literature study

Search terms

“Twisted tube heat exchanger”

“Twisted tube” + “heat exchanger”

“Heat exchanger with twisted tube”

Search tools used

Science Direct (Elsevier)

Science Direct is an information source for scientific, technical, and medical research. It is searched using the Scirus search engine. Scirus is one of the most comprehensive science-specific search engine available on the Internet. Driven by the latest search engine technology, it enables scientists, students and anyone searching for scientific information to chart and pinpoint data, locate university sites and find reports and articles quickly and easily. It was launched by Elsevier Science, the leading international publisher of scientific information.

Address: <http://www.sciencedirect.com/>

Compendex (Engineering Village 2)

Compendex is one of the most comprehensive interdisciplinary engineering database in the world with over 9 million records referencing 5,000 engineering journals and conference materials dating from 1884.

Address: <http://www.engineeringvillage2.org>

Google scholar

Google Scholar is a freely-accessible web search engine that indexes the full text of scholarly literature across an array of publishing formats and disciplines. Released in November 2004, the Google Scholar index includes most peer-reviewed online journals of the world's largest scholarly publishers. It is similar in function to the freely-available Scirus from Elsevier, CiteSeer, and getCITED. It is also similar to the subscription-based tools, Elsevier's Scopus and Thomson ISI's Web of Science.

Address: <http://scholar.google.com/>

Google

As of August 2007, Google is the most used search engine on the web with a 53.6% market share, ahead of Yahoo (19.9%) and Live Search (12.9%). Google indexes billions of Web pages, so that users can search for the information they desire, through the use of keywords and operators, although at any given time it will only return a maximum of 1,000 results for any specific search query.

Address: <http://www.google.com>

Appendix B Measurement data 25-HA-113 twisted tube

Date	Tin HC [°C]	Tout HC [°C]	Flow HC [°C]	Tin W [°C]	Tout W [°C]	Flow W [l/hr]	P in [bar]	P out [bar]	DP [bar]	Duty [kW]	C1 [%]	C2 [%]	C3 [%]	N2 [%]	U [W/m²K]	LMTD [°C]	Faktor	A [m²]
26.11.08 23:00	69,12	11,83	524,17	5,93	16,11	1399,40	17,61	16,95	0,66	15907,86	53,50578	28,66585	0,576576	17,25179	692,7	21,46405	1,000	1070
28.11.08 0:00	69,24	11,84	519,92	6,95	16,17	1469,66	17,42	16,77	0,65	15815,43	53,318	29,06156	0,578248	17,04219	731,4	20,20787	1,000	1070
28.11.08 5:30	69,15	11,75	518,86	6,83	16,10	1459,20	17,37	16,72	0,65	15781,50	53,25	29,14	0,58	17,03	729,1	20,23034	1,000	1070
29.11.08 0:00	69,50	11,77	518,32	6,86	16,08	1474,07	16,92	16,25	0,67	15840,91	53,14	29,37	0,58	16,90	728,9	20,31121	1,000	1070
29.11.08 6:30	69,85	11,79	518,29	6,81	16,16	1461,73	16,90	16,23	0,67	15935,00	53,05	29,50	0,58	16,87	727,2	20,47847	1,000	1070
29.11.08 17:00	71,42	11,93	522,73	6,83	16,41	1468,30	17,12	16,44	0,68	16403,63	52,53	29,25	0,57	17,66	730,8	20,9769	1,000	1070
01.12.08 0:00	71,85	11,52	520,79	6,37	16,04	1465,95	16,94	16,27	0,67	16539,50	51,97	29,66	0,56	17,80	727,1	21,25998	1,000	1070
01.12.08 20:00	67,57	11,27	511,69	6,53	15,45	1451,34	16,48	15,82	0,66	15103,57	51,89	29,81	0,55	17,74	714,1	19,76681	1,000	1070
03.12.08 6:00	72,34	11,89	521,20	6,69	16,50	1450,76	17,01	16,30	0,70	16591,66	51,52	30,18	0,55	17,75	727,0	21,32783	1,000	1070
03.12.08 3:00	72,24	11,79	521,25	6,60	16,38	1454,80	17,01	16,34	0,68	16590,73	51,53	30,13	0,55	17,79	727,0	21,32781	1,000	1070
06.12.08 12:00	67,73	10,69	542,55	6,38	13,99	1848,51	19,00	18,35	0,65	16409,17	56,72	24,95	0,00	18,33	783,0	19,58468	1,000	1070
06.12.08 14:00	66,24	10,63	542,72	6,43	13,85	1849,03	19,04	18,39	0,65	16005,92	56,48	25,39	0,01	18,13	783,8	19,0859	1,000	1070
07.12.08 18:00	71,32	10,68	524,05	6,20	14,06	1841,94	18,07	17,42	0,65	16879,18	53,22	29,54	0,02	17,22	761,8	20,7063	1,000	1070
24.12.08 3:00	61,18	9,57	548,91	5,85	12,49	1915,42	16,74	15,98	0,76	14851,12	52,78	29,99	0,05	17,19	793,5	17,49224	1,000	1070
31.12.08 3:00	61,56	9,71	551,97	5,95	12,63	1927,87	17,21	16,45	0,76	15025,78	52,56	30,16	0,03	17,25	797,9	17,59976	1,000	1070
03.01.09 3:00	65,51	10,22	540,33	5,73	14,39	1539,78	17,24	16,52	0,71	15560,45	50,87	30,34	0,04	18,75	758,9	19,16214	1,000	1070
06.01.09 3:00	65,91	10,14	515,86	5,68	14,32	1500,79	16,92	16,23	0,68	15132,19	53,91	28,21	0,22	17,66	734,4	19,25728	1,000	1070
17.01.09 3:00	70,48	9,95	500,40	5,27	14,52	1497,00	16,92	16,28	0,64	16155,52	59,41	22,90	0,60	17,09	730,4	20,67236	1,000	1070
19.01.09 3:00	65,20	9,83	531,92	5,12	14,36	1445,34	17,70	17,00	0,70	15578,73	52,57	30,10	0,52	16,81	751,3	19,37897	1,000	1070
21.01.09 12:00	68,08	9,21	524,58	4,28	13,94	1451,96	17,78	17,11	0,68	16372,50	52,91	29,73	0,51	16,86	744,8	20,54393	1,000	1070
26.01.09 3:00	72,29	9,54	521,09	4,34	14,58	1441,89	17,04	16,34	0,70	17219,34	51,60	30,31	0,45	17,64	737,4	21,82318	1,000	1070
28.01.09 13:00	71,94	9,56	492,43	4,65	14,32	1443,60	16,90	16,28	0,63	16282,56	52,33	30,44	0,46	16,76	711,0	21,404	1,000	1070
29.01.09 3:00	72,91	9,68	519,00	4,43	14,74	1442,27	17,33	16,65	0,68	17357,33	52,16	30,07	0,46	17,31	737,3	22,00106	1,000	1070
31.01.09 3:00	69,45	9,82	530,40	4,74	14,71	1452,89	17,46	16,75	0,72	16895,66	54,01	29,79	0,44	15,76	756,2	20,88223	1,000	1070
02.02.09 0:00	61,88	9,32	520,26	4,97	13,49	1458,30	18,62	18,00	0,62	14498,33	53,76	29,06	0,10	17,07	741,2	18,28089	1,000	1070
Average	68,56	10,64	524,15	5,86	14,87	1542,07	17,39	16,71	0,68	16029,34	53,24	29,03	0,38	17,35	742,3	20,21	1,00	1070,00

Appendix C Measurement data 25-HA-113 double helix

Date	Tin HC [°C]	Tout HC [°C]	Flow HC [°C]	Tin W [°C]	Tout W [°C]	Flow W [l/h/m]	P in [bar]	P out [bar]	DP [bar]	Duty [kWh]	C1 [%]	C2 [%]	C3 [%]	N2 [%]	U [W/m²K]	LMTD [°C]	F faktor	A [m²]
15.08.08 6:00	58,01	9,82	546,13	6,74	14,10	1677,94	0,00	0,00	0,00	14402,07	61,40	27,82	0,20	10,58	596,6	15,35726	1,000	1571,9
20.08.08 12:00	57,55	9,96	552,03	6,94	14,10	1726,28	0,00	0,00	0,00	14411,09	63,01	26,33	0,11	10,55	604,7	15,16131	1,000	1571,9
26.08.08 0:00	57,49	10,52	564,04	7,35	14,72	1695,30	0,00	16,93	-16,93	14582,01	63,20	26,46	0,04	10,30	609,1	15,22983	1,000	1571,9
26.08.08 6:00	58,15	9,97	536,86	6,93	14,19	1673,10	0,00	16,54	-16,54	14172,79	62,32	26,76	0,08	10,84	588,2	15,32797	1,000	1571,9
27.08.08 7:00	59,37	9,75	533,17	6,86	13,71	1812,39	0,00	16,27	-16,27	14498,15	62,12	27,02	0,09	10,77	594,8	15,50612	1,000	1571,9
27.08.08 12:00	59,73	9,89	532,48	7,01	13,85	1824,29	0,00	16,25	-16,25	14562,98	62,06	27,28	0,09	10,57	596,3	15,53781	1,000	1571,9
28.08.08 18:00	59,92	10,04	532,76	6,88	14,37	1668,13	17,71	16,07	16,07	14563,63	61,81	27,51	0,09	10,59	583,5	15,87798	1,000	1571,9
30.08.08 18:00	54,27	9,61	524,72	6,99	13,44	1693,40	16,77	15,11	1,66	12746,76	62,44	27,02	0,01	10,53	582,2	13,92829	1,000	1571,9
01.09.08 1:00	64,03	9,90	499,68	6,91	14,32	1745,78	17,34	15,88	1,45	15106,60	67,28	22,68	0,22	9,81	578,0	16,62812	1,000	1571,9
01.09.08 21:00	65,09	10,50	529,33	7,13	15,14	1717,22	17,76	16,14	1,62	16033,74	66,37	22,75	0,21	10,67	590,5	17,27295	1,000	1571,9
05.09.08 12:00	65,80	10,70	550,92	7,02	15,50	1675,29	17,58	15,81	1,77	16585,97	62,29	25,75	0,20	11,76	591,6	17,83664	1,000	1571,9
06.09.08 9:00	56,60	9,97	529,24	7,11	13,99	1714,70	16,71	14,98	1,72	13762,25	69,00	22,36	0,01	8,63	595,3	14,70621	1,000	1571,9
07.09.08 3:00	65,07	10,53	541,20	7,04	15,23	1695,30	16,87	15,08	1,79	16191,67	64,17	24,67	0,03	11,12	591,0	17,13231	1,000	1571,9
07.09.08 18:00	64,71	10,48	530,82	7,15	15,07	1705,24	16,64	14,90	1,74	15748,51	63,84	24,73	0,04	11,40	584,8	17,13231	1,000	1571,9
08.09.08 21:00	71,06	11,76	573,77	7,55	16,99	1699,19	17,49	15,53	1,95	18708,11	63,16	25,47	0,04	11,33	609,3	19,53467	1,000	1571,9
09.09.08 13:00	69,80	11,26	556,36	7,29	16,36	1688,88	16,92	15,02	1,90	17875,71	63,03	25,71	0,04	11,22	597,5	19,03418	1,000	1571,9
10.09.08 3:00	70,48	11,17	562,62	7,06	16,36	1687,32	16,96	15,02	1,94	18307,23	62,83	25,89	0,04	11,24	600,2	19,40453	1,000	1571,9
10.09.08 20:00	67,11	10,97	583,35	6,84	15,95	1673,85	17,05	14,98	2,06	17785,27	59,13	29,67	0,04	11,16	605,4	18,68815	1,000	1571,9
11.09.08 6:00	65,83	10,90	577,49	6,93	15,77	1668,55	16,83	14,79	2,04	17211,96	59,14	29,81	0,04	11,01	602,0	18,19019	1,000	1571,9
14.09.08 0:00	64,48	10,62	574,28	6,85	15,32	1670,76	16,37	14,29	2,08	16514,23	56,24	31,33	0,05	12,39	594,5	17,67304	1,000	1571,9
16.09.08 6:00	65,35	10,90	563,61	7,21	15,62	1657,22	16,09	14,08	2,02	16257,56	54,42	32,19	0,05	13,34	584,0	17,7106	1,000	1571,9
17.09.08 21:00	59,32	10,31	536,33	7,26	14,49	1641,02	15,32	13,40	1,92	13836,93	54,18	32,73	0,05	13,04	566,5	15,53761	1,000	1571,9
19.09.08 12:00	63,12	10,71	563,87	7,12	15,21	1675,99	16,42	14,45	1,98	15829,70	58,76	28,46	0,17	12,61	588,7	17,10661	1,000	1571,9
Average	62,71	10,45	547,61	7,05	14,95	1699,44	16,87	15,03	1,84	15638,91	61,83	26,97	0,08	11,11	592,8	16,77	1,00	1571,90

Appendix D Data sheets for measurement sensors

HC GAS PRESSURE MEASUREMENTS

2600T Pressure Transmitters
Model 264DS, 264PS, 264VS

SS/264XS_1

Functional Specifications

Range and span limits

Sensor Code	Upper Range Limit (URL)	Lower Range Limit (LRL)			Minimum span	
		264DS differential	264PS gauge	264VS absolute	264DS differential 264PS gauge	264VS absolute
B	4kPa 40mbar 16inH ₂ O	-4kPa -40mbar -16inH ₂ O	-4kPa -40mbar -16inH ₂ O		0.134kPa 1.34mbar 0.54inH ₂ O	
E	16kPa 160mbar 64inH ₂ O	-16kPa -160mbar -64inH ₂ O	-16kPa -160mbar -64inH ₂ O	0.07kPa abs 0.7mbar abs 0.5mmHg	0.27kPa 2.7mbar 1.08inH ₂ O	0.27kPa 2.7mbar 2mmHg
F	40kPa 400mbar 160inH ₂ O	-40kPa -400mbar -160inH ₂ O	-40kPa -400mbar -160inH ₂ O	0.07kPa abs 0.7mbar abs 0.5mmHg	0.4kPa 4mbar 1.6inH ₂ O	0.67kPa 6.7mbar 5mmHg
G	65kPa 650mbar 260inH ₂ O	-65kPa -650mbar -260inH ₂ O	-65kPa -650mbar -260inH ₂ O	0.07kPa abs 0.7mbar abs 0.5mmHg	0.65kPa 6.5mbar 2.6inH ₂ O	1.1kPa 11mbar 8mmHg
H	160kPa 1600mbar 642inH ₂ O	-160kPa -1600mbar -642inH ₂ O	1kPa abs 10mbar abs 0.15 psia	0.07kPa abs 0.7mbar abs 0.5mmHg	1.6kPa 16mbar 6.4inH ₂ O	2.67kPa 26.7mbar 20mmHg
M	600kPa 6bar 87psi	-600kPa -6bar -87psi	1kPa abs 10mbar abs 0.15 psia	0.07kPa abs 0.7mbar abs 0.5mmHg	6kPa 0.06bar 0.87psi	10kPa 0.1bar 1.45psi
P	2400kPa 24bar 348psi	-2400kPa -24bar -348psi	1kPa abs 10mbar abs 0.15 psia	0.07kPa abs 0.7mbar abs 0.5mmHg	24kPa 0.24bar 3.5psi	40kPa 0.4bar 5.8psi
Q	8000kPa 80bar 1160psi	-8000kPa -80bar -1160psi	1kPa abs 10mbar abs 0.15 psia	0.07kPa abs 0.7mbar abs 0.5mmHg	80kPa 0.8bar 11.6psi	134kPa 1.34bar 19.4psi
S	16000kPa 160bar 2320psi	-16000kPa -160bar -2320psi	1kPa abs 10mbar abs 0.15 psia	0.07kPa abs 0.7mbar abs 0.5mmHg	160kPa 1.6bar 23.2psi	267kPa 2.67bar 38.7psi

Span limits

Maximum span = URL
(can be further adjusted up to \pm URL (TD = 0.5) for differential models, within the range limits)

IT IS RECOMMENDED TO SELECT THE TRANSMITTER SENSOR CODE PROVIDING THE TURNDOWN VALUE AS LOWEST AS POSSIBLE TO OPTIMIZE PERFORMANCE CHARACTERISTICS.

Zero suppression and elevation

Zero and span can be adjusted to any value within the range limits detailed in the table as long as:

- calibrated span \geq minimum span

Damping

Selectable time constant : 0, 0.25, 0.5, 1, 2, 4, 8 or 16s.
This is in addition to sensor response time

Turn on time

Operation within specification in less than 1s with minimum damping.

Insulation resistance

> 100M Ω at 1000VDC (terminals to earth)

Performance specifications

Stated at reference condition to IEC 60770 ambient temperature of 20°C (68°F), relative humidity of 65%, atmospheric pressure of 1013hPa (1013mbar), mounting position with vertical diaphragm and zero based range for transmitter with isolating diaphragms in AISI 316L ss or Hastelloy and silicone oil fill or ABB fill and HART digital trim values equal to 4–20mA span end points, in linear mode.

Unless otherwise specified, errors are quoted as % of span.

Some performance data are affected by the actual turndown (TD) as ratio between Upper Range Limit (URL) and calibrated span.

IT IS RECOMMENDED TO SELECT THE TRANSMITTER SENSOR CODE PROVIDING THE TURNDOWN VALUE AS LOWEST AS POSSIBLE TO OPTIMIZE PERFORMANCE CHARACTERISTICS.

Dynamic performance (according to IEC 61298–1 definition)

- Dead time: 40ms
- Time constant (63.2% of total step change):
 - sensors M to S: ≤ 70ms
 - sensor H: 100ms
 - sensor G: 130ms
 - sensor F: 180ms
- Response time (total) = dead time + time constant

Accuracy rating

% of calibrated span, including combined effects of terminal based linearity, hysteresis and repeatability.

For fieldbus versions SPAN refer to analog input function block outscale range

- Model 264DS, 264PS
 - ±0.075% for TD from 1:1 to 15:1
 (±0.10% for sensor code B for TD from 1:1 to 10:1)
 - ±0.005% x $\frac{URL}{Span}$ for TD from 15:1 to 60:1
 (30:1 for sensor code E)
 - (±0.01% x $\frac{URL}{Span}$ for sensor code B for TD from 10:1 to 20:1)
- Models 264VS
 - ±0.075% for TD from 1:1 to 10:1
 - ±0.0075% x $\frac{URL}{Span}$ for TD from 10:1 to 20:1

Operating influences

Ambient temperature

per 20K (36°F) change between the limits of –20°C to +65°C (–4 to +150°F) :

Model	Sensor Code	for TD up to	
264DS	E to S	15:1	± (0.04% URL + 0.065% span)
264PS	B	10:1	± (0.06% URL + 0.10% span)
264VS	E to S	10:1	± (0.08% URL + 0.13% span)

Optional CoMeter and ProMeter ambient temperature

Total reading error per 20K (36°F) change between the ambient limits of –20 and +70°C (–4 and +158°F) :

±0.15% of max span (16mA).

Static pressure (zero errors can be calibrated out at line pressure)

- per 2MPa, 20bar or 290psi (sensor code B)
- per 7MPa, 70bar or 1015psi (sensor codes E to S)

Model 264DS

- zero error: ±0.15% of URL
- span error: ±0.15% of reading
- Multiply by 1.5 the errors for sensor code E.

Supply voltage

Within voltage/load specified limits the total effect is less than 0.005% of URL per volt.

Load

Within load/voltage specified limits the total effect is negligible.

Radio frequency interference

Total effect : less than 0.10% of span from 20 to 1000MHz and for field strengths up to 30V/m when tested with shielded conduit and grounding, with or without meter.

Common mode interference

No effect from 100Vrms @ 50Hz, or 50VDC

Mounting position

Rotations in plane of diaphragm have negligible effect. A tilt to 90° from vertical causes a zero shifts up to 0.5kPa, 5mbar or 2inH₂O, which can be corrected with the zero adjustment. No span effect.

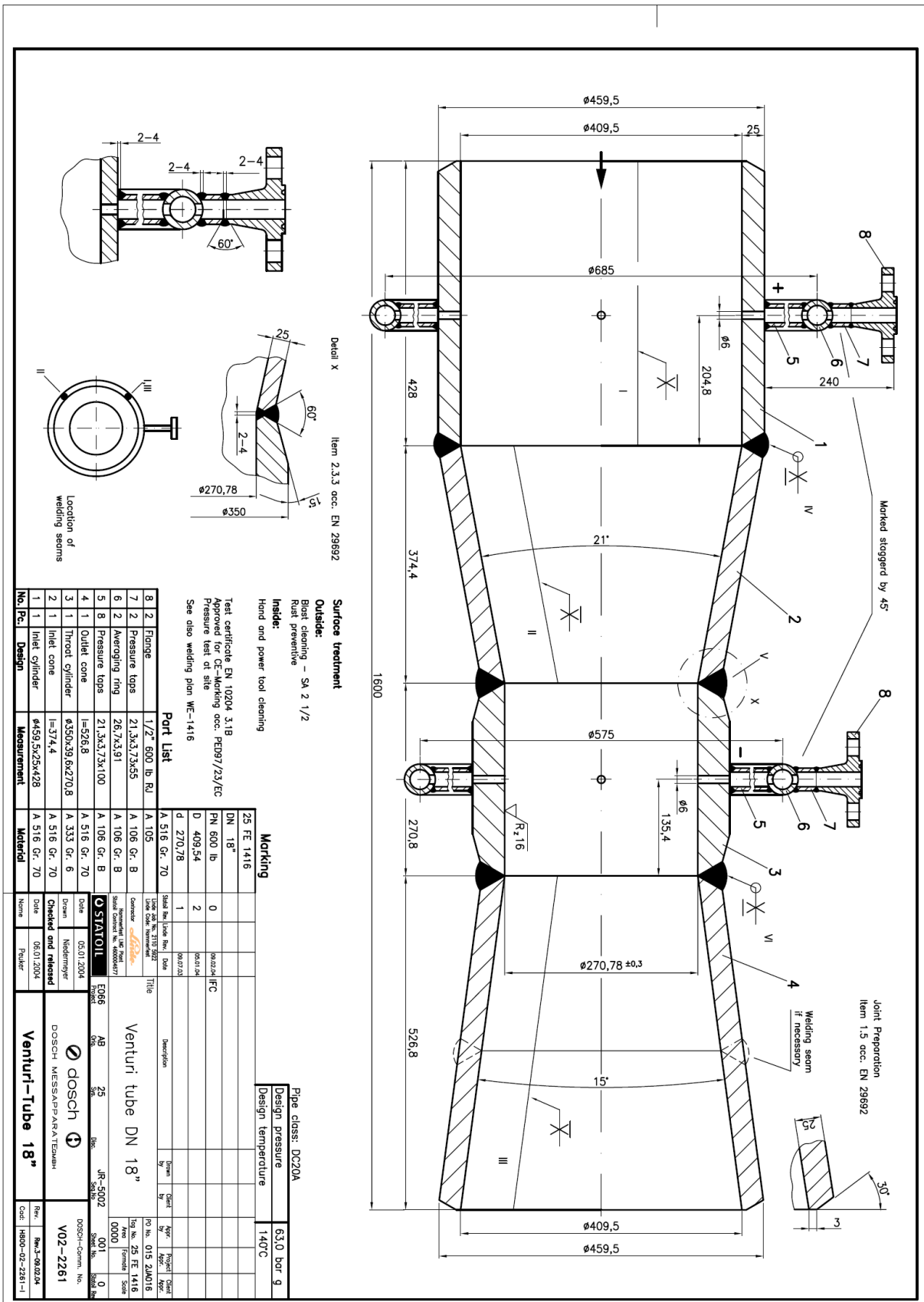
Stability

±0.10% of URL over a thirty-six-month period

Vibration effect

±0.10% of URL (according to IEC 61298–3)

HC GAS FLOW MEASUREMENTS BY VENTURI TUBE



2600T Series Pressure Transmitter

Model 261GS Gauge
Model 261AS Absolute
standard overload

- **Base accuracy: $\pm 0.15\%$**
- **Span limits**
 - 0.3 to 60000 kPa; 1.2 inH₂O to 8700 psi
 - 0.3 to 3000 kPa abs; 2.25 mmHg to 435 psia
- **Reliable sensing system coupled with very latest digital technologies**
 - provides large turn down ratio up to 20:1
- **Stainless steel housing**
 - optimized for rough environment
 - extreme robust
- **Flexible configuration facilities**
 - local zero and span button
 - local configuration with keys on LCD indicator
 - remote configuration with hand terminal or PC based software
- **Full compliance with PED Category III**



ABB 2600T Series
Engineered solutions
for all applications



Functional Specifications

Range and span limits

Sensor Code	Upper Range Limit (URL)	Lower Range Limit (LRL) für 261GS	Minimum span	
			261GS gauge	261AS absolute
C	6 kPa 60 mbar 24 inH ₂ O	-6 kPa -60 mbar -24 inH ₂ O	0.3 kPa 3 mbar 1.2 inH ₂ O	0.3kPa 3 mbar 2.25 mmHg
F	40 kPa 400 mbar 160 inH ₂ O	-40 kPa -400 mbar -160 inH ₂ O	2 kPa 20 mbar 8 inH ₂ O	2 kPa 20 mbar 15 mmHg
L	250 kPa 2500 mbar 1000 inH ₂ O	0 absolute	12.5 kPa 125 mbar 50 inH ₂ O	12.5 kPa 125 mbar 93.8 mmHg
D	1000 kPa 10 bar 145 psi	0 absolute	50 kPa 500 mbar 7.25 psi	50 kPa 500 mbar 375 mmHg
U	3000 kPa 30 bar 435 psi	0 absolute	150 kPa 1.5 bar 21.7 psi	150 kPa 1.5 bar 21.7 psi
R	10000 kPa 100 bar 1450 psi	0 absolute	500 kPa 5 bar 72.5 psi	
V	60000 kPa 600 bar 8700 psi	0 absolute	3000 kPa 30 bar 435 psi	

Note:

Lower Range Limit (LRL) for 261AS is 0 absolute for all ranges.

Span limits

Maximum span = Upper range limit (URL)
IN ORDER TO OPTIMISE THE TRANSMITTER PERFORMANCE IT IS ADVISABLE TO SELECT THE TRANSMITTER SENSOR TO PROVIDE THE MINIMUM POSSIBLE TURNDOWN.
Turndown = Upper range limit / Calibrated span

Zero suppression and elevation

Zero and span can be adjusted to any value within the range limits detailed in the table as long as:
- calibrated span ≥ minimum span

Damping

Adjustable time constant: 0 to 60 s. This is in addition to sensor response time. Can be adjusted via local indicator, hand terminal or PC based software.

Turn on time

Operation within specification in less than 10 s with minimum damping.

Insulation resistance

> 100 MΩ at 500 V DC (terminals to earth)

Operative limits

Temperature limits °C (°F):

Ambient temperature limits (is the operating temperature)

white oil filling: -40°C and +85°C (-40°F and +185°F)
-6°C and +85°C (-21°F and +185°F)
Lower limit for LCD indicator and Viton gasket: -20°C (-4°F)
Lower limit for perfluoroelastomer gasket: -25°C/-15°C (-13°F/+5°F) (ref. to section "Pressure Limits")
Upper limit for perfluoroelastomer gasket: +80°C (+176°F)
Upper limit for LCD indicator: +70°C (+158°F)

Note:

For Hazardous Atmosphere applications see the temperature range specified on the certificate/approval relevant to the aimed type of protection.

Process temperature limits

Lower limit
- -50°C (-58°F); -20°C (-4°F) for Viton gasket
-25°C/-15°C (-13°F/+5°F) for perfluoroelastomer gasket (ref. to section "Pressure Limits")
-6°C (+21°F) for white oil filling
Upper limit
- +120°C (+250°F)
- +80°C (+176°F) for perfluoroelastomer gasket

Storage temperature limits

Lower limit: -50°C (-58°F), -40°C (-40°F) for LCD indicators
-6°C (+21°F) for white oil filling
Upper limit: +85°C (+185°F)

Pressure limits

Overpressure limits (without damage to the transmitter)

0 absolute to
- 1 MPa, 10 bar, 145 psi for sensor codes C, F
- 0.5 MPa, 5 bar, 72.5 psi for sensor code L
- 2 MPa, 20 bar, 290 psi für Sensorcode D
- 6 MPa, 60 bar, 870 psi for sensor code U
- 20 MPa, 200 bar, 2900 psi for sensor code R
- 90 MPa, 900 bar, 13050 psi for sensor code V
- 0.6 MPa abs, 6 bar abs, 87 psia for perfluoroelastomer gasket, T ≥ -15 °C (+5 °F)
- 0.18 MPa abs, 1.8 bar abs, 26 psia for perfluoroelastomer gasket, T ≥ -25 °C (-13 °F)

Proof pressure

The transmitter can be exposed to line pressure for pressure test up to:
refer to Overpressure limits

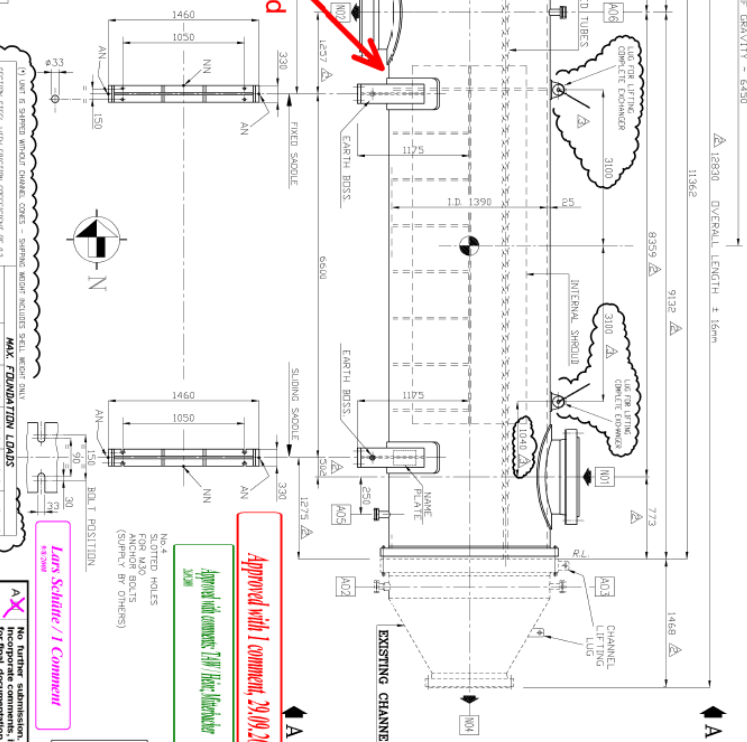
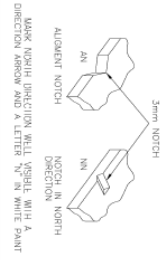
Appendix E Technical drawings of 25-HA-113 twisted tube

NOTE GENERAL

- 1) GENERAL WORK FOR ASSEMBLY
- 2) GENERAL WORK FOR ASSEMBLY
- 3) GENERAL WORK FOR ASSEMBLY
- 4) GENERAL WORK FOR ASSEMBLY
- 5) GENERAL WORK FOR ASSEMBLY
- 6) GENERAL WORK FOR ASSEMBLY
- 7) GENERAL WORK FOR ASSEMBLY
- 8) GENERAL WORK FOR ASSEMBLY
- 9) GENERAL WORK FOR ASSEMBLY
- 10) GENERAL WORK FOR ASSEMBLY
- 11) GENERAL WORK FOR ASSEMBLY
- 12) GENERAL WORK FOR ASSEMBLY
- 13) GENERAL WORK FOR ASSEMBLY
- 14) GENERAL WORK FOR ASSEMBLY
- 15) GENERAL WORK FOR ASSEMBLY
- 16) GENERAL WORK FOR ASSEMBLY
- 17) GENERAL WORK FOR ASSEMBLY
- 18) GENERAL WORK FOR ASSEMBLY
- 19) GENERAL WORK FOR ASSEMBLY
- 20) GENERAL WORK FOR ASSEMBLY
- 21) GENERAL WORK FOR ASSEMBLY
- 22) GENERAL WORK FOR ASSEMBLY
- 23) GENERAL WORK FOR ASSEMBLY
- 24) GENERAL WORK FOR ASSEMBLY
- 25) GENERAL WORK FOR ASSEMBLY
- 26) GENERAL WORK FOR ASSEMBLY
- 27) GENERAL WORK FOR ASSEMBLY
- 28) GENERAL WORK FOR ASSEMBLY
- 29) GENERAL WORK FOR ASSEMBLY
- 30) GENERAL WORK FOR ASSEMBLY
- 31) GENERAL WORK FOR ASSEMBLY

1 Show shell reinforced plate item 78!

No comment by H.Schule THK



Approved with 1 comment, 29/09/2008, T.T. Nguyen

Approved and reviewed by H.Schule

Luis Schuler / I Comment

NO.	DESCRIPTION	UNIT	QTY	REMARKS
1	NOZZLE	PC	1	
2	SHELL	PC	1	
3	TUBE	PC	1	

NO.	DESCRIPTION	UNIT	QTY	REMARKS
4	NOZZLE	PC	1	
5	SHELL	PC	1	
6	TUBE	PC	1	

ITEM NO.	DESCRIPTION	UNIT	QTY	REMARKS
1	NOZZLE	PC	1	
2	SHELL	PC	1	
3	TUBE	PC	1	

NO.	DESCRIPTION	UNIT	QTY	REMARKS
1	NOZZLE	PC	1	
2	SHELL	PC	1	
3	TUBE	PC	1	

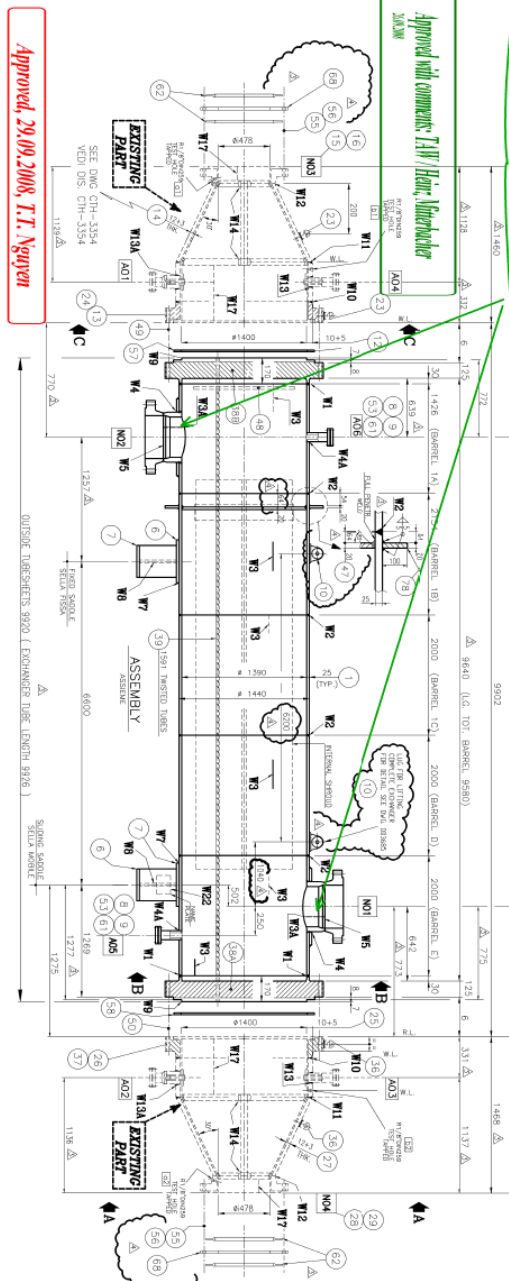
NO.	DESCRIPTION	UNIT	QTY	REMARKS
4	NOZZLE	PC	1	
5	SHELL	PC	1	
6	TUBE	PC	1	

NO.	DESCRIPTION	UNIT	QTY	REMARKS
7	NOZZLE	PC	1	
8	SHELL	PC	1	
9	TUBE	PC	1	

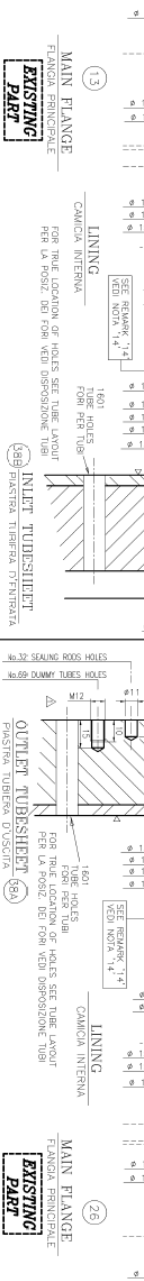
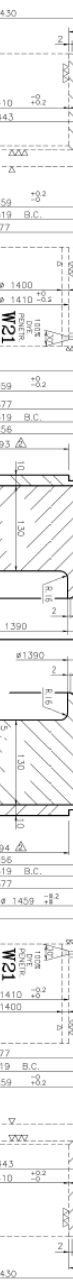
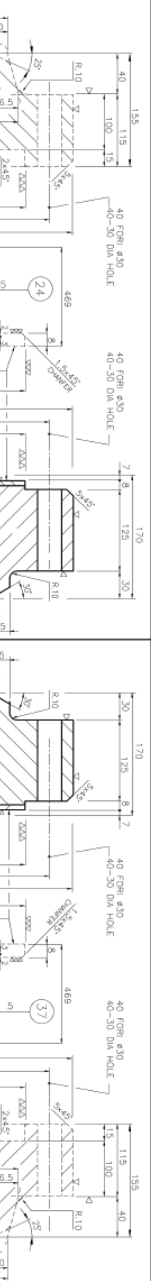
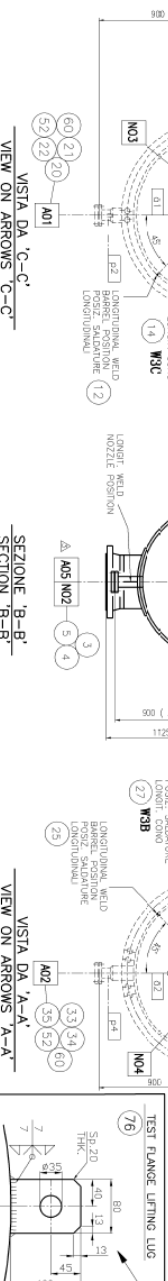
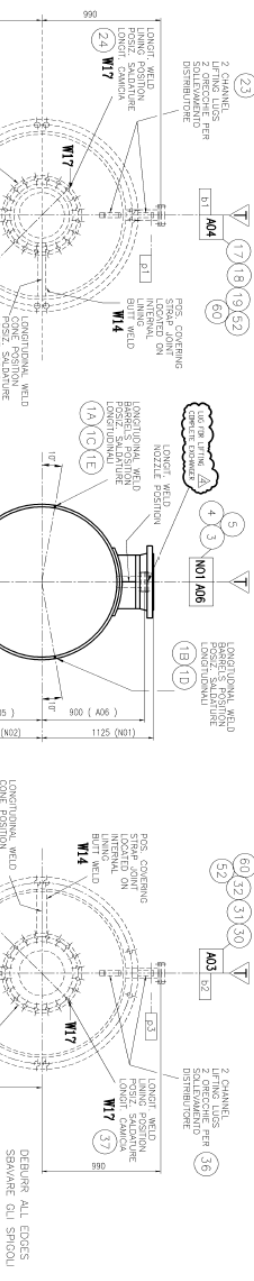
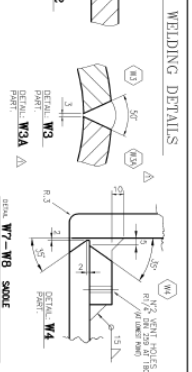
NO.	DESCRIPTION	UNIT	QTY	REMARKS
10	NOZZLE	PC	1	
11	SHELL	PC	1	
12	TUBE	PC	1	

NO.	DESCRIPTION	UNIT	QTY	REMARKS
13	NOZZLE	PC	1	
14	SHELL	PC	1	
15	TUBE	PC	1	

Approved with comments TAV Hair, Mechanical
MAIWA
 For clarity, please, whether W23 is existing or not!
 The drawings are for the revision of the design for the inspection and Test Plan TP-2005, etc.



Approved: 29.09.2008, T.T. Nguyen



TEST FLANGES LIFTING LUG
 OPEN ALL ENDS
 SPRAYED OIL SPRAY

TEST FLANGES 'W'
 VISTA DA PROVA

GENERAL DETAIL
 NO. 01
 DATE: 18/03/2008
 LINDE AG Engineering Division
 001200226

No.	Description	Date
1	REVISED (SEELED) FOR APPROVAL	
2	REVISED (SEELED) FOR APPROVAL	
3	REVISED (SEELED) FOR APPROVAL	
4	REVISED (SEELED) FOR APPROVAL	
5	REVISED (SEELED) FOR APPROVAL	
6	REVISED (SEELED) FOR APPROVAL	
7	REVISED (SEELED) FOR APPROVAL	
8	REVISED (SEELED) FOR APPROVAL	
9	REVISED (SEELED) FOR APPROVAL	
10	REVISED (SEELED) FOR APPROVAL	

OSATOIL
 1300 x 10000
 1117 85 m2
 1 1334 2400
 1 1334 2400
 1 1334 2400

LINDE
ALLOY
GENERAL DETAIL
 NO. 01
 DATE: 18/03/2008
 LINDE AG Engineering Division
 001200226

OSATOIL
 1300 x 10000
 1117 85 m2
 1 1334 2400
 1 1334 2400
 1 1334 2400

LINDE AG
STAMMIL HYDRO
2194 E
GD-3685

No comment by Hsdiol, TMC
 Lens Schiller no Comment
 Approved: 01.10.2008, T.D.

Appendix F Technical drawings of 25-HA-113 double helix

Appendix G Thermodynamic properties of HC gas

The properties are evaluated at for the following HC gas composition

CH₄ 53,2%
 C₂H₆ 29,0%
 C₃H₈ 0,4%
 N₂ 17,4%

Run Information:

Run Date: 03.06.2009 20:06

Flash Method: Integral

Liquid method: Advanced_Peng-Robinson

Vapor method: Advanced_Peng-Robinson

Pressure: 1884,00 kPa			Vapor Properties			
Temperature (C)	Enthalpy (kJ/kg)	Weight Fraction Vapor	Density (kg/m ³)	Viscosity (mN-s/m ²)	Thermal Cond. (W/m-C)	Heat Capacity (kJ/kg-C)
10,000	411,165	1,00000	19,1769	0,0114	0,0281	1,9170
15,767	422,235	1,00000	18,7036	0,0115	0,0289	1,9223
21,533	433,337	1,00000	18,2563	0,0117	0,0297	1,9284
27,300	444,478	1,00000	17,8327	0,0119	0,0305	1,9353
33,067	455,659	1,00000	17,4308	0,0121	0,0312	1,9429
38,833	466,887	1,00000	17,0488	0,0122	0,0320	1,9511
44,600	478,163	1,00000	16,6851	0,0124	0,0328	1,9598
50,367	489,491	1,00000	16,3383	0,0126	0,0336	1,9691
56,133	500,874	1,00000	16,0072	0,0127	0,0344	1,9788
61,900	512,314	1,00000	15,6907	0,0129	0,0352	1,9890

* - Denotes dew/bubble point.

Pressure: 1884,00 kPa			Vapor Properties			
Temperature (C)	Enthalpy (kJ/kg)	Weight Fraction Vapor	Density (kg/m ³)	Viscosity (mN-s/m ²)	Thermal Cond. (W/m-C)	Heat Capacity (kJ/kg-C)
10,640	412,392	1,00000	19,1230	0,0114	0,0282	1,9175
17,076	424,752	1,00000	18,5999	0,0116	0,0291	1,9236
23,511	437,154	1,00000	18,1084	0,0118	0,0299	1,9307
29,947	449,604	1,00000	17,6457	0,0120	0,0308	1,9387
36,382	462,109	1,00000	17,2088	0,0122	0,0317	1,9475
42,818	474,673	1,00000	16,7956	0,0123	0,0326	1,9571
49,253	487,300	1,00000	16,4040	0,0125	0,0335	1,9673
55,689	499,995	1,00000	16,0322	0,0127	0,0344	1,9781
62,124	512,761	1,00000	15,6786	0,0129	0,0352	1,9894
68,560	525,601	1,00000	15,3418	0,0131	0,0361	2,0012

* - Denotes dew/bubble point.

Pressure: 1739,00 kPa			Vapor Properties			
Temperature (C)	Enthalpy (kJ/kg)	Weight Fraction Vapor	Density (kg/m ³)	Viscosity (mN-s/m ²)	Thermal Cond. (W/m-C)	Heat Capacity (kJ/kg-C)
10,000	413,026	1,00000	17,6001	0,0113	0,0280	1,9043
15,767	424,025	1,00000	17,1729	0,0115	0,0288	1,9104
21,533	435,061	1,00000	16,7685	0,0117	0,0295	1,9173
27,300	446,139	1,00000	16,3851	0,0118	0,0303	1,9249
33,067	457,262	1,00000	16,0209	0,0120	0,0311	1,9330
38,833	468,435	1,00000	15,6744	0,0122	0,0319	1,9418
44,600	479,659	1,00000	15,3441	0,0124	0,0327	1,9510
50,367	490,937	1,00000	15,0289	0,0125	0,0335	1,9607
56,133	502,274	1,00000	14,7277	0,0127	0,0343	1,9709
61,900	513,669	1,00000	14,4395	0,0129	0,0351	1,9815

* - Denotes dew/bubble point.

Pressure: 1739,00 kPa			Vapor Properties			
Temperature (C)	Enthalpy (kJ/kg)	Weight Fraction Vapor	Density (kg/m ³)	Viscosity (mN-s/m ²)	Thermal Cond. (W/m-C)	Heat Capacity (kJ/kg-C)
10,640	414,245	1,00000	17,5515	0,0113	0,0281	1,9049
17,076	426,527	1,00000	17,0792	0,0115	0,0289	1,9119
23,511	438,856	1,00000	16,6348	0,0117	0,0298	1,9198
29,947	451,238	1,00000	16,2157	0,0119	0,0307	1,9285
36,382	463,680	1,00000	15,8196	0,0121	0,0316	1,9380
42,818	476,184	1,00000	15,4445	0,0123	0,0325	1,9481
49,253	488,755	1,00000	15,0886	0,0125	0,0333	1,9588
55,689	501,398	1,00000	14,7504	0,0127	0,0342	1,9701
62,124	514,114	1,00000	14,4285	0,0129	0,0351	1,9819
68,560	526,908	1,00000	14,1216	0,0131	0,0360	1,9941

* - Denotes dew/bubble point.

Pressure: 1814,00 kPa			Vapor Properties			
Temperature (C)	Enthalpy (kJ/kg)	Weight Fraction Vapor	Density (kg/m ³)	Viscosity (mN-s/m ²)	Thermal Cond. (W/m-C)	Heat Capacity (kJ/kg-C)
10,000	412,065	1,00000	18,4135	0,0113	0,0281	1,9108
15,767	423,100	1,00000	17,9626	0,0115	0,0288	1,9165
21,533	434,170	1,00000	17,5363	0,0117	0,0296	1,9230
27,300	445,280	1,00000	17,1323	0,0119	0,0304	1,9303
33,067	456,434	1,00000	16,7487	0,0120	0,0312	1,9381
38,833	467,634	1,00000	16,3840	0,0122	0,0320	1,9466
44,600	478,885	1,00000	16,0365	0,0124	0,0328	1,9556
50,367	490,190	1,00000	15,7051	0,0126	0,0336	1,9651
56,133	501,550	1,00000	15,3885	0,0127	0,0344	1,9750
61,900	512,968	1,00000	15,0857	0,0129	0,0352	1,9853

* - Denotes dew/bubble point.

Pressure: 1814,00 kPa			Vapor Properties			
Temperature (C)	Enthalpy (kJ/kg)	Weight Fraction Vapor	Density (kg/m ³)	Viscosity (mN-s/m ²)	Thermal Cond. (W/m-C)	Heat Capacity (kJ/kg-C)
10,640	413,288	1,00000	18,3621	0,0114	0,0281	1,9114
17,076	425,609	1,00000	17,8638	0,0116	0,0290	1,9179
23,511	437,976	1,00000	17,3953	0,0117	0,0299	1,9254
29,947	450,394	1,00000	16,9538	0,0119	0,0308	1,9338
36,382	462,868	1,00000	16,5368	0,0121	0,0316	1,9429
42,818	475,403	1,00000	16,1421	0,0123	0,0325	1,9527
49,253	488,003	1,00000	15,7679	0,0125	0,0334	1,9632
55,689	500,672	1,00000	15,4124	0,0127	0,0343	1,9742
62,124	513,414	1,00000	15,0742	0,0129	0,0352	1,9857
68,560	526,232	1,00000	14,7519	0,0131	0,0361	1,9978

* - Denotes dew/bubble point.

Pressure: 1671,00 kPa			Vapor Properties			
Temperature (C)	Enthalpy (kJ/kg)	Weight Fraction Vapor	Density (kg/m ³)	Viscosity (mN-s/m ²)	Thermal Cond. (W/m-C)	Heat Capacity (kJ/kg-C)
10,000	413,896	1,00000	16,8668	0,0113	0,0279	1,8984
15,767	424,862	1,00000	16,4605	0,0115	0,0287	1,9049
21,533	435,868	1,00000	16,0758	0,0116	0,0295	1,9121
27,300	446,917	1,00000	15,7108	0,0118	0,0303	1,9200
33,067	458,013	1,00000	15,3638	0,0120	0,0311	1,9285
38,833	469,160	1,00000	15,0335	0,0122	0,0318	1,9375
44,600	480,359	1,00000	14,7186	0,0124	0,0326	1,9469
50,367	491,615	1,00000	14,4179	0,0125	0,0334	1,9569
56,133	502,930	1,00000	14,1304	0,0127	0,0342	1,9672
61,900	514,305	1,00000	13,8552	0,0129	0,0351	1,9780

* - Denotes dew/bubble point.

Pressure: 1671,00 kPa			Vapor Properties			
Temperature (C)	Enthalpy (kJ/kg)	Weight Fraction Vapor	Density (kg/m ³)	Viscosity (mN-s/m ²)	Thermal Cond. (W/m-C)	Heat Capacity (kJ/kg-C)
10,640	415,112	1,00000	16,8206	0,0113	0,0280	1,8991
17,076	427,357	1,00000	16,3714	0,0115	0,0289	1,9065
23,511	439,652	1,00000	15,9485	0,0117	0,0297	1,9148
29,947	452,003	1,00000	15,5494	0,0119	0,0306	1,9238
36,382	464,416	1,00000	15,1719	0,0121	0,0315	1,9336
42,818	476,892	1,00000	14,8143	0,0123	0,0324	1,9440
49,253	489,438	1,00000	14,4749	0,0125	0,0333	1,9549
55,689	502,055	1,00000	14,1521	0,0127	0,0342	1,9664
62,124	514,749	1,00000	13,8447	0,0129	0,0351	1,9784
68,560	527,520	1,00000	13,5516	0,0131	0,0360	1,9908

* - Denotes dew/bubble point.

Appendix H Correction of thermodynamic properties

Deviation in operation point compared to design

The calculations is based on thermodynamic properties from Appendix G and the table below

	Design	Averaged operation point	Units
$T_{h,i}$	61,9	68,6	°C
$T_{h,o}$	10	10,6	°C
$p_{h,i}$	18,84	17,4	bar
$p_{h,o}$	18,14	16,7	bar

Viscosity HC gas

Design pressure, averaged temperature for all 25 measurements

$$\frac{\mu_{h,i} + \mu_{h,o}}{\mu_{h,i \text{ design}} + \mu_{h,o \text{ design}}} = \frac{0,0131 + 0,0114}{0,0129 + 0,0113} = 1,0124$$

Correction term for viscosity with respect off design temperature

$$0,00186(T_{h,i} - T_{h,i \text{ design}}) + 1$$

The changes in pressure have a negligible effect on the viscosity.

Specific heat capacity HC gas

Design temperature, averaged pressure for all 25 measurements

$$\frac{Cp_{h,i} + Cp_{h,o}}{Cp_{h,i \text{ design}} + Cp_{h,o \text{ design}}} = \frac{1,9815 + 1,8984}{1,9890 + 1,9108} = 0,9949$$

Correction term for specific heat capacity with respect to off design pressure

$$0,0035(p_{h,i} - p_{h,i \text{ design}}) + 1$$

The changes is temperature have a negligible effect on the specific heat capacity.

Density of HC gas

Design temperature, averaged pressure for all 25 measurements

$$\frac{\rho_{h,i} + \rho_{h,o}}{\rho_{h,i \text{ design}} + \rho_{h,o \text{ design}}} = \frac{14,4395 + 16,8668}{15,6907 + 18,4135} = 0,9180$$


Correction term for specific heat capacity with respect to off design pressure

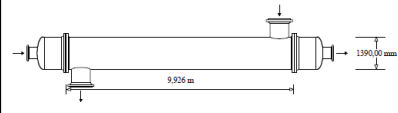
$$0,0566(p_{h,i} - p_{h,i \text{ design}}) + 1$$

The changes in temperature have a negligible effect on the specific heat capacity.

Appendix I TEMA specification sheets printed from HTRI

CHAPTER 3: SPECIFICATION SHEET FOR TWISTED TUBE HEAT EXCHANGER

		HEAT EXCHANGER SPECIFICATION SHEET				Page 1	
						SI Units	
Customer		Linde AG for Statoil AS		Job No.			
Address				Reference No.		8422-25HA113-00	
Plant Location		Hammerfest LNG Plant		Proposal No.		8422r/07	
Service of Unit		Subcooling Cycle Compressor Intercooler		Date		05.08.2008 Rev 0	
Size		1390,00 x 9926,00 mm		Type		BEM	
Surf/Unit (Gross/Eff)		1102,64 / 1070,87 m ²		Horz.		Connected In	
		Shell/Unit		1		Surf/Shell (Gross/Eff)	
						1102,64 / 1070,87 m ²	
PERFORMANCE OF ONE UNIT							
Fluid Allocation		Shell Side			Tube Side		
Fluid Name		N2/C1/C2 HC Refrigerant			Sea Water		
Fluid Quantity, Total		kg/hr			500206		
Vapor (In/Out)		500206			500206		
Liquid					1590428		
Steam					1590428		
Water							
Noncondensables							
Temperature (In/Out)		C			61,90 10,00		
Specific Gravity					1,0267 1,0243		
Viscosity		mN-s/m ²			0,0120 0,0110		
Molecular Weight, Vapor							
Molecular Weight, Noncondensables							
Specific Heat		kJ/kg-C			2,1000 2,0400		
Thermal Conductivity		W/m-C			0,0350 0,0282		
Latent Heat		kJ/kg					
Inlet Pressure		kPa			1884,03		
Velocity		m/s			13,54		
Pressure Drop, Allow/Calc		kPa			70,001 81,352		
Fouling Resistance (min)		m ² -K/W			0,000180		
Heat Exchanged W		14917752			MTD (Corrected)		
					17,7 C		
Transfer Rate, Service		787,18 W/m ² -K			Clean		
					1176,56 W/m ² -K		
					Actual		
					940,55 W/m ² -K		
CONSTRUCTION OF ONE SHELL				Sketch (Bundle/Nozzle Orientation)			
		Shell Side		Tube Side			
Design/Test Pressure		kPaG		2500,04 / 1750,03 /			
Design Temperature		C		140,00 50,00			
No Passes per Shell		1		1			
Corrosion Allowance		mm					
Connections		In mm		1 @ 814,000			
Size & Rating		Out mm		1 @ 814,000			
		Intermediate		@			
Tube No.		1591		OD 22,225 mm			
		Thk(Avg)		1,734 mm			
		Length		9,926 m			
		Pitch		27,781 mm			
		Layout		60			
Tube Type		Twisted		Material TITANIUM-GRADE 2			
Shell		ID 1390,00 mm		OD mm			
Channel or Bonnet				Shell Cover			
Tubesheet-Stationary				Channel Cover			
Floating Head Cover				Tubesheet-Floating			
Baffles-Cross		Type NONE		%Cut (Diam) Spacing(c/c) 9640,02			
Baffles-Long				Inlet mm			
Supports-Tube				Seal Type			
Bypass Seal Arrangement				U-Bend Type			
Expansion Joint				Tube-Tubesheet Joint			
Rho-V2-Inlet Nozzle		4555,05 kg/m-s ²		Bundle Entrance Bundle Exit kg/m-s ²			
Gaskets-Shell Side				Tube Side			
				-Floating Head			
Code Requirements				TEMA Class			
Weight/Shell		26877,8		Filled with Water 45059,5			
				Bundle 10074,7 kg			
Remarks: Case 03							
Note: Reported duty and flow rates include a user-specified multiplier of 1.05. Reprinted with Permission (v5 SP2)							



CHAPTER 6: SPECIFICATION SHEET FOR CONVENTIONAL HEAT EXCHANGER

HTRI		HEAT EXCHANGER SPECIFICATION SHEET				Page 1 SI Units
Customer		Linde AG for Statoil AS		Job No.		
Address				Reference No. 8422-25HA113-00		
Plant Location		Hammerfest LNG Plant		Proposal No. 8422r/07		
Service of Unit		Subcooling Cycle Compressor Intercooler		Date 11.06.2009 Rev 0		
Size		1400,00 x 9929,88 mm Type BEM Horz.		Connected In 1 Parallel 1 Series		
Surf/Unit (Gross/Eff)		2137,69 / 2109,03 m2		Shell/Unit 1 Surf/Shell (Gross/Eff) 2137,69 / 2109,03 m2		
PERFORMANCE OF ONE UNIT						
Fluid Allocation		Shell Side		Tube Side		
Fluid Name		N2/C1/C2 HC Refrigerant		Sea Water		
Fluid Quantity, Total		kg/hr 500206		1590428		
Vapor (In/Out)		500206 500206				
Liquid				1590428 1590428		
Steam						
Water						
Noncondensables						
Temperature (In/Out) C		61,90 9,87		6,10 14,13		
Specific Gravity				1,0267 1,0243		
Viscosity mN-s/m2		0,0120 0,0110		1,4690 1,1842		
Molecular Weight, Vapor						
Molecular Weight, Noncondensables						
Specific Heat kJ/kg-C		2,1000 2,0399		4,2001 4,1900		
Thermal Conductivity W/m-C		0,0350 0,0282		0,5832 0,5955		
Latent Heat kJ/kg						
Inlet Pressure kPa		1884,03		610,009		
Velocity m/s		7,21		1,44		
Pressure Drop, Allow/Calc kPa		70,001 45,586		100,002 24,945		
Fouling Resistance (min) m2-K/W				0,000180		
Heat Exchanged W		14963998		MTD (Corrected) 17,2 C		
Transfer Rate, Service		412,88 W/m2-K Clean		527,56 W/m2-K Actual 411,35 W/m2-K		
CONSTRUCTION OF ONE SHELL				Sketch (Bundle/Nozzle Orientation)		
		Shell Side		Tube Side		
Design/Test Pressure kPaG		2500,04 /		1750,03 /		
Design Temperature C		140,00		50,00		
No Passes per Shell		1		1		
Corrosion Allowance mm						
Connections		In mm 1 @ 814,000		1 @ 488,000		
Size & Rating		Out mm 1 @ 814,000		1 @ 488,000		
		Intermediate @		@		
Tube No. 1435		OD 22,225 mm		Thk(Avg) 1,734 mm		Length 9,930 m Pitch 26,781 mm Layout 30
Tube Type Low Fin				Material TITANIUM-GRADE 2		
Shell ID 1400,00 mm		OD mm		Shell Cover		
Channel or Bonnet				Channel Cover		
Tubesheet-Stationary				Tubesheet-Floating		
Floating Head Cover				Impingement Plate Circular plate		
Baffles-Cross		Type NTIW-SEG.		%Cut (Diam) 24,00		Spacing(c/c) 1500,00 Inlet 2571,95 mm
Baffles-Long				Seal Type		
Supports-Tube				U-Bend Type		
Bypass Seal Arrangement				Tube-Tubesheet Joint		
Expansion Joint				Type		
Rho-V2-Inlet Nozzle		4555,05 kg/m-s2		Bundle Entrance 1523,69		Bundle Exit 852,29 kg/m-s2
Gaskets-Shell Side				Tube Side		
-Floating Head						
Code Requirements				TEMA Class		
Weight/Shell 25648,0		Filled with Water 44283,9		Bundle 8665,46 kg		
Remarks: Supports/baffle space = 4. Case 03						
Note: Reported duty and flow rates include a user-specified multiplier of 1.05.						
Reprinted with Permission (v5 SP2)						

CHAPTER 6: SPECIFICATION SHEET FOR DOUBLE HELIX HEAT EXCHANGER

HTRI		HEAT EXCHANGER SPECIFICATION SHEET					Page 1 SI Units						
Customer		Linde AG for Statoil AS			Job No.								
Address					Reference No.		8422-25HA113-00						
Plant Location		Hammerfest LNG Plant			Proposal No.		8422r/07						
Service of Unit		Subcooling Cycle Compressor Intercooler			Date		11.06.2009 Rev 0						
Size		1400,00 x 9993,88 mm		Type BEM		Horz.		Connected In 1 Parallel 1 Series					
Surf/Unit (Gross/Eff)		1627,88 / 1618,85 m ²		Shell/Unit		1		Surf/Shell (Gross/Eff) 1627,88 / 1618,85 m ²					
PERFORMANCE OF ONE UNIT													
Fluid Allocation			Shell Side			Tube Side							
Fluid Name			N2/C1/C2 HC Refrigerant			Sea Water							
Fluid Quantity, Total			kg/hr			500206							
Vapor (In/Out)			500206			500206							
Liquid						1590428							
Steam						1590428							
Water													
Noncondensables													
Temperature (In/Out)			C			61,90 15,30 6,10 13,29							
Specific Gravity						1,0267 1,0246							
Viscosity			mN-s/m ²			0,0120 0,0111 1,4690 1,2102							
Molecular Weight, Vapor													
Molecular Weight, Noncondensables													
Specific Heat			kJ/kg-C			2,1000 2,0462 4,2001 4,1911							
Thermal Conductivity			W/m-C			0,0350 0,0289 0,5832 0,5942							
Latent Heat			kJ/kg										
Inlet Pressure			kPa			1884,03 610,009							
Velocity			m/s			9,66 1,91							
Pressure Drop, Allow/Calc			kPa			70,001 22,397 100,002 39,611							
Fouling Resistance (min)			m ² -K/W			0,000180							
Heat Exchanged W			13423961			MTD (Corrected) 23,8 C							
Transfer Rate, Service			348,17 W/m ² -K			Clean Actual 424,49 W/m ² -K 345,87 W/m ² -K							
CONSTRUCTION OF ONE SHELL						Sketch (Bundle/Nozzle Orientation)							
			Shell Side		Tube Side								
Design/Test Pressure			kPaG		2500,04 / 1750,03 /								
Design Temperature			C		140,00 50,00								
No Passes per Shell			1		1								
Corrosion Allowance			mm										
Connections			In mm		1 @ 814,000 1 @ 488,000								
Size & Rating			Out mm		1 @ 814,000 1 @ 488,000								
			Intermediate		@ @								
Tube No.		1078		OD 19,050 mm		Thk(Avg) 1,250 mm		Length 9,994 m		Pitch 32,000 mm		Layout 45	
Tube Type		Low Fin		Material		TITANIUM-GRADE 2							
Shell		ID 1400,00 mm		OD		mm		Shell Cover					
Channel or Bonnet				Channel Cover									
Tubesheet-Stationary				Tubesheet-Floating									
Floating Head Cover				Impingement Plate		Rods							
Baffles-Cross		Type DOUBLE HELIX		%Cut (Diam)		Spacing(c/c) 1212,00		Inlet 684,949 mm					
Baffles-Long				Seal Type									
Supports-Tube				U-Bend		Type							
Bypass Seal Arrangement				Tube-Tubesheet Joint									
Expansion Joint				Type									
Rho-V2-Inlet Nozzle		4555,05 kg/m-s ²		Bundle Entrance		2064,00		Bundle Exit		2139,25 kg/m-s ²			
Gaskets-Shell Side				Tube Side									
-Floating Head													
Code Requirements				TEMA Class									
Weight/Shell		23797,4		Filled with Water		43841,0		Bundle		6744,19 kg			
Remarks: Case 03													
Note: Reported duty and flow rates include a user-specified multiplier of 1.05.													
Reprinted with Permission (v5 SP2)													